Thermomechanical Postbuckling of Geometrically Imperfect Anisotropic Flat and Doubly Curved Sandwich Panels

by

Terry J. Hause

Dissertation Submitted To The Faculty of
Virginia Polytechnic Institute and State University
In Partial Fulfillment for the Degree of

Doctor of Philosophy

in

Engineering Mechanics

Department of Engineering Science and Mechanics

Virginia Polytechnic Institute and State University

Approved By:

Dr. L. Librescu (Chairman)
Dr. M. Hajj
Dr. E.G. Henneke
Dr. R.K. Kapania
Dr. S. Thangjitham

April 17, 1998

Blacksburg, Virginia

Keywords: Sandwich Structures, Buckling and Postbuckling, Geometrically Nonlinearities, Snap-Through, Geometric Imperfections

Thermomechanical Postbuckling of Geometrically Imperfect Anisotropic Flat and Doubly Curved Sandwich Panels

by

Terry J. Hause

Committee Chairman: Dr. L. Librescu
Engineering Science and Mechanics

Abstract

Sandwich structures constitute basic components of advanced supersonic/hypersonic flight and launch vehicles. These advanced flight vehicles operate in hostile environments consisting of high temperature, moisture, and pressure fields. As a result, these structures are exposed to large lateral pressures, large compressive edge loads, and high temperature gradients which can create large stresses and strains within the structure and can produce the instability of the structure. This creates the need for a better understanding of the behavior of these structures under these complex loading conditions. Moreover, a better understanding of the load carrying capacity of sandwich structures constitutes an essential step towards a more rational design and exploitation of these constructions.

In order to address these issues, a comprehensive geometrically non-linear theory of doubly curved sandwich structures constructed of anisotropic laminated face sheets with an orthotropic core under various loadings for simply supported edge conditions is developed. The effects of the radii of curvature, initial geometric imperfections, pressure, uniaxial compressive edge loads, biaxial edge loading consisting of compressive/tensile edge loads, and thermal loads will be analyzed. The effect of the structural tailoring of the facesheets upon the load carrying capacity of the structure under these various loading conditions are analyzed. In addition, the movability/immovability of the unloaded edges and the end-shortening are examined.

To pursue this study, two different formulations of the theory are developed. One of these formulations is referred to as the mixed formulation, While the second formulation is referred to as the displacement formulation. Several results are presented encompassing buckling, postbuckling, and stress/strain analysis in conjunction with the application of the structural tailoring technique. The great effects of this technique are explored. Moreover, comparisons with the available theoretical and experimental results are presented and good agreements are reported.

Acknowledgements

I want to express my thanks to Dr. Liviu Librescu who served as my committee chairperson who provided me with the opportunity to work with him on a grant with NASA Langley Research Center for three years and who guided and encouraged me to persevere throughout the Phd program.

This work was supported by NASA Langley Research Center under the Grant NAG1-1689. I would like to express my thanks to Dr. Theodore F. Johnson, the monitor of the grant who gave me this wonderful opportunity to prepare for my future and spend several weeks during the summer at NASA Langley Research Center.

Additional thanks are expressed towards Dr. M. Hajj, Dr. E. G. Henneke, Dr. R. K. Kapania, and Dr. S. Thangjitham for serving on my committee.

Special thanks are addressed to Dr. E. G. Henneke as the head of the ESM Department, for his thoughtful advices offered to me.

Above all, I would like to express my thanks to God for his care over me.

Table of Contents

List of Figures

List of Tables

1 Introduction

1.1 Overview

Sandwich type construction, due to its outstanding features(listed below), is of great promise in the design of advanced flight and launch vehicles. In its simplest form the sandwich construction is composed of two stiff layers (face layers) separated by a thick mid layer of low density material (core layer). The considerable advantages offered by fibrous composite materials over conventional materials and the need for overcoming the technical challenges involving the design of advanced supersonic/hypersonic flight vehicles have prompted an increased use of sandwich structures with laminated composite facesheets.

The field of sandwich construction has become popular in recent years as a result of improvements in manufacturing techniques. Prior to modern times the prohibitive cost of sandwich construction has limited its use. As new manufacturing techniques are now being developed which make the use of sandwich structures financially feasible, more research work is becoming increasingly important. The next generation of supersonic/hypersonic flight and launch vehicles has to be designed to meet increasingly stringent performance requirements. These flight vehicles are likely to operate in hostile environments consisting of high temperature, moisture, and pressure fields. The temperatures under which these flight vehicles are likely to operate range from the extreme lows of cryogenic fuels and low radiation from the sun to the extreme high temperatures of aerodynamic heating and heat from propulsion units.

The sandwich structures encompasse a number of properties of exceptional importance the fulfillment of the high demands imposed upon these vehicles. Among others are

- High bending stiffness characteristics with little resultant weight penalty
- a smoother aerodynamic surface in a higher speed range
- Excellent thermal and sound insulation
- Increased strength at elevated temperatures
- Increased operational time as compared to stiffened-reinforced structures which are weakened by the occurence of stress concentrations

Traditionally, standard sandwich type constructions were composed of a thick core separating two identical thin metallic face sheets. This construction allowed the various load components to be distributed in a specialized way such that the bending moments were predominantly taken up as tensile and compressive stresses in the faces, while the core carried only transverse shear stresses (weak core). The ability to design the faces and the core according to their specific

needs yields the high stiffness and strength per unit weight of such constructions. From this emerges the efficiency and the success of their usage.

However, with advanced sandwich type constructions, this separation of tasks becomes questionable. This is the case within the advanced sandwich type construction consisting of anisotropic fiber-reinforced laminated composite facesheets featuring symmetry/non-symmetry properties with respect to their own midsurfaces and of a core layer capable of carrying in plane stresses as well as transverse shear stresses (strong core).

Because these advanced sandwich structures used in high speed flight vehicles will experience large lateral loads, large compressive edge loads, and high temperature gradients, determination of the response to these loading conditions constitutes an issue of considerable importance towards their rational design. This study is likely to contribute to a better understanding and exploitation of their load carrying capacity. Such an investigation will provide among others, important information about the character of the snap-through behavior (which is a damaging phenomenon), the influence the initial geometric imperfections, compressive edge loads, lateral loads, and the immovability of the edges, and the influence of a number of other geometrical and physical parameters on the response behavior of these sandwich structures.

In spite of the practical importance of these problems, based on the information available in the most comprehensive survey paper on sandwich structures [74], one can conclude that these issues have not yet either been addressed or the results are very limited in scope and depth. The study of these problems constitutes the topic of this dissertation.

1.2 Scope and Content

One of the goals of this dissertation is to develop a comprehensive structural model of sandwich structures with anisotropic laminated composite facesheets and to study the behavior of these structures under a variety of loading conditions, both mechanical and thermal. It is supposed that the faces are symmetrically laminated with respect to their local midsurfaces as well as the global midsurface, which runs through the middle surface of the core. The core will be assumed to exhibit the weak core behavior. The assumed temperature profile will exhibit an antisymmetric linear variation through the thickness of the sandwich panel. Finally, all edges will be assumed to be simply supported.

The effects of the radii of curvature, initial geometric imperfections, pressure, uniaxially compressive edge loads, biaxial edge loading consisting of compressive/tensile edge loads, and thermal loads will be analyzed. The effect of the structural tailoring of the face sheets upon the load carrying capacity and of the snap-through behavior will be analyzed. In addition, the effect of the movability/immovability of the unloaded edges will be examined.

To undertake this study, two different formulations of sandwich constructions will be developed. One of these representations is in terms of the Airy's potential function, transversal

deflection, and two displacement measures and is referred to as the *mixed formulation*. The second formulation is in terms of displacement measures and is referred to as the *displacement formulation*. Although more difficult to handle for the problem at hand, the latter has the advantage of allowing one to treat the sandwich panel in the most general conditions.

Results in the form of plots and tables are presented and discussed in the results and discussion section. In addition, comparisons are made between theoretical and experimental results, cited in the literature.

1.3 Brief Literature Review

During the last few decades a tremendous amount of research has been devoted to modeling, analysis and manufacturing of sandwich constructions. According to the survey paper by Noor, Burton, and Bert [74], sandwich panels were introduced into aircraft structures during World War II. In addition, because their light weight coupled with high stiffness, structural efficiency and durability, sandwich panels have been widely used in shipbuilding, construction, and other industries. First generation sandwich panels used in aircraft structures were composed of plywood or wood pulp fiber facings in conjunction with a core made from cork, balsa wood or synthetic materials. Newer sandwich constructions used in aircraft or spacecraft applications consist of faces and cores composed of aluminum alloys, titanium, and stainless steel. Modern sandwich construction consists of anisotropic laminated facesheets with either a honeycomb, truss, or a foam core.

A substanial amount of literature exists on the subject of sandwich construction, the main emphasis being placed on the linear theories in contrast to the nonlinear theory. This deficiency with the nonlinear theory prompted the research involved with this dissertation. Volmir [92] developed a linear theory for circular cylindrical sandwich panels which incorporated isotropic facings and a transversely isotropic core with complete structural symmetry for both simply supported and clamped boundary conditions.

Tennison and Chan [89] developed a linear theory for sandwich cylinders under axial compression with axisymmetric imperfections incorporated into the theory. In addition, the facings were isotropic with orthotropic cores. They presented several results as a function of imperfection amplitude, wavelength, and core shear flexibility efficiency. They also considered nonshear deformable cores.

Akkas [4] developed a linear theory for shallow spherical and conical shells where emphasis was placed on the conical cap. The boundary value problem associated with an axisymmetrical, asymmetrical, and initial postbuckling behavior of a clamped conical sandwich shell under a uniform pressure with complete structural symmetry were introduced. The results revealed that the buckling and initial postbuckling response of a sandwich cap are similar to the response of a conical homogenious cap.

Rao [83] developed the force-deformation relations of a cylindrically curved symmetric anisotropic sandwich plate utilizing Castigliano's theorem of minimum complementary energy. He then adopted the Raleigh-Ritz method to determine the buckling response of fiber reinforced plastic faced curved sandwich panels under combined axial and bending loads. His results showed that the buckling strength is maximum when the fiber orientation is around 40^o with respect to the circumferential direction. In addition, he showed that the buckling response is very sensitive to the combined effect of low aspect ratio, low radius,, and bending load coefficient. Further work has been developed in Rao and Maeyer-piening [80] where the effect of shear loading has been integrated into the theory. Here they showed the quantitative difference between positive and negative shear buckling loads. In addition they showed that panels of small aspect ratios efficiently carry negative shear loads and those of large aspect ratios are able to carry marginally higher positive shear loads. They finally showed that a fiber orientation angle of 50 degrees measured from the curved edge provides maximum shear buckling strength and that a deeply curved sandwich shell resists larger negative shear loads while shallow shells resist larger positive shear loads.

Kim and Hong [40] developed a linear theory to determine the buckling strengths of unbalanced anisotropic sandwich plates with finite bonding stiffness for simply supported boundary conditions. The theory accounts for dissimilar anisotropic laminated facings and adhesive layers with finite bonding stiffness. As a result, the coupling effects within the facings are accounted for. It was found that the bonding stiffness is critical for sandwich plates composed of thin faces and a stiff core when it is smaller than the threshold value.

In contrast, Pearce and Webber [76] developed a linear theory with similar face sheets as far as symmetry is concerned to determine the buckling strengths of flat sandwich panels with simply supported edge conditions constructed of fiber reinforced laminated facings and a honeycomb core, subjected to compressive edge loadings with the effect of wrinkling included within the theory. They showed that the stiffness of the core has a substantial effect on the critical wrinkling loads. Their theory is developed from an elasticity approach as opposed to an energy approach. In addition they also showed that carbon fiber faced panels can be manufactured lighter than sandwich panels with aluminum alloy facings.

Other significant contributions on the subject matter have been developed by Ko and Jackson [41]. Their work encompassed buckling analysis of flat sandwich panels with anisotropic laminated facings made from metal matrix composites with titanium honeycomb cores under severe thermal environments coupled with inplane compressive edge and shear loadings. Their solution process utilized the Rayleigh-Ritz method. The results showed that slender rectangular sandwich panels have the most advantageous stiffness to weight ratios for aerospace structural applications. In addition it was found that the degradation of the buckling strength under thermal effects was faster in shear than in compression. They also found that the buckling strength was a function of both the loading condition and the panel aspect ratio. Finally, under the same specific weight and panel aspect ratio they showed that metal matrix composite face sheets give higher buckling strengths than the monolithic face sheet counterpart.

In addition to the linear theories a few geometrically nonlinear theories have been developed to aid in the advancement of the theory and application. Ebcioglu [20] developed one of the most comprehensive nonlinear theories for flat sandwich panels encompassing most of the general effects. His theoretical developments were approached from energy variational methods which aided in future refinements of the theory. His theory encompassed sandwich panels with each layer being different in thickness and anisotropic material having one plane of elastic symmetry. Transverse shear, transverse normal strain, inertia effects, and thermal effects are all included within his theory.

Grigoljuk and Chulkov [28] presented a nonlinear theory of sandwich shells where the faces are constructed from different materials and thicknesses but are homogeneous and isotropic in nature. In addition, the Kirchhoff-Love assumptions are introduced into the facings. The core material is considered to be incompressible in the transverse direction exhibiting transversely-isotropic properties. In addition, the inplane displacements are considered to be a function of the transverse coordinate.

Librescu [55] presents a nonlinear theory for anisotropic sandwich plates for both weak and strong cores where he included the body forces, the thermal effects, and the inertia effects. He developed his theory via variational energy methods. In addition, he refines his theory for special simplified cases.

Among all of these nonlinear theories, Fulton [26] presents one of the best developments from a organized well thought out solution process. His approach to the theory and the solution of the governing equations have influenced the developments in this dissertation. His theory was generalized for shallow sandwich shells with dissimilar facesheets both from a geometrical and a material point of view. Hamilton's variational method is used in conjunction with the stress potential method to aid in the solution process. The Extended Galerkin Method is utilized to solve the governing equations. For a comprehensive literature review of sandwich structures see Noor, Burton, and Bert [74].

2 Basic Equations

2.1 Preliminaries and Basic Assumptions

The global middle surface of the structure which is selected to coincide with the middle surface of the core layer, is referred to a curvilinear and orthogonal coordinate system $x_\alpha (\alpha = 1,2)$. The normal coordinate x_3 is considered positive when it is measured in the direction of the downward normal. The uniform thickness of the core is $2\bar{h}$ while those of the bottom and upper faces are h' and h'', respectively. As a result, $H(\equiv h' + 2\bar{h} + h'')$ is the total thickness of the structure. For the sake of identification, unless otherwise specified, the quantities associated with the core will be accompanied by a superposed bar, while those associated with the lower and upper faces by a single and double primes, respectively, placed on the right or left of the

respective quantity. In the forthcoming developments, in addition to the mid-surface of the entire structure(the global midsurface), the mid-surfaces of the upper and lower composite facings will also be considered in the analysis (see Fig. 2.1).

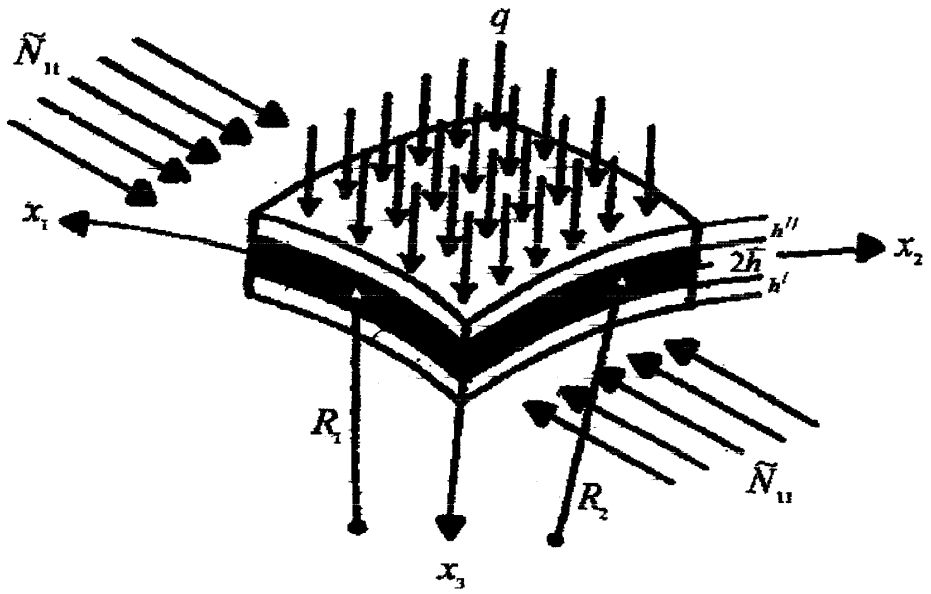

Fig. 2.1. The depiction of a sandwich-shell element.

The geometrically non-linear theory of doubly curved sandwich panels developed herein is based on a number of assumptions, namely:

- The face sheets are constructed of a number of orthotropic material layers, the axes of orthotropy of the individual plies being not necessarily coincident with the geometrical axes x_α of the structure.

- The thickness of the core is much larger than those of the face sheets, i.e., $2\bar{h} \rangle\rangle h', h''$.

- The core material features orthotropic properties, the axes of orthotropy being parallel to the geometrical axes x_α .

- The cases of both the *weak* and *strong* core type sandwich structures are considered. In the former case, the core is capable of carrying transverse shear stresses only, whereas in the latter case, the core can carry both tangential and transverse shear stresses.

- A perfect bonding between the facesheets and between the faces and the core is postulated.

- The core and face layers are incompressible in the transverse normal direction.
- The geometrical non-linearities, in the Von-Karman sense, together with the effect of initial geometric imperfections are included in the model.
- The principles of shallow shell theory are applied in this study.

2.2 Displacement Field

The 3-D displacement field in the facings and the core are represented as

Bottom Face

$$\left.\begin{aligned} {}^{/}V_1(x_\alpha, x_3) &= {}^{/}V_1^{\circ}(x_\alpha) + (x_3 - a^{/})\psi_1^{/}(x_\alpha) \\ {}^{/}V_2(x_\alpha, x_3) &= {}^{/}V_2^{\circ}(x_\alpha) + (x_3 - a^{/})\psi_2^{/}(x_\alpha) \\ {}^{/}V_3(x_\alpha, x_3) &= {}^{/}v_3(x_\alpha) \end{aligned}\right\} \quad (\bar{h} \le x_3 \le \bar{h} + {}^{/}h) \tag{2.1a-c}$$

Core Layer

$$\left.\begin{aligned} \bar{V}_1(x_\alpha, x_3) &= \bar{V}_1^{\circ}(x_\alpha) + x_3\bar{\psi}_1(x_\alpha) \\ \bar{V}_2(x_\alpha, x_3) &= V_2^{\circ}(x_\alpha) + x_3\bar{\psi}_2(x_\alpha) \\ \bar{V}_3(x_\alpha, x_3) &= \bar{v}_3(x_\alpha) \end{aligned}\right\} \quad (-\bar{h} \le x_3 \le \bar{h}) \tag{2.2a-c}$$

Top Face

$$\left.\begin{aligned} {}^{//}V_1(x_\alpha, x_3) &= {}^{//}V_1^{\circ}(x_\alpha) + (x_3 + a^{//})\psi_1^{//}(x_\alpha) \\ {}^{//}V_2(x_\alpha, x_3) &= {}^{//}V_2^{\circ}(x_\alpha) + (x_3 + a^{//})\psi_2^{//}(x_\alpha) \\ {}^{//}V_3(x_\alpha, x_3) &= {}^{//}v_3(x_\alpha) \end{aligned}\right\} \quad (-\bar{h} - h^{//} \le x_3 \le -\bar{h}) \tag{2.3a-c}$$

In these equations, ${}^{/}V_\alpha^{\circ}, \psi_\alpha^{/}, {}^{//}V_\alpha^{\circ}, \psi_\alpha^{//}$, and $\bar{V}_\alpha^{\circ}, \bar{\psi}_\alpha$ denote the tangential displacements and the shear angles of the points of the mid-surface of the bottom and upper faces and of the core,

respectively. In addition, $a'(\equiv \bar{h} + h'/2)$ and $a''(\equiv \bar{h} + h''/2)$ denote the distances between the global mid-surface and the mid-surfaces of the bottom and top facings, respectively.

Fulfillment of the kinematic continuity conditions at the interfaces between the core and the facings is expressed mathematically as

(2.4a-d)

$$ {}^{\prime}V_1\Big|_{x_3=\bar{h}} = \overline{V}_1\Big|_{x_3=\bar{h}} \;,\; {}^{\prime}V_2\Big|_{x_3=\bar{h}} = \overline{V}_2\Big|_{x_3=\bar{h}} \;,\; {}^{\prime\prime}V_1\Big|_{x_3=-\bar{h}} = \overline{V}_1\Big|_{x_3=-\bar{h}} \;,\; {}^{\prime\prime}V_2\Big|_{x_3=-\bar{h}} = \overline{V}_2\Big|_{x_3=-\bar{h}} $$

And when used in conjunction with Eqs. (2.1) - (2.3), results in the following expressions of the 3-D displacement components.

$$ \left.\begin{aligned} {}^{\prime}V_1(x_\alpha, x_3) &= \xi_1(x_\alpha) + \eta_1(x_\alpha) + (x_3 - a^{\prime})\psi_1^{\prime}(x_\alpha) \\ {}^{\prime}V_2(x_\alpha, x_3) &= \xi_2(x_\alpha) + \eta_2(x_\alpha) + (x_3 - a^{\prime})\psi_2^{\prime}(x_\alpha) \\ {}^{\prime}V_3(x_\alpha, x_3) &= v_3(x_\alpha) \end{aligned}\right\} \quad (\bar{h} \le x_3 \le \bar{h} + h^{\prime}) \qquad (2.5a\text{-}c) $$

$$ \left.\begin{aligned} \overline{V}_1(x_\alpha, x_3) &= \xi_1(x_\alpha) - \frac{1}{4}\left[{}^{\prime}h\psi_1^{\prime}(x_\alpha) - {}^{\prime\prime}h\psi_1^{\prime\prime}(x_\alpha)\right] + \\ &\quad + (x_3/\bar{h})\left\{\eta_1(x_\alpha) - \frac{1}{4}\left[{}^{\prime}h\psi_1^{\prime}(x_\alpha) + {}^{\prime\prime}h\psi_1^{\prime\prime}(x_\alpha)\right]\right\} \\ \overline{V}_2(x_\alpha, x_3) &= \xi_2(x_\alpha) - \frac{1}{4}\left[{}^{\prime}h\psi_2^{\prime}(x_\alpha) - {}^{\prime\prime}h\psi_2^{\prime\prime}(x_\alpha)\right] + \\ &\quad + (x_3/\bar{h})\left\{\eta_2(x_\alpha) - \frac{1}{4}\left[{}^{\prime}h\psi_2^{\prime}(x_\alpha) + {}^{\prime\prime}h\psi_2^{\prime\prime}(x_\alpha)\right]\right\} \\ \overline{V}_3(x_{\alpha,}, x_3) &= v_3(x_\alpha) \end{aligned}\right\} \quad (-\bar{h} \le x_3 \le \bar{h}) \qquad (2.6a\text{-}c) $$

$$ \left.\begin{aligned} {}^{\prime\prime}V_1(x_\alpha, x_3) &= \xi_1(x_\alpha) - \eta_1(x_\alpha) + (x_3 + a^{\prime\prime})\psi_1^{\prime\prime}(x_\alpha) \\ {}^{\prime\prime}V_2(x_\alpha, x_3) &= \xi_2(x_\alpha) - \eta_2(x_\alpha) + (x_3 + a^{\prime\prime})\psi_2^{\prime\prime}(x_\alpha) \\ {}^{\prime\prime}V_3(x_\alpha, x_3) &= v_3(x_\alpha) \end{aligned}\right\} \quad (-\bar{h} - {}^{\prime\prime}h \le x_3 \le \bar{h}) \qquad (2.7a\text{-}c) $$

In these equations, the newly defined 2-D tangential displacement measures $\xi_\alpha(x_1, x_2)$ and $\eta_\alpha(x_1, x_2)$ are

$$\begin{aligned} \xi_1 &= \left({}'V_1^\circ + {}''V_1^\circ\right)/2 \quad , \quad \xi_2 = \left({}'V_2^\circ + {}''V_2^\circ\right)/2 \\ \eta_1 &= \left({}'V_1^\circ - {}''V_1^\circ\right)/2 \quad , \quad \eta_2 = \left({}'V_2^\circ - {}''V_2^\circ\right)/2 \end{aligned} \tag{2.8a-d}$$

Hence, it can be seen that the 2-D displacement measures reduce to

$$\xi_1(x_1, x_2),\ \xi_2(x_1, x_2),\ \eta_1(x_1, x_2),\ \eta_2(x_1, x_2),\ v_3(x_1, x_2),\ {}'\psi_1(x_1, x_2),\ {}'\psi_2(x_1, x_2),\ {}''\psi_1(x_1, x_2),\ {}''\psi_2(x_1, x_2)$$

2.3 Strain Displacement Relationships

Assuming that the structure features a stress-free initial geometric imperfection $V_3^\circ\ (\equiv v_3^\circ(x_\alpha))$ and in conjunction with the strain-displacement relationships, in a 3-D space, in the Lagrangian description, adopting the concept of small strains and moderately small rotations [58] and the principles of shallow shell theory, one obtains the 3-D strain quantities in terms of the 2-D strain measures which are expressed as

Bottom facings

$$\begin{aligned} {}'e_{11} &= {}'\varepsilon_{11} + (x_3 - a')\kappa'_{11} \\ {}'e_{22} &= {}'\varepsilon_{22} + (x_3 - a')\kappa'_{22} \qquad (\bar{h} \le x_3 \le \bar{h} + h') \\ 2{}'e_{12} &= {}'\gamma_{12} + (x_3 - a')\kappa'_{12} \\ 2{}'e_{13} &= {}'\gamma_{13}, \quad 2{}'e_{23} = {}'\gamma_{23} \end{aligned} \tag{2.9a-e}$$

Core Layer

$$\begin{aligned} \bar{e}_{11} &= \bar{\varepsilon}_{11} + x_3\bar{\kappa}_{11} \\ \bar{e}_{22} &= \bar{\varepsilon}_{22} + x_3\bar{\kappa}_{22} \qquad \left(-\bar{h} \le x_3 \le \bar{h}\right) \\ 2\bar{e}_{12} &= \bar{\gamma}_{12} + x_3\bar{\kappa}_{12} \\ 2\bar{e}_{13} &= \bar{\gamma}_{13}, \quad 2\bar{e}_{23} = \bar{\gamma}_{23} \end{aligned} \tag{2.10a-e}$$

Upper facings

$$\begin{aligned} {}^{//}e_{11} &= {}^{//}\varepsilon_{11} + (x_3 + a^{//})\kappa^{//}_{11} \\ {}^{//}e_{22} &= {}^{//}\varepsilon_{22} + (x_3 + a^{//})\kappa^{//}_{22} \qquad \left(-\bar{h} - h^{//} \le x_3 \le -\bar{h}\right) \\ 2^{//}e_{12} &= {}^{//}\gamma_{12} + (x_3 + a^{//})\kappa^{//}_{12} \\ 2^{//}e_{13} &= {}^{//}\gamma_{13}, \quad 2^{//}e_{23} = {}^{//}\gamma_{23} \end{aligned} \tag{2.11a-e}$$

In these equations ε_{11}, ε_{22}, $\varepsilon_{12}(\equiv \gamma_{12}/2)$, and $\varepsilon_{13}(\equiv \gamma_{13}/2)$, $\varepsilon_{23}(\equiv \gamma_{23}/2)$ denote the 2-D tangential and the transverse shear strain measures, respectively. Their expressions in terms of the 2-D displacement measures are displayed in Appendix 1.

When the Love-Kirchhoff hypothesis is adopted for both the upper and bottom facings, Eqs. (2.5)-(2.7) can be specialized in the sense of

$$\psi^{/}_{\alpha} = \psi^{//}_{\alpha} = -\partial v_3/\partial x_{\alpha} \tag{2.12}$$

Furthermore, for a symmetric sandwich structure, one should stipulate

$$h^{/} = h^{//} \equiv h, \qquad a^{/} = a^{//}\left(\equiv a\right) = \bar{h} + h/2 \tag{2.13}$$

2.4 Stress-Strain Relationships

It should be recalled that within the 3-D geometrically non-linear elasticity theory, the constitutive equations are described by linear relationships between the second Piola-Kirchhoff

stress and the Lagrange strain tensor components [58]. As a result, for an anisotropic material featuring monoclinic symmetry and the consideration of the temperature and moisture effects, the generalized Hooke's law for a constituent *kth layer* of the bottom face sheets can be expressed as

$$\begin{Bmatrix} {}'S_{11} \\ {}'S_{22} \\ {}'S_{12} \end{Bmatrix}_k = \begin{bmatrix} {}'\hat{Q}_{11} & {}'\hat{Q}_{12} & {}'\hat{Q}_{16} \\ {}'\hat{Q}_{12} & {}'\hat{Q}_{22} & {}'\hat{Q}_{26} \\ {}'\hat{Q}_{16} & {}'\hat{Q}_{26} & {}'\hat{Q}_{66} \end{bmatrix}_k \begin{Bmatrix} {}'e_1 \\ {}'e_2 \\ 2'e_6 \end{Bmatrix} - \begin{Bmatrix} {}'\hat{\lambda}_1 \\ {}'\hat{\lambda}_2 \\ {}'\hat{\lambda}_6 \end{Bmatrix}_k T - \begin{Bmatrix} {}'\hat{\mu}_1 \\ {}'\hat{\mu}_2 \\ {}'\hat{\mu}_6 \end{Bmatrix}_k M \qquad \text{(2.14a,b)}$$

$$\begin{Bmatrix} {}'S_{23} \\ {}'S_{13} \end{Bmatrix}_k = {}'K^2 \begin{bmatrix} {}'Q_{44} & {}'Q_{45} \\ {}'Q_{45} & {}'Q_{55} \end{bmatrix}_k \begin{Bmatrix} 2'e_{23} \\ 2'e_{13} \end{Bmatrix}$$

In these equations, S_{ij} denotes the second Piola-Kirchoff stress tensor,

$\hat{Q}_{ij}\left(\equiv Q_{ij} - \dfrac{Q_{i3}Q_{j3}}{Q_{33}} \right)$ denotes the reduced elastic moduli,

$\hat{\lambda}_J\left(\equiv \lambda_J - \dfrac{Q_{I3}}{Q_{33}}\lambda_{33} \right)$ denotes the reduced thermal moduli,

$\hat{\mu}_J\left(\equiv \mu_J - \dfrac{Q_{I3}}{Q_{33}}\mu_{33} \right)$ denotes the reduced moisture moduli,

and

$T(\equiv T(x_\alpha, x_3))$ and $M(\equiv M(x_\alpha, x_3))$ represent the excess temperature and moisture with respect to the stress free temperature and moisture T_r and M_r, respectively. Herein, the index I takes on the values 1, 2, or 6 when the index J assumes the values 11, 22, or 12, respectively. The generalized Hooke's law for the core and the upper face is obtained by replacing single primes with a superposed bar and double primes, respectively.

An anisotropic material featuring a monoclinic symmetry can be simulated by an orthotropic material whose axes of orthotropy are rotated with respect to the geometrical axes of the

structure. The associated elastic, thermal, and moisture moduli, $\hat{Q}_{ij}$, $\hat{\lambda}_J$, and $\hat{\mu}_J$, respectively, can be expressed in terms of their associated counterparts in the on-axis configuration and the ply-angles by which the principle material axes are rotated with respect to the geometrical ones. These relationships are displayed in Appendix 2.

2.5 Stress and Stress Couple Resultants

Consistent with the concept of shallow shell theory, the stress resultants and stress couples associated with the bottom facings can be represented as

$$\left\{N'_{\alpha\beta}, M'_{\alpha\beta}\right\} = \sum_{k=1}^{n'} \int_{(x_3)_{k-1}}^{(x_3)_k} \left({}'S_{\alpha\beta}\right)_k \left\{1, \left(x_3 - {}'a\right)\right\} dx_3 \tag{2.15a,b}$$

$$N'_{\alpha 3} = \sum_{k=1}^{n'} \int_{(x_3)_{k-1}}^{(x_3)_k} \left({}'S_{\alpha\beta}\right)_k dx_3 \qquad (\alpha, \beta = 1,2)$$

and the ones associated with the core as

$$\left\{\overline{N}_{\alpha\beta}, \overline{M}_{\alpha\beta}\right\} = \int_{-\overline{h}}^{\overline{h}} \overline{S}_{\alpha\beta} \left\{1, x_3\right\} dx_3 \qquad (\alpha, \beta = 1,2) \tag{2.16a,b}$$

$$\overline{N}_{\alpha 3} = \int_{-\overline{h}}^{\overline{h}} \overline{S}_{\alpha\beta} dx_3$$

The stress resultants and stress couples for the upper facings can be obtained from Eqs. (2.15a,b) by replacing single primes by double primes, a' by $-a''$ and n' by n''. Herein, n' and n'' denote the number of constituent layers of the bottom and upper facings, respectively, while $(x_3)_k$ and $(x_3)_{k-1}$ denote the distances from the global reference surface (coinciding with that of

the core layer) to the upper and bottom interfaces of the *kth* layer, respectively. These definitions of the stress and stress couple resultants are similiar to the ones in references [55] and [57].

2.6 Constitutive Equations

Substituting Eqs. (2.14) into Eqs. (2.15) results in the constitutive equations for the bottom face sheets. These expressions are

$$
\begin{aligned}
{}'N_{11} &= A'_{11}\varepsilon'_{11} + A'_{12}\varepsilon'_{22} + A'_{16}\gamma'_{12} + E'_{11}\kappa'_{11} + E'_{12}\kappa'_{22} + E'_{16}\kappa'_{12} \\
&\quad -{}'N^{T}_{11} - {}'N^{m}_{11} \qquad (1 \overrightarrow{\leftarrow} 2) \\
{}'N_{12} &= A'_{16}\varepsilon'_{11} + A'_{26}\varepsilon'_{22} + A'_{66}\gamma'_{12} + E'_{16}\kappa'_{11} + E'_{26}\kappa'_{22} + E'_{66}\kappa'_{12} \\
&\quad -{}'N^{T}_{12} - {}'N^{m}_{12} \\
{}'N_{13} &= {}'K^{2}\left[{}'A_{45}\gamma'_{23} + {}'A_{55}\gamma'_{13}\right] \\
{}'N_{23} &= {}'K^{2}\left[{}'A_{44}\gamma'_{23} + {}'A_{45}\gamma'_{13}\right] \qquad \text{(2.17a-f)} \\
{}'M_{11} &= E'_{11}\varepsilon'_{11} + E'_{12}\varepsilon'_{22} + E'_{16}\gamma'_{12} + F'_{11}\kappa'_{11} + F'_{12}\kappa'_{22} + F'_{16}\kappa'_{12} \\
&\quad -{}'M^{T}_{11} - {}'M^{m}_{11} \qquad (1 \overrightarrow{\leftarrow} 2) \\
{}'M_{12} &= E'_{16}\varepsilon'_{11} + E'_{26}\varepsilon'_{22} + E'_{66}\gamma'_{12} + F'_{16}\kappa'_{11} + F'_{26}\kappa'_{22} + F'_{66}\kappa'_{12} \\
&\quad -{}'M^{T}_{12} - {}'M^{m}_{12}
\end{aligned}
$$

The stiffnesses and the thermal and moisture stress and stress couple resultants appearing in Eqs. (2.17) are defined as

$$
\left\{A'_{\omega\rho}, B'_{\omega\rho}, D'_{\omega\rho}\right\} = \sum_{k=1}^{n'} \int_{(x_3)_{k-1}}^{(x_3)_k} \left(\hat{Q}'_{\omega\rho}\right)_{(k)} \left(1, x_3, x_3^2\right) dx_3 \qquad (\omega, \rho = 1,2,6)
$$

$$A'_{IJ} = {}'K^2 \sum_{k=1}^{n'} \int_{(x_3)_{k-1}}^{(x_3)_k} \left(Q'_{IJ}\right) dx_3 \qquad (I, J = 4,\ 5)$$

$$E'_{\omega\rho} = B'_{\omega\rho} - a' A'_{\omega\rho} \qquad (2.18a\text{-}h)$$

$$F'_{\omega\rho} = D'_{\omega\rho} - 2a' B'_{\omega\rho} + a'^2 A'_{\omega\rho}$$

$${}'N^T_{\alpha\beta} = \sum_{k=1}^{n'} \int_{(x_3)_{k-1}}^{(x_3)_k} \left({}'\hat{\lambda}_{\alpha\beta}\right)_k T dx_3 \qquad (\alpha, \beta = 1,2)$$

$${}'N^m_{\alpha\beta} = \sum_{k=1}^{n'} \int_{(x_3)_{k-1}}^{(x_3)_k} \left({}'\hat{\mu}_{\alpha\beta}\right)_k M dx_3$$

$${}'M^T_{\alpha\beta} = \sum_{k=1}^{n'} \int_{(x_3)_{k-1}}^{(x_3)_k} \left(x_3 - a'\right)\left({}'\hat{\lambda}_{\alpha\beta}\right)_k T dx_3$$

$${}'M^m_{\alpha\beta} = \sum_{k=1}^{n'} \int_{(x_3)_{k-1}}^{(x_3)_k} \left(x_3 - a'\right)\left({}'\hat{\mu}_{\alpha\beta}\right)_k M dx_3$$

If the facesheets feature full symmetry about their respective local mid-surface, $E'_{\omega\rho} \equiv 0$. The expressions of the stiffness quantities, the stress resultants, and the stress couples for the upper facings can be formally obtained from Eqs. (2.17) and (2.18) by replacing single primes by double primes, a' by $-a'$, and n' by n''.

For the core considered as an orthotropic body (the axes of orthotropy coinciding with the geometrical axes), the constitutive equations are given as

$$\overline{N}_{11} = 2\overline{h}\left[\overline{Q}_{11}\overline{\varepsilon}_{11} + \overline{Q}_{12}\overline{\varepsilon}_{12}\right] - \overline{N}^T_{11} - \overline{N}^m_{11} \qquad (1 \overrightarrow{\leftarrow} 2)$$

$$\overline{N}_{12} = 2\overline{h}\,\overline{Q}_{66}\overline{\gamma}_{12}$$

$$\overline{N}_{13} = 2\overline{h}\,\overline{K}^{2}\overline{Q}_{55}\overline{\gamma}_{13} \tag{2.19a-e}$$

$$\overline{M}_{11} = (2/3)\overline{h}^{3}\left[\overline{Q}_{11}\overline{\kappa}_{11} + \overline{Q}_{12}\overline{\kappa}_{22}\right] - \overline{M}_{11}^{T} - \overline{M}_{11}^{m} \qquad (1 \overset{\rightarrow}{\leftarrow} 2)$$

$$\overline{M}_{12} = (2/3)\overline{h}^{3}\overline{Q}_{66}\overline{\kappa}_{12}$$

here the thermal and moisture stress and stress couples are defined as

$$\left(\overline{N}_{\alpha\beta}^{T}, \overline{M}_{\alpha\beta}^{T}\right) = \int_{-\overline{h}}^{\overline{h}} (1, x_3)\overline{\lambda}_{\alpha\beta} T dx_3$$

$$(\alpha, \beta = 1,2) \tag{2.20a,b}$$

$$\left(\overline{N}_{\alpha\beta}^{m}, \overline{M}_{\alpha\beta}^{m}\right) = \int_{-\overline{h}}^{\overline{h}} (1, x_3)\overline{\mu}_{\alpha\beta} M dx_3$$

In Eqs. (2.17), (2.18), and (2.19) $'K^2$ and $\overline{K}^2$ are referred to as the shear correction factors associated with the facings and the core, respectively.

3 Equations of Motion/Equilibrium and Boundary Conditions

3.1 Hamilton's Variational Principle

Hamilton's variational principle is used to derive the equations of motion/equilibrium and the associated boundary conditions of the theory of shallow sandwich shells. Hamilton's variational principle may be stated as

$$\delta J = \delta \int_{t_0}^{t_1} (U - W - T) dt \tag{3.1}$$

where t_0 and t_1 are two arbitrary instants of time, U denotes the strain energy, W denotes the work done by surface tractions, edge loads, and body forces, and T denotes the kinetic energy of the 3-D body of the sandwich structure, while δ denotes the variation sign.

3.2 Strain Energy

The strain energy stored in a 3-D elastic body can be expressed as

$$U = \frac{1}{2}\int_{\tau} \sigma_{ij}\varepsilon_{ij}\, d\tau \tag{3.2}$$

It should be stressed that the total strain energy, in a sandwich structure, is simply a summation of the strain energies in the upper and the lower faces and in the core. As a result, one can express δU as

$$\delta U = \frac{1}{2}\int_{\sigma}\left[\int_{\bar{h}}^{\bar{h}+h'} {}'S_{ij}\delta e'_{ij} + \int_{-\bar{h}}^{\bar{h}} \bar{S}_{ij}\delta\bar{e}_{ij} + \int_{-\bar{h}-h''}^{-\bar{h}} {}''S_{ij}\delta e''_{ij}\right] dx_3 d\sigma \qquad (i, j = 1,2,3) \tag{3.3}$$

Herein, the usual summation convention over a repeated index is employed, S_{ij} denotes the second Piola-Kirchhoff stress tensor and σ denotes the undeformed mid-surface of the sandwich shell. Upon discarding the moisture effects, an alternative form of δU which will prove useful in the next developments is given by

$$\begin{aligned}\delta U = \frac{1}{2}\delta\int_{\sigma}\Bigg\{&\int_{\bar{h}}^{\bar{h}+h'}\left(\hat{Q}'_{\alpha\beta\omega\rho}e'_{\alpha\beta}e'_{\omega\rho} - 2\hat{\lambda}'_{\alpha\beta}Te'_{\alpha\beta}\right)dx_3 + \int_{-\bar{h}-h''}^{\bar{h}}\left(\hat{Q}''_{\alpha\beta\omega\rho}e''_{\alpha\beta}e''_{\omega\rho} - 2\hat{\lambda}''_{\alpha\beta}Te''_{\alpha\beta}\right)dx_3 + \\ &+\int_{-\bar{h}}^{\bar{h}}\left(\underline{\hat{\bar{Q}}_{\alpha\beta\omega\rho}\bar{e}_{\alpha\beta}\bar{e}_{\omega\rho} - 2\hat{\bar{\lambda}}_{\alpha\beta}T\bar{e}_{\alpha\beta}} + \hat{\bar{Q}}_{\alpha 3\omega 3}\bar{e}_{\alpha 3}\bar{e}_{\omega 3}\right)dx_3\Bigg\}d\sigma\end{aligned} \tag{3.4}$$

where the Greek indices assume the values 1 and 2 and the usual summation convention over a repeated index is employed. For the case of the weak core, the underlined term should be discarded. In addition,

$$\hat{Q}_{\alpha\beta\omega\rho}\left(\equiv Q_{\alpha\beta\omega\rho}-\frac{Q_{\alpha\beta 33}Q_{33\omega\rho}}{Q_{3333}}\right) \quad \text{and} \quad \hat{\lambda}_{\alpha\beta}\left(\equiv \lambda_{\alpha\beta}-\frac{Q_{\alpha\beta 33}}{Q_{3333}}\lambda_{33}\right) \tag{3.5a,b}$$

denote the modified elastic moduli and thermal compliance expansion coefficients, respectively. One also assumes that the reduced elastic and thermal coefficients are temperature independent.

3.3 Kinetic Energy

The contribution of kinetic energy in Hamilton's variational principle can be expressed as

$$\int_{t_0}^{t_1}\delta T dt=-\int_{t_0}^{t_1}\left[\int_{\sigma}\left\{\int_{\bar{h}}^{\bar{h}+h'}\rho\ddot{V}_i\delta V_i dx_3+\int_{-\bar{h}}^{\bar{h}}\rho\ddot{V}_i\delta V_i dx_3+\int_{-\bar{h}-h''}^{-\bar{h}}\rho\ddot{V}_i\delta V_i dx_3\right\}d\sigma\right]dt \tag{3.6}$$

Here, in conjunction with Hamilton's condition, $\delta V_i=0$ at $t=t_0,t_1$.

3.4 Work Done by External Loads

The work done by external loads is given as

$$\delta W=\int_{\sigma}\left[\int_{\bar{h}}^{\bar{h}+h'}\rho H_i\delta V_i dx_3+\int_{-\bar{h}}^{\bar{h}}\rho H_i\delta V_i dx_3+\int_{-\bar{h}-h''}^{-\bar{h}}\rho H_i\delta V_i dx_3\right]d\sigma+\int_{\Omega_s}\tilde{S}_i\delta V_i d\Omega \tag{3.7}$$

ρ denotes the mass density, $\tilde{S}_i=\tilde{S}_{ij}n_j$ represents the components of the stress vector prescribed

on the part Ω_s of the external boundary Ω, n_i are the components of the outward unit vector normal to Ω, while H_i denotes the components of the body force vector. The work due to external loadings can be cast as

$$\delta W = \delta W_B + \delta W_E \tag{3.8}$$

where δW_B is the variation in the work due to body forces and δW_E is the variation in the work due to external loadings. The variation in the work due to external loadings can also be expressed as

$$\delta W_E = \delta W_{EL} + \delta W_S \tag{3.9}$$

where δW_{EL} is the variation in the work due to edge loads and δW_S is the variation in the work due to lateral loads. The variation in the work due to lateral loads is given as

$$\delta W_S = \int_0^{l_2} \int_0^{l_1} q_3(x_1, x_2) \delta v_3 dx_1 dx_2 \tag{3.10}$$

The variation in the work due to the edge loads consists of the contributions from both facings and the core. This can be expressed as

$$\delta W_{EL} = \delta W_{EL}^{/} + \delta \overline{W}_{EL} + \delta W_{EL}^{//} \tag{3.11}$$

where each contribution is detailed as

Bottom Facings

$$\delta W_{EL}^{/} = \int_0^{l_1} \left\{ {}^{/}\tilde{N}_{22}\delta {}^{/}V_2^{\circ} + {}^{/}\tilde{N}_{21}\delta {}^{/}V_1^{\circ} + {}^{/}\tilde{N}_{23}\delta {}^{/}V_3 + {}^{/}\tilde{M}_{22}\delta {}^{/}\psi_2 + {}^{/}\tilde{M}_{21}\delta {}^{/}\psi_1 \right\} dx_1 + \int_0^{l_2} \left\{ {}^{/}\tilde{N}_{11}\delta {}^{/}V_1^{\circ} + {}^{/}\tilde{N}_{12}\delta {}^{/}V_2^{\circ} + {}^{/}\tilde{N}_{13}\delta {}^{/}V_3 + {}^{/}\tilde{M}_{11}\delta {}^{/}\psi_1 + {}^{/}\tilde{M}_{12}\delta {}^{/}\psi_2 \right\} dx_2 \tag{3.12}$$

Using the following relations

$$\begin{aligned} {}^{/}V_1^{\circ} &= \xi_1 + \eta_1 \\ {}^{/}V_2^{\circ} &= \xi_2 + \eta_2 \\ {}^{/}V_3 &= \nu_3 \end{aligned} \tag{3.13a-c}$$

The $\delta W_{EL}^{/}$ can be expressed as

(3.14)

$$\delta W_{EL}^{/} = \int_0^{l_1} \left\{ {}^{/}\tilde{N}_{22}\delta\xi_2 + {}^{/}\tilde{N}_{22}\delta\eta_2 + {}^{/}\tilde{N}_{21}\delta\xi_1 + {}^{/}\tilde{N}_{21}\delta\eta_1 + {}^{/}\tilde{N}_{23}\delta\nu_3 + {}^{/}\tilde{M}_{22}\delta\psi_2^{/} + {}^{/}\tilde{M}_{21}\delta\psi_1^{/} \right\} dx_1 + \int_0^{l_2} \left\{ {}^{/}\tilde{N}_{11}\delta\xi_1 + {}^{/}\tilde{N}_{11}\delta\eta_1 + {}^{/}\tilde{N}_{12}\delta\xi_2 + {}^{/}\tilde{N}_{12}\delta\eta_2 + {}^{/}\tilde{N}_{13}\delta\nu_3 + {}^{/}\tilde{M}_{11}\delta\psi_1^{/} + {}^{/}\tilde{M}_{12}\delta\psi_2^{/} \right\} dx_2$$

Core Layer

$$\delta \overline{W}_{EL} = \int_0^{l_1} \left\{ \overline{\tilde{N}}_{22}\delta\overline{V}_2^{\circ} + \overline{\tilde{N}}_{21}\delta\overline{V}_1^{\circ} + \overline{\tilde{N}}_{23}\delta\overline{V}_3 + \overline{\tilde{M}}_{22}\delta\overline{\psi}_2 + \overline{\tilde{M}}_{21}\delta\overline{\psi}_1 \right\} dx_1 + \int_0^{l_2} \left\{ \overline{\tilde{N}}_{11}\delta\overline{V}_1^{\circ} + \overline{\tilde{N}}_{12}\delta\overline{V}_2^{\circ} + \overline{\tilde{N}}_{13}\delta\overline{V}_3 + \overline{\tilde{M}}_{11}\delta\overline{\psi}_1 + \overline{\tilde{M}}_{12}\delta\overline{\psi}_2 \right\} dx_2 \tag{3.15}$$

Using the following relations

$$\begin{aligned}
\overline{V}_1^{\circ} &= \xi_1 - \frac{{}^{/}h}{4}{}^{/}\psi_1 + \frac{{}^{//}h}{4}{}^{//}\psi_1 \\
\overline{V}_2^{\circ} &= \xi_2 - \frac{{}^{/}h}{4}{}^{/}\psi_2 + \frac{{}^{//}h}{4}{}^{//}\psi_2 \\
\overline{\psi}_1 &= \frac{\eta_1}{\overline{h}} - \frac{{}^{/}h}{4\overline{h}}{}^{/}\psi_1 - \frac{{}^{//}h}{4\overline{h}}{}^{//}\psi_1 \\
\overline{\psi}_2 &= \frac{\eta_2}{\overline{h}} - \frac{{}^{/}h}{4\overline{h}}{}^{/}\psi_2 - \frac{{}^{//}h}{4\overline{h}}{}^{//}\psi_2
\end{aligned} \tag{3.16a-d}$$

$\delta\overline{W}_{EL}$ can be cast as

(3.17)

$$\begin{aligned}
\delta\overline{W}_{EL} = \int_0^{l_1} \Bigg\{ & \tilde{\overline{N}}_{22}\delta\xi_2 + \tilde{\overline{N}}_{21}\delta\xi_1 + \frac{\tilde{\overline{M}}_{21}}{\overline{h}}\delta\eta_1 + \frac{\tilde{\overline{M}}_{22}}{\overline{h}}\delta\eta_2 - \left(\tilde{\overline{N}}_{21}\frac{{}^{/}h}{4} + \tilde{\overline{M}}_{21}\frac{{}^{/}h}{4\overline{h}}\right)\delta\psi_1^{/} + \left(\tilde{\overline{N}}_{21}\frac{{}^{//}h}{4}\right. \\
& \left. - \tilde{\overline{M}}_{21}\frac{{}^{//}h}{4\overline{h}}\right)\delta\psi_1^{//} - \left(\tilde{\overline{N}}_{22}\frac{{}^{/}h}{4} + \tilde{\overline{M}}_{22}\frac{{}^{/}h}{4\overline{h}}\right)\delta\psi_2^{/} + \left(\tilde{\overline{N}}_{22}\frac{{}^{//}h}{4} - \tilde{\overline{M}}_{22}\frac{{}^{//}h}{4\overline{h}}\right)\delta\psi_2^{//} + \tilde{\overline{N}}_{23}\delta v_3\Bigg\}dx_1 + \\
& \int_0^{l_2} \Bigg\{ \tilde{\overline{N}}_{12}\delta\xi_2 + \tilde{\overline{N}}_{11}\delta\xi_1 + \frac{\tilde{\overline{M}}_{12}}{\overline{h}}\delta\eta_2 + \frac{\tilde{\overline{M}}_{11}}{\overline{h}}\delta\eta_1 - \left(\tilde{\overline{N}}_{12}\frac{{}^{/}h}{4} + \tilde{\overline{M}}_{12}\frac{{}^{/}h}{4\overline{h}}\right)\delta\psi_2^{/} + \left(\tilde{\overline{N}}_{12}\frac{{}^{//}h}{4} - \right. \\
& \left. \tilde{\overline{M}}_{12}\frac{{}^{//}h}{4\overline{h}}\right)\delta\psi_2^{//} - \left(\tilde{\overline{N}}_{11}\frac{{}^{/}h}{4} + \tilde{\overline{M}}_{11}\frac{{}^{/}h}{4\overline{h}}\right)\delta\psi_1^{/} + \left(\tilde{\overline{N}}_{11}\frac{{}^{//}h}{4} - \tilde{\overline{M}}_{11}\frac{{}^{//}h}{4\overline{h}}\right)\delta\psi_1^{//} + \tilde{\overline{N}}_{13}\delta v_3\Bigg\}dx_2
\end{aligned}$$

Upper Facings

$$\begin{aligned}
\delta^{//}W_{EL} = & \int_0^{l_1} \left\{ {}^{//}\tilde{N}_{22}\delta^{//}V_2^{\circ} + {}^{//}\tilde{N}_{21}\delta^{//}V_1^{\circ} + {}^{//}\tilde{N}_{23}\delta V_3^{//} + {}^{//}\tilde{M}_{22}\delta\psi_2^{//} + {}^{//}\tilde{M}_{21}\delta\psi_1^{//} \right\}dx_1 + \\
& \int_0^{l_2} \left\{ {}^{//}\tilde{N}_{11}\delta^{//}V_1^{\circ} + {}^{//}\tilde{N}_{12}\delta^{//}V_2^{\circ} + {}^{//}\tilde{N}_{13}\delta V_3^{//} + {}^{//}\tilde{M}_{11}\delta\psi_1^{//} + {}^{//}\tilde{M}_{12}\delta\psi_2^{//} \right\}dx_2
\end{aligned} \tag{3.18}$$

Using the following relations

$$
\begin{aligned}
{}^{//}V_1^{\circ} &= \xi_1 - \eta_1 \\
{}^{//}V_2^{\circ} &= \xi_2 - \eta_2 \\
{}^{//}V_3 &= \nu_3
\end{aligned}
\tag{3.19a-c}
$$

$\delta W_{EL}^{//}$ can be modified as

(3.20)

$$
\begin{aligned}
\delta W_{EL}^{//} = &\int_0^{l_1} \left\{ {}^{//}\tilde{N}_{22}\delta\xi_2 - {}^{//}\tilde{N}_{22}\delta\eta_2 + {}^{//}\tilde{N}_{21}\delta\xi_1 - {}^{//}\tilde{N}_{21}\delta\eta_1 + {}^{//}\tilde{N}_{23}\delta\nu_3 + {}^{//}\tilde{M}_{22}\delta\psi_2^{//} + {}^{//}\tilde{M}_{21}\delta\psi_1^{//} \right\} dx_1 \\
&+ \int_0^{l_2} \left\{ {}^{//}\tilde{N}_{11}\delta\xi_1 - {}^{//}\tilde{N}_{11}\delta\eta_1 + {}^{//}\tilde{N}_{12}\delta\xi_2 - {}^{//}\tilde{N}_{12}\delta\eta_2 + {}^{//}\tilde{N}_{13}\delta\nu_3 + {}^{//}\tilde{M}_{11}\delta\psi_1^{//} + {}^{//}\tilde{M}_{12}\delta\psi_2^{//} \right\} dx_2
\end{aligned}
$$

The total variation in the work due to the edge loads can now be expressed as

(3.21)

$$
\begin{aligned}
\delta W_{EL} = &\int_0^{l_1} \left\{ \tilde{N}_{12}\delta\xi_1 + \tilde{N}_{22}\delta\xi_2 + \frac{\hat{\tilde{L}}_{12}}{\bar{h}}\delta\eta_1 + \frac{\hat{\tilde{L}}_{22}}{\bar{h}}\delta\eta_2 - \hat{\tilde{H}}_{12}\delta\psi_1^{/} - \hat{\tilde{H}}_{22}\delta\psi_2^{/} + \hat{\tilde{H}}_{12}\delta\psi_1^{//} + \right. \\
&\left. + \hat{\tilde{H}}_{22}\delta\psi_2^{//} + \tilde{N}_{23}\delta\nu_3 \right\} dx_1 \\
&+ \int_0^{l_2} \left\{ \tilde{N}_{11}\delta\xi_1 + \tilde{N}_{12}\delta\xi_2 + \frac{\hat{\tilde{L}}_{11}}{\bar{h}}\delta\eta_1 + \frac{\hat{\tilde{L}}_{12}}{\bar{h}}\delta\eta_2 - \hat{\tilde{H}}_{11}\delta\psi_1^{/} - \hat{\tilde{H}}_{12}\delta\psi_2^{/} + \hat{\tilde{H}}_{11}\delta\psi_1^{//} \right. \\
&\left. + \hat{\tilde{H}}_{12}\delta\psi_2^{//} + \tilde{N}_{13}\delta\nu_3 \right\} dx_2
\end{aligned}
$$

3.5 Equations of Motion/Equilibrium

3.5.1 The Mixed Formulation

From Eq (3.1), considered in conjunction with Eqs. (3.3) and (3.7), and the strain-displacement relationships, Eqs. (2.9)-(2.11), carrying out the integration with respect to x_3, integrating by parts wherever possible, using the expressions of global stress and stress couple resultants (to be defined later), and invoking the arbitrary and independent character of variations $\delta\xi_1$, $\delta\xi_2$, $\delta\eta_1$, $\delta\eta_2$, $\delta\psi_1^{/}$, $\delta\psi_2^{/}$, $\delta\psi_1^{//}$, $\delta\psi_2^{//}$, and δv_3 the equations of motion/equilibrium and the boundary conditions are derived as

$$
\begin{aligned}
\delta\xi_1 :&\quad N_{11,1} + N_{12,2} = 0 \\
\delta\xi_2 :&\quad N_{22,2} + N_{12,1} = 0 \\
\delta\eta_1 :&\quad L_{11,1} + L_{12,2} - \overline{N}_{13} = 0 \\
\delta\eta_2 :&\quad L_{22,2} + L_{12,1} - N_{13} = 0 \\
\delta\psi_1^{/} :&\quad \hat{H}_{11,1} + \hat{H}_{12,2} + N_{13}^{/} - \left(h^{/}/4\overline{h}\right)\overline{N}_{13} = 0 \\
\delta\psi_2^{/} :&\quad \hat{H}_{22,2} + \hat{H}_{12,1} + N_{23}^{/} - \left(h^{/}/4\overline{h}\right)\overline{N}_{23} = 0 \\
\delta\psi_1^{//} :&\quad \hat{\hat{H}}_{11,1} + \hat{\hat{H}}_{12,2} + N_{13}^{//} + \left(h^{//}/4\overline{h}\right)\overline{N}_{13} = 0 \\
\delta\psi_2^{//} :&\quad \hat{\hat{H}}_{22,2} + \hat{\hat{H}}_{12,1} + N_{23}^{//} - \left(h^{//}/4\overline{h}\right)\overline{N}_{23} = 0 \\
\delta v_3 :&\quad N_{11}\left(v_{3,11} + \overset{\circ}{v}_{3,11} + 1/R_1\right) + 2N_{12}\left(v_{3,12} + \overset{\circ}{v}_{3,12}\right) + N_{22}\left(v_{3,22} + \overset{\circ}{v}_{3,22} + 1/R_2\right) \\
&\quad + N_{13,1} + N_{23,2} + q_3 = m_o\ddot{v}_3
\end{aligned}
\qquad \text{(3.22a-i)}
$$

Herein, $1/R_1$ and $1/R_2$ denote the principal curvatures of the global mid-surface, $(\bullet)_{,\alpha}$ denotes partial differentiation with respect to surface coordinates x_α and q_3 denotes the distributed transversal load. In the above equations of motion/equilibrium only the transverse inertia term was retained. In addition, these equations are expressed in terms of the global stress resultants and stress couple resultants defined as

$$
\begin{aligned}
N_{11} &= N_{11}^{/} + \overline{N}_{11} + N_{11}^{//} && (1\overset{\rightarrow}{\leftarrow}2)\\
N_{12} &= N_{12}^{/} + \overline{N}_{12} + N_{12}^{//}\\
N_{13} &= N_{13}^{/} + \overline{N}_{13} + N_{13}^{//}\\
L_{11} &= \overline{h}\left(N_{11}^{/} - N_{11}^{//}\right) + \overline{M}_{11} && (1\overset{\rightarrow}{\leftarrow}2)\\
L_{12} &= \overline{h}\left(N_{12}^{/} - N_{12}^{//}\right) + \overline{M}_{12}\\
\hat{H}_{11} &= \left(h^{/}/4\right)\left(\overline{N}_{11} + \overline{M}_{11}/\overline{h}\right) - M_{11}^{/} && (1\overset{\rightarrow}{\leftarrow}2)\\
\hat{H}_{12} &= \left(h^{/}/4\right)\left(\overline{N}_{12} + \overline{M}_{12}/\overline{h}\right) - M_{12}^{/}\\
\hat{\hat{H}}_{11} &= \left(h^{//}/4\right)\left(\overline{N}_{11} - \overline{M}_{11}/\overline{h}\right) + M_{11}^{//} && (1\overset{\rightarrow}{\leftarrow}2)\\
\hat{\hat{H}}_{12} &= \left(h^{//}/4\right)\left(\overline{N}_{12} - \overline{M}_{12}/\overline{h}\right) + M_{12}^{//}
\end{aligned}
\qquad \text{(3.23a-i)}
$$

The associated boundary conditions at the edge x_n = constant ($n = 1,2$) result in

$$
\begin{aligned}
N_{nn} &= \tilde{N}_{nn} && \text{or} && \xi_n = \tilde{\xi}_n\\
N_{nt} &= \tilde{N}_{nt} && \text{or} && \xi_t = \tilde{\xi}_t\\
L_{nn} &= \tilde{L}_{nn} && \text{or} && \eta_n = \tilde{\eta}_n\\
L_{nt} &= \tilde{L}_{nt} && \text{or} && \eta_t = \tilde{\eta}_t\\
\hat{H}_{nn} &= \tilde{\hat{H}}_{nn} && \text{or} && \psi_n^{/} = \tilde{\psi}_n^{/}\\
\hat{H}_{nt} &= \tilde{\hat{H}}_{nt} && \text{or} && \psi_t^{/} = \tilde{\psi}_t^{/}\\
\hat{\hat{H}}_{nn} &= \tilde{\hat{\hat{H}}}_{nn} && \text{or} && \psi_n^{//} = \tilde{\psi}_n^{//}\\
\hat{\hat{H}}_{nt} &= \tilde{\hat{\hat{H}}}_{nt} && \text{or} && \psi_t^{//} = \tilde{\psi}_t^{//}\\
\hat{\hat{H}}_{nn} &= \tilde{\hat{\hat{H}}}_{nn} && \text{or} && \psi_n^{//} = \tilde{\psi}_n^{//}\\
\hat{\hat{H}}_{nt} &= \tilde{\hat{\hat{H}}}_{nt} && \text{or} && \psi_t^{//} = \tilde{\psi}_t^{//}\\
N_{nt}\left(v_{3,t} + v_{3,t}^{\circ}\right) + N_{nn}\left(v_{3,n} + v_{3,n}^{\circ}\right) + N_{n3} &= \tilde{N}_{n3} && \text{or} && v_3 = \tilde{v}_3
\end{aligned}
\qquad \text{(3.24a-k)}
$$

Here the subscripts n and t are used to designate the normal and tangential in-plane directions to an edge and hence, $n = 1$ when $t = 2$, and vice-versa. There are nine boundary conditions which means that the governing equations are of the eighteenth order. Several special cases associated with these equations will be displayed next.

Special Cases

Case I) The discarding of transverse shear effects in the facings

In the case of thin facings or when the constituent materials feature large transverse shear characteristics, the Love-Kirchhoff hypothesis can be adopted for the facings. In this case, using the variational principle, Eq. (3.1), in conjunction with Eq. (2.12), the equations of motion/equilibrium become

$$
\begin{aligned}
\delta\xi_1: \quad & N_{11,1} + N_{12,2} = 0 \\
\delta\xi_2: \quad & N_{22,2} + N_{12,1} = 0 \\
\delta\eta_1: \quad & L_{11,1} + L_{12,2} - \overline{N}_{13} = 0 \\
\delta\eta_2: \quad & L_{22,2} + L_{12,1} - \overline{N}_{23} = 0 \\
\delta v_3: \quad & N_{11}\left(v_{3,11} + \overset{\circ}{v}_{3,11} + 1/R_1\right) + 2N_{12}\left(v_{3,12} + \overset{\circ}{v}_{3,12}\right) + N_{22}\left(v_{3,22} + \overset{\circ}{v}_{3,22} + 1/R_2\right) \\
& -C_2\left(\overline{N}_{11,11} + 2\overline{N}_{12,12} + \overline{N}_{22,22}\right) + \left(1 + C_1/\overline{h}\right)\left(\overline{N}_{13,1} + \overline{N}_{23,2}\right) + M_{11,11} + 2M_{12,12} + \\
& + M_{22,22} + q_3 = m_o \ddot{v}_3
\end{aligned}
\tag{3.25a-e}
$$

The associated boundary conditions become

$$
\begin{aligned}
& N_{nn} = \tilde{\overline{N}}_{nn} && \text{or} && \xi_n = \tilde{\overline{\xi}}_n \\
& N_{nt} = \tilde{\overline{N}}_{nt} && \text{or} && \xi_t = \tilde{\overline{\xi}}_t \\
& L_{nn} = \tilde{\overline{L}}_{nn} && \text{or} && \eta_n = \tilde{\overline{\eta}}_n \\
& L_{nt} = \tilde{\overline{L}}_{nt} && \text{or} && \eta_t = \tilde{\overline{\eta}}_t \\
& C_2\overline{N}_{nn} - M_{nn} = C_2\tilde{\overline{N}}_{nn} - \tilde{M}_{nn} && \text{or} && v_{3,n} = \tilde{v}_{3,n} \\
& N_{nt}\left(v_{3,t} + \overset{\circ}{v}_{3,t}\right) + N_{nn}\left(v_{3,n} + \overset{\circ}{v}_{3,n}\right) + M_{nn,n} && \text{or} && v_3 = \tilde{v}_3 \\
& +2M_{nt,t} - C_2\left(\overline{N}_{nn,n} + 2\overline{N}_{nt,t}\right) + \left(1 + C_1/\overline{h}\right)\overline{N}_{n3} = \\
& -C_2\tilde{\overline{N}}_{nt,t} + \tilde{M}_{nt,t} + \tilde{\overline{N}}_{n3}
\end{aligned}
\tag{3.26a-f}
$$

In this case, the global stress and stress couple resultants are reduced to

$$
\begin{aligned}
N_{11} &= N_{11}^{/} + \overline{N}_{11} + N_{11}^{//} \qquad (1\overrightarrow{\leftarrow}2)\\
N_{12} &= N_{12}^{/} + \overline{N}_{12} + N_{12}^{//}\\
N_{13} &= \overline{N}_{13}\\
L_{11} &= \overline{h}\left(N_{11}^{/} - N_{11}^{//}\right) + \overline{M}_{11} \qquad (1\overrightarrow{\leftarrow}2)\\
L_{12} &= \overline{h}\left(N_{12}^{/} - N_{12}^{//}\right) + \overline{M}_{12}\\
M_{11} &= {}^{/}M_{11} + {}^{//}M_{11} - \left(C_1/\overline{h}\right)\overline{M}_{11} \qquad (1\overrightarrow{\leftarrow}2)\\
M_{12} &= {}^{/}M_{12} + {}^{//}M_{12} - \left(C_1/\overline{h}\right)\overline{M}_{12}
\end{aligned}
\tag{3.27a-f}
$$

where

$$
C_1 = \left(h^{/} + h^{//}\right)/4, \qquad C_2 = \left(h^{/} - h^{//}\right)/4 \tag{3.28a,b}
$$

In this case, there are six boundary conditions required at each edge. This reduces the order of the governing equations to the twelfth order.

Case II) Weak(Soft) Core Sandwich Shell with Symmetric Faces

If the core is capable of carrying only transverse shear stresses, $\overline{N}_{\alpha\beta}$ and $\overline{M}_{\alpha\beta}$ become immaterial. In this case, the equations of motion/equilibrium, the stress and stress couple resultants, and the associated boundary conditions can be further simplified. In addition, if the faces are symmetric with respect to the global mid-surface, then $C_1 = h/2$ and $C_2 = 0$. As a result, the equations of motion/equilibrium modify as

$$
\begin{aligned}
\delta\xi_1 &: \quad N_{11,1} + N_{12,2} = 0\\
\delta\xi_2 &: \quad N_{22,2} + N_{12,1} = 0\\
\delta\eta_1 &: \quad L_{11,1} + L_{12,2} - \overline{N}_{13} = 0\\
\delta\eta_2 &: \quad L_{22,2} + L_{12,1} - \overline{N}_{23} = 0
\end{aligned}
\tag{3.29a-e}
$$

$$\delta v_3: \quad N_{11}\left(v_{3,11}+\overset{\circ}{v}_{3,11}+1/R_1\right)+2N_{12}\left(v_{3,12}+\overset{\circ}{v}_{3,12}\right)+$$
$$N_{22}\left(v_{3,22}+\overset{\circ}{v}_{3,22}+1/R_2\right)+\left(1+h/2\bar{h}\right)\left(\overline{N}_{13,1}+\overline{N}_{23,2}\right)+$$
$$M_{11,11}+2M_{12,12}+M_{22,22}+q_3=m_o\ddot{v}_3$$

The associated boundary conditions simplify to

$$\begin{aligned}
N_{nn} &= \tilde{\tilde{N}}_{nn} && \text{or} && \xi_n = \tilde{\tilde{\xi}}_n \\
N_{nt} &= \tilde{\tilde{N}}_{nt} && \text{or} && \xi_t = \tilde{\tilde{\xi}}_t \\
L_{nn} &= \tilde{\tilde{L}}_{nn} && \text{or} && \eta_n = \tilde{\tilde{\eta}}_n \\
L_{nt} &= \tilde{\tilde{L}}_{nt} && \text{or} && \eta_t = \tilde{\tilde{\eta}}_t \\
M_{nn} &= \tilde{\tilde{M}}_{nn} && \text{or} && v_{3,n} = \tilde{\tilde{v}}_{3,n} \\
N_{nt}\left(v_{3,t}+\overset{\circ}{v}_{3,t}\right)+N_{nn}\left(v_{3,n}+\overset{\circ}{v}_{3,n}\right)+M_{nn,n} & && \text{or} && v_3 = \tilde{\tilde{v}}_3 \\
+2M_{nt,t}+\left(1+h/2\bar{h}\right)\overline{N}_{n3} &= \tilde{\tilde{M}}_{nt,t}+\tilde{\tilde{\overline{N}}}_{n3}
\end{aligned} \qquad \text{(3.30a-f)}$$

The global stress and stress couple resultants reduce to

$$\begin{aligned}
N_{11} &= N_{11}^{/}+N_{11}^{//} && (1\overset{\rightarrow}{\leftarrow}2) \\
N_{12} &= N_{12}^{/}+N_{12}^{//} \\
L_{11} &= \bar{h}\left(N_{11}^{/}-N_{11}^{//}\right) && (1\overset{\rightarrow}{\leftarrow}2) \\
L_{12} &= \bar{h}\left(N_{12}^{/}-N_{12}^{//}\right) \\
M_{11} &= M_{11}^{/}+M_{11}^{//} && (1\overset{\rightarrow}{\leftarrow}2) \\
M_{12} &= M_{12}^{/}+M_{12}^{//}
\end{aligned} \qquad \text{(3.31a-f)}$$

At this point it should be recalled that two formulations of governing equations will be presented. One of these is in terms of a Airy's function and three 2-D displacement measures, while the other one is in terms of the 2-D displacement measures. These two formulations will be referred to as the mixed formulation and the displacement formulation, respectively.

3.5.2 The Displacement Formulation

For the purposes of this dissertation, the displacement formulation has been utilized to develop the governing equations for a sandwich structure exhibiting the following properties: The faces are symmetric with respect to their mid-surfaces as well as the global mid-surface, the faces are of an anisotropic material, and the core exhibits the strong type behavior. The thermal terms have also been included for the analysis of the thermomechanical behavior. From Eq. (3.1), considered in conjunction with Eq. (3.4) and Eq. (3.7), using the strain displacement relationships Eqs. (2.9)-(2.11) considered in conjunction with Eqs. (2.12) and (2.13), carrying out the integration with respect to x_3 and integrating by parts wherever feasible utilizing Eqs. (2.18), and invoking the independent character of variations $\delta\xi_1$, $\delta\xi_2$, $\delta\eta_1$, $\delta\eta_2$, δv_3, the governing equations in terms of displacement quantities are obtained as

(3.32a)

$\delta\xi_1$:

$$\Lambda_{11}\left\{\xi_{1,11}+v_{3,1}v_{3,11}+\overset{\circ}{v}_{3,11}v_{3,1}+\overset{\circ}{v}_{3,1}v_{3,11}-(1/R_1)v_{3,1}\right\}+\Lambda_{66}\left\{\xi_{1,22}+\xi_{2,12}+v_{3,2}v_{3,12}+\right.$$
$$+v_{3,1}v_{3,22}+v_{3,2}\overset{\circ}{v}_{3,12}+\overset{\circ}{v}_{3,1}v_{3,22}+\overset{\circ}{v}_{3,2}v_{3,12}+v_{3,1}\overset{\circ}{v}_{3,22}\left.\right\}+\Lambda_{12}\left\{\xi_{2,12}+v_{3,2}v_{3,12}+v_{3,2}\overset{\circ}{v}_{3,12}\right.$$
$$+\overset{\circ}{v}_{3,2}v_{3,12}-(1/R_2)v_{3,1}\left.\right\}-A_{16}\left\{2\xi_{1,12}+\xi_{2,11}+2v_{3,1}v_{3,12}+2v_{3,1}\overset{\circ}{v}_{3,12}+2\overset{\circ}{v}_{3,1}v_{3,12}+v_{3,2}v_{3,11}\right.$$
$$+v_{3,2}\overset{\circ}{v}_{3,11}+\overset{\circ}{v}_{3,2}v_{3,11}-(1/R_1)v_{3,2}\left.\right\}-A_{26}\left\{\xi_{2,22}+v_{3,2}v_{3,22}+v_{3,2}\overset{\circ}{v}_{3,22}+\overset{\circ}{v}_{3,2}v_{3,22}-\right.$$
$$\left.(1/R_2)v_{3,2}\right\}-N^T_{11,1}-N^T_{12,2}=0$$

(3.32b)

$\delta\xi_2$:

$$\Lambda_{22}\left\{\xi_{2,22}+v_{3,2}v_{3,22}+\overset{\circ}{v}_{3,22}v_{3,2}+\overset{\circ}{v}_{3,2}v_{3,22}-(1/R_2)v_{3,2}\right\}+\Lambda_{66}\left\{\xi_{2,11}+\xi_{1,12}+v_{3,1}v_{3,12}+\right.$$
$$+v_{3,2}v_{3,11}+v_{3,1}\overset{\circ}{v}_{3,12}+\overset{\circ}{v}_{3,2}v_{3,11}+\overset{\circ}{v}_{3,1}v_{3,12}+v_{3,2}\overset{\circ}{v}_{3,11}\left.\right\}+\Lambda_{12}\left\{\xi_{1,12}+v_{3,1}v_{3,12}+v_{3,1}\overset{\circ}{v}_{3,12}+\right.$$
$$+\overset{\circ}{v}_{3,1}v_{3,12}-(1/R_1)v_{3,2}\left.\right\}-A_{26}\left\{2\xi_{2,12}+\xi_{1,22}+2v_{3,2}v_{3,12}+2v_{3,2}\overset{\circ}{v}_{3,12}+2\overset{\circ}{v}_{3,2}v_{3,12}+v_{3,1}v_{3,22}\right.$$
$$+v_{3,1}\overset{\circ}{v}_{3,22}+\overset{\circ}{v}_{3,1}v_{3,22}-(1/R_2)v_{3,1}\left.\right\}-A_{16}\left\{\xi_{1,11}+v_{3,1}v_{3,11}+v_{3,1}\overset{\circ}{v}_{3,11}+\overset{\circ}{v}_{3,1}v_{3,11}-\right.$$
$$\left.(1/R_1)v_{3,1}\right\}-N^T_{22,2}-N^T_{12,1}=0$$

(3.32c)

$\delta\eta_1$:

$$\hat{\Lambda}_{11}\eta_{1,11}+\frac{h\bar{h}\overline{Q}_{11}}{3}v_{3,111}+\hat{\Lambda}_{66}\{\eta_{1,22}+\eta_{2,12}\}+\frac{2h\bar{h}\overline{Q}_{66}}{3}v_{3,122}+\hat{\Lambda}_{12}\eta_{2,12}+\frac{h\bar{h}\overline{Q}_{12}}{3}v_{3,122}+$$
$$A_{16}\{2\eta_{1,12}+\eta_{2,11}\}+A_{26}\eta_{2,22}-d_1\{\eta_1+av_{3,1}\}-(1/\bar{h})\hat{N}^T_{11,1}-(1/\bar{h})\hat{N}^T_{12,2}=0$$

(3.32d)

$\delta\eta_2$:

$$\hat{\Lambda}_{22}\eta_{2,22}+\frac{h\bar{h}\overline{Q}_{22}}{3}v_{3,222}+\hat{\Lambda}_{66}\{\eta_{2,11}+\eta_{1,12}\}+\frac{2h\bar{h}\overline{Q}_{66}}{3}v_{3,112}+\hat{\Lambda}_{12}\eta_{1,12}+\frac{h\bar{h}\overline{Q}_{12}}{3}v_{3,112}+$$
$$A_{26}\{2\eta_{2,12}+\eta_{1,22}\}+A_{16}\eta_{1,11}-d_2\{\eta_2+av_{3,2}\}-(1/\bar{h})\hat{N}^T_{2,22}-(1/\bar{h})\hat{N}^T_{12,1}=0$$

(3.32e)

δv_3:

$$\Lambda_{11}\Big\{\xi_{1,1}v_{3,11}+\xi_{1,1}v^{\circ}_{3,11}+(1/2)v^2_{3,1}v_{3,11}+(1/2)v^{\circ}_{3,11}v^2_{3,1}+v^{\circ}_{3,1}v^{\circ}_{3,11}v_{3,1}+v^{\circ}_{3,1}v_{3,1}v_{3,11}+(1/R_1)\Big[\xi_{1,1}+$$
$$+(1/2)v^2_{3,1}+v^{\circ}_{3,1}v_{3,1}-v_3v_{3,11}-v_3v^{\circ}_{3,11}-v_3/R_1\Big]\Big\}-\frac{h\bar{h}\overline{Q}_{11}}{3}\{\eta_{1,111}+(h/2)v_{3,1111}\}+\Lambda_{22}\{\xi_{2,2}v_{3,22}+$$
$$\xi_{2,2}v^{\circ}_{3,22}+(1/2)v^2_{3,2}v_{3,22}+(1/2)v^{\circ}_{3,22}v^2_{3,2}+v^{\circ}_{3,2}v^{\circ}_{3,22}v_{3,2}+v^{\circ}_{3,2}v_{3,2}v_{3,22}+(1/R_2)\Big[\xi_{2,2}+(1/2)v^2_{3,2}+$$
$$2v^{\circ}_{3,1}v_{3,1}v_{3,12}+2v^{\circ}_{3,1}v_{3,1}v^{\circ}_{3,12}+(1/R_1)\Big[\xi_{1,2}+\xi_{2,1}+v_{3,1}v_{3,2}+v^{\circ}_{3,1}v_{3,2}+v_{3,1}v^{\circ}_{3,2}-2v_3v_{3,12}-2v_3v^{\circ}_{3,12}\Big]\Big\}$$
$$+A_{26}\Big\{2\xi_{2,2}v_{3,12}+2\xi_{2,2}v^{\circ}_{3,12}+\xi_{1,2}v_{3,22}+\xi_{2,1}v_{3,22}+\xi_{1,2}v^{\circ}_{3,22}+\xi_{2,1}v^{\circ}_{3,22}+v_{3,12}v^2_{3,2}+v^{\circ}_{3,12}v^2_{3,2}+$$
$$v^{\circ}_{3,2}v_{3,2}-v_3v_{3,22}-v_3v^{\circ}_{3,22}-v_3/R_2\Big]\Big\}-\frac{h\bar{h}\overline{Q}_{22}}{3}\{\eta_{2,222}+(h/2)v_{3,2222}\}+\Lambda_{66}\{2\xi_{1,2}v_{3,12}+2\xi_{2,1}v_{3,12}$$
$$+\ 2\xi_{1,2}v^{\circ}_{3,12}+2\xi_{2,1}v^{\circ}_{3,12}+2v_{3,1}v_{3,2}v_{3,12}+2v_{3,1}v_{3,2}v^{\circ}_{3,12}+2v^{\circ}_{3,1}v_{3,2}v_{3,12}+2v_{3,1}v^{\circ}_{3,2}v_{3,12}+$$
$$2v_{3,1}v^{\circ}_{3,2}v^{\circ}_{3,12}+2v^{\circ}_{3,1}v_{3,2}v^{\circ}_{3,12}\Big\}-\frac{2h\bar{h}\overline{Q}_{66}}{3}\Big\{\eta_{1,122}++\eta_{2,112}+hv_{3,1122}\Big\}+\Lambda_{12}\Big\{\xi_{1,1}v_{3,22}+\xi_{1,1}v^{\circ}_{3,22}+$$
$$\xi_{2,2}v_{3,11}+\xi_{2,2}v^{\circ}_{3,11}+(1/2)v_{3,11}v^2_{3,2}+(1/2)v_{3,22}v^2_{3,1}+(1/2)v^{\circ}_{3,22}v^2_{3,1}+(1/2)v^{\circ}_{3,11}v^2_{3,2}++v^{\circ}_{3,1}v_{3,1}v_{3,22}$$
$$+v^{\circ}_{3,2}v_{3,2}v_{3,11}+v^{\circ}_{3,1}v_{3,1}v^{\circ}_{3,22}+v^{\circ}_{3,2}v_{3,2}v^{\circ}_{3,11}+(1/R_1)\Big[\xi_{2,2}+(1/2)v^2_{3,2}+v_{3,2}v^{\circ}_{3,2}-v_3v_{3,22}-v_3v^{\circ}_{3,22}\Big]$$
$$+(1/R_2)\Big[\xi_{1,1}+(1/2)v^2_{3,1}+v_{3,1}v^{\circ}_{3,1}-v_3v_{3,11}-v_3v^{\circ}_{3,11}\Big]-\frac{2v_3}{R_1R_2}\Big\}-\frac{h\bar{h}\overline{Q}_{12}}{3}\{\eta_{1,122}+\eta_{2,112}+$$

$$(h/2)v_{3,1122}\Big\} + A_{16}\Big\{2\xi_{1,1}v_{3,12} + 2\xi_{1,1}\overset{\circ}{v}_{3,12} + \xi_{1,2}v_{3,11} + \xi_{2,1}v_{3,11} + \xi_{1,2}\overset{\circ}{v}_{3,11} + \xi_{2,1}\overset{\circ}{v}_{3,11} + v_{3,12}v_{3,1}^2 +$$
$$\overset{\circ}{v}_{3,12}v_{3,1}^2 + v_{3,1}v_{3,2}v_{3,11} + v_{3,1}v_{3,2}\overset{\circ}{v}_{3,11} + \overset{\circ}{v}_{3,1}v_{3,2}v_{3,11} + v_{3,1}\overset{\circ}{v}_{3,2}v_{3,11} + \overset{\circ}{v}_{3,1}v_{3,2}\overset{\circ}{v}_{3,11} + v_{3,1}\overset{\circ}{v}_{3,2}\overset{\circ}{v}_{3,11} +$$
$$v_{3,1}v_{3,2}v_{3,22} + \overset{\circ}{v}_{3,1}v_{3,2}v_{3,22} + v_{3,1}\overset{\circ}{v}_{3,2}v_{3,22} + v_{3,1}v_{3,2}\overset{\circ}{v}_{3,22} + \overset{\circ}{v}_{3,1}v_{3,2}\overset{\circ}{v}_{3,22} + v_{3,1}\overset{\circ}{v}_{3,2}\overset{\circ}{v}_{3,22} + 2\overset{\circ}{v}_{3,2}v_{3,2}v_{3,12}$$
$$+2\overset{\circ}{v}_{3,2}v_{3,2}\overset{\circ}{v}_{3,12} + (1/R_2)\Big[\xi_{1,2} + \xi_{2,1} + v_{3,1}v_{3,2} - F_{11}v_{3,1111} + \overset{\circ}{v}_{3,1}v_{3,2} + v_{3,1}\overset{\circ}{v}_{3,2} - 2v_3v_{3,12} - 2v_3\overset{\circ}{v}_{3,12}\Big]\Big\}$$
$$-F_{22}v_{3,2222} - 2F_{12}v_{3,1122} - 4F_{16}v_{3,1112} - 4F_{26}v_{3,1222} - 4F_{66}v_{3,1122} + d_1a\Big\{\eta_{1,1} + av_{3,11}\Big\} + d_2a\Big\{\eta_{2,2} +$$
$$av_{3,22}\Big\} + q_3 - N_{11}^T\Big\{v_{3,11} + \overset{\circ}{v}_{3,11} + (1/R_1)\Big\} - N_{22}^T\Big\{v_{3,22} + \overset{\circ}{v}_{3,22} + (1/R_2)\Big\} - 2N_{12}^T\Big\{v_{3,12} + \overset{\circ}{v}_{3,12}\Big\} -$$
$$N_{11,1}^T\Big\{v_{3,1} + \overset{\circ}{v}_{3,1}\Big\} - N_{22,2}^T\Big\{v_{3,2} + \overset{\circ}{v}_{3,2}\Big\} - N_{12,1}^T\Big\{v_{3,2} + \overset{\circ}{v}_{3,2}\Big\} - N_{12,2}^T\Big\{v_{3,1} + \overset{\circ}{v}_{3,1}\Big\} - \hat{M}_{11,1}^T - \hat{M}_{22,2}^T$$
$$-2\hat{M}_{12,12}^T = 0$$

It should also be noted that the fifth equilibrium equation, Eq. (3.32e) has been simplified with the use of the first two equilibrium equations, Eqs. (3.32a,b). This has been accomplished from the fact that the first two equilibrium equations can be identified in the last equilibrium equation. Since these equilibrium equations are homogeneous, this results in all of the terms contained within these two equilibrium equations summing to zero. It should also be mentioned that Eq. (3.32e) contains terms involving the squares of the imperfection. For the case of small imperfections, which is usually the case, these terms can be discarded. The associated boundary conditions are:

$$\begin{aligned}
&N_{nn} = \tilde{N}_{nn} && \text{or} && \xi_n = \tilde{\xi}_n \\
&N_{nt} = \tilde{N}_{nt} && \text{or} && \xi_t = \tilde{\xi}_t \\
&L_{nn} = \tilde{L}_{nn} && \text{or} && \eta_n = \tilde{\eta}_n \\
&L_{nt} = \tilde{L}_{nt} && \text{or} && \eta_t = \tilde{\eta}_t \\
&M_{nn} = \tilde{M}_{nn} && \text{or} && v_{3,n} = \tilde{v}_{3,n} \\
&N_{nt}\left(v_{3,t} + \overset{\circ}{v}_{3,t}\right) + N_{nn}\left(v_{3,n} + \overset{\circ}{v}_{3,n}\right) + M_{nn,n} + && \text{or} && v_3 = \tilde{v}_3 \\
&2M_{nt,t} + (a/\bar{h})\bar{N}_{n3} = \tilde{M}_{nt,t} + \tilde{\bar{N}}_{n3}
\end{aligned} \qquad \text{(3.33a-f)}$$

The stiffness coefficients appearing in the equilibrium equations are defined as

$$
\begin{aligned}
\Lambda_{11} &= A_{11} + 2\bar{h}\,\overline{Q}_{11} \qquad (1^{\rightarrow}_{\leftarrow}2)\\
\Lambda_{12} &= A_{12} + 2\bar{h}\,\overline{Q}_{12}\\
\Lambda_{66} &= A_{66} + 2\bar{h}\,\overline{Q}_{66}\\
\hat{\Lambda}_{11} &= A_{11} + \left(2\bar{h}/3\right)\overline{Q}_{11} \qquad (1^{\rightarrow}_{\leftarrow}2)\\
\hat{\Lambda}_{12} &= A_{12} + \left(2\bar{h}/3\right)\overline{Q}_{12}\\
\hat{\Lambda}_{66} &= A_{66} + \left(2\bar{h}/3\right)\overline{Q}_{66}
\end{aligned}
\tag{3.34a-f}
$$

where the global mechanical stiffness measures are defined as

$$
\begin{aligned}
A_{\omega\rho} &= {}^{/}A_{\omega\rho} + {}^{//}A_{\omega\rho} \qquad (\omega,\rho = 1,\ 2,\ 6)\\
F_{\omega\rho} &= {}^{/}F_{\omega\rho} + {}^{//}F_{\omega\rho}
\end{aligned}
\tag{3.35a,b}
$$

If both the upper and bottom face sheets are symmetric with respect to their local and global mid-surfaces, then

$$
\begin{aligned}
{}^{/}A_{\omega\rho} &= {}^{//}A_{\omega\rho}\\
{}^{/}F_{\omega\rho} &= {}^{//}F_{\omega\rho}
\end{aligned}
\tag{3.36a,b}
$$

The global thermal stress and stress couple resultants appearing in the governing equations are defined as

$$
\begin{aligned}
N_{11}^{T} &= {}^{/}N_{11}^{T} + \overline{N}_{11}^{T} + {}^{//}N_{11}^{T} \qquad (1^{\rightarrow}_{\leftarrow}2)\\
N_{12}^{T} &= {}^{/}N_{12}^{T} + {}^{//}N_{12}^{T}\\
\hat{N}_{11}^{T} &= \bar{h}\left({}^{/}N_{11}^{T} - {}^{//}N_{11}^{T}\right) \qquad (1^{\rightarrow}_{\leftarrow}2)\\
\hat{N}_{12}^{T} &= \bar{h}\left({}^{/}N_{12}^{T} - {}^{//}N_{12}^{T}\right)\\
\hat{M}_{11}^{T} &= {}^{/}M_{11}^{T} + {}^{//}M_{11}^{T} - \left(h/2\bar{h}\right)\overline{M}_{11}^{T} \qquad (1^{\rightarrow}_{\leftarrow}2)\\
\hat{M}_{12}^{T} &= {}^{/}M_{12}^{T} + {}^{//}M_{12}^{T}
\end{aligned}
\tag{3.37a-f}
$$

and

$$d_1 = \frac{2\overline{K}^2 G_{13}}{\overline{h}} \qquad (1\overrightarrow{\leftarrow}2) \qquad (3.38)$$

A more direct method to obtain the governing equations in terms of displacements consists of expressing the global stress and stress couple resultants in terms of displacements and then substituting these expressions into the equations of equilibrium.

3.6 Boundary Conditions

The case of simply supported boundary conditions on all four edges will be considered next. Having in view, that in geometrically nonlinear problems of plates and shells the bending and stretching problems are coupled, the boundary conditions concern both bending and tangential contributions. The formulation of the tangential boundary conditions gives rise to two tangential types of boundary conditions, which are movable and immovable edge conditions. These correspond to the cases when the motion of the unloaded edges is either unrestrained or completely restrained, respectively, in the plane tangent to the structure's midsurface, normal to the respective edge. As a result, the following two cases become apparent.

Case I) *The edges* $x_n = \text{const}$ *are loaded in compression and freely movable.* In this case, along these edges, the following conditions have to be fulfilled.

$$N_{nn} = -\tilde{N}_{nn}, \quad N_{nt} = 0, \quad \eta_n = 0, \quad \eta_{\mathrm{t}} = 0, \quad M_{nn} = 0, \quad v_3 = 0 \qquad (3.39)$$

Case II) *The edges* $x_n = \text{const}$ *are unloaded and immovable.* In this case, along these edges, the following conditions have to be fulfilled.

$$\xi_n = 0, \quad N_{nt} = 0, \quad \eta_n = 0, \quad \eta_{\mathrm{t}} = 0, \quad M_{nn} = 0, \quad v_3 = 0 \qquad (3.40)$$

As stated earlier, the subscripts n and t are used to designate the normal and tangential in-plane directions to an edge and hence, $n = 1$ when $t = 2$, and vice-versa.

The condition expressing the immovability of the edges, $\xi_n = 0$ on , is fulfilled in an average sense expressed as

$$\int_0^{L_2} \int_0^{L_1} \frac{\partial \xi_n}{\partial x_n} dx_n dx_t = 0 \tag{3.41}$$

This condition, in conjunction with the expression for $\varepsilon_{11}^{/}$ and $\varepsilon_{11}^{//}$, Eqs. (5.2a) and (5.4a), and in conjunction with the constitutive equations provides the fictious edge load $\tilde{N}_{nn}$ rendering the edges $x_n = \text{const}$, immovable.

In addition, the following tangential static boundary conditions, Eqs. (3.39a,b) and (3.40b) are fulfilled in an average sense. These are expressed as

$$\int_0^{L_t} N_{nn} dx_t = -\tilde{N}_{nn} L_n$$

$$\begin{pmatrix} n = 1,\ 2 \\ \mathrm{t} = 2,\ 1 \end{pmatrix} \qquad \sum_{n,t} , \tag{3.42a,b}$$

$$\int_0^{L_t} N_{nt} dx_t = 0$$

where $\tilde{N}_{nn}$ denote the compressive edge loads on the edges $x_n = 0,\ L_n$. The sign $\sum_{n,t}$ indicates no summation over the indices n and t.

4 The Thermomechanical Postbuckling Solution of the Governing Equations

The basic equations necessary for the thermomechanical postbuckling solution have been presented except for the compatibility equation. The next task is to solve the equations to generate the postbuckling solution. The method of solution is different for each of the two formulations. It should be mentioned that for this case within the mixed formulation the temperature effects have been neglected. For this case only the mechanical postbuckling solution

is presented. This results from the mathematical limitations on the use of the stress potential method. Since all of the general effects can be introduced with the use of the displacement formulation, the desired temperature effects have been included in this formulation.

4.1 Airy's Potential Function Involving the Mixed Formulation

A representation of the governing equations most suitable for the buckling and postbuckling of sandwich shell type structures for the case of a weak core with cross-ply laminated faces being both symmetric with respect to both their local midsurfaces and the global mid-surface will be utilized. This representation can be seen as a generalization for the case of sandwich shells used in the case of shear deformable shallow shell theory [59] as well for flat sandwich structures [55]. For the case considered here, the representation is presented in terms of the Airy's potential function $\phi(x_1, x_2)$, the transverse displacement v_3, and the displacement measures η_1 and η_2. The Extended Galerkin Method will be the chosen method to arrive at a postbuckling solution. The Extended Galerkin Method consists of retaining the unfulfilled equation(s) of motion/equilibrium and the boundary terms in the energy functional, substituting in the appropriate functions in which the unfulfilled equations of motion/equilibrium and boundary terms are expressed in terms of, multiplying by the variation in the coefficients of each of the unfulfilled expressions, and finally, integrating over the domain. The advantage in using the Extended Galerkin Method consists of the compensation of the non-fulfillment of static boundary conditions via retaining these in the energy functional.

The equilibrium Eqs. (3.29a,b) can be fulfilled by expressing the stress resultants in terms of the Airy's potential function $\phi(\equiv \phi(x_\omega))$ in the following form

$$N_{\alpha\beta} = c_{\alpha\omega} c_{\beta\rho} \phi_{,\omega\rho} \tag{4.1}$$

where $c_{\alpha\beta}$ denotes the 2-D permutation symbol. The first two equilibrium equations being eliminated establishes a need for a compatibility equation involving the tangential strain measures to be established and fulfilled. By eliminating the displacements from the strain displacement relationships, a compatibility equation can be obtained. For weak core doubly curved sandwich panels this equation is

$$\varepsilon_{11,22} + \varepsilon_{22,11} - \gamma_{12,12} + (2/R_1)v_{3,22} + (2/R_2)v_{3,11} - 2v_{3,12}^2 + 2v_{3,11}v_{3,22} + 2v_{3,11}^{\circ}v_{3,22} - 4v_{3,12}v_{3,12}^{\circ} + 2v_{3,11}v_{3,22}^{\circ} = 0 \tag{4.2}$$

where

$$\varepsilon_{11} = {}^{/}\varepsilon_{11} + {}^{//}\varepsilon_{11}, \quad \varepsilon_{22} = {}^{/}\varepsilon_{22} + {}^{//}\varepsilon_{22}, \quad \gamma_{12} = {}^{/}\gamma_{12} + {}^{//}\gamma_{12} \tag{4.3a-c}$$

By performing a partial inversion of the constitutive equations, Eqs. (2.18a,b), Eq. (4.2) can be expressed in terms of the basic functions mentioned above. Having this in view these formulations considered in conjunction with Eq (4.1) , the compatibility equation can be expressed as

$$\begin{aligned} &A_{22}^{*}\phi_{,1111} + A_{11}^{*}\phi_{,2222} + (A_{66}^{*} + 2A_{12}^{*})\phi_{,1122} + (2/R_1)v_{3,22} + (2/R_2)v_{3,11} - 2v_{3,12}^{2} + 2v_{3,11}v_{3,22} + \\ &2v_{3,11}^{\circ}v_{3,22} + 2v_{3,11}v_{3,22}^{\circ} - 4v_{3,12}v_{3,12}^{\circ} = 0 \end{aligned} \tag{4.4}$$

where the stiffness quantities $A_{\alpha\beta}^{*}$ represent the inverted counterparts of $A_{\alpha\beta}$. The remaining three equilibrium equations, Eqs. (3.29c,d,e) expressed in terms of $\phi,\ \eta_1,\ \eta_2,$ and v_3 appear as follows

(4.5a-c)

$$A_{11}\eta_{1,11} + A_{16}\eta_{2,11} + A_{66}\eta_{1,22} + (A_{12} + A_{66})\eta_{2,12} + 2A_{16}\eta_{1,12} + A_{26}\eta_{2,22} - d_1(\eta_1 + av_{3,1}) = 0$$

$$A_{22}\eta_{2,22} + A_{26}\eta_{1,22} + A_{66}\eta_{2,11} + (A_{12} + A_{66})\eta_{1,12} + 2A_{26}\eta_{2,12} + A_{16}\eta_{1,11} - d_2(\eta_2 + av_{3,2}) = 0$$

$$\begin{aligned} &\phi_{,22}(v_{3,11} + v_{3,11}^{\circ} + 1/R_1) - 2\phi_{,12}(v_{3,12} + v_{3,12}^{\circ}) + \phi_{,11}(v_{3.22} + v_{3,22}^{\circ} + 1/R_2) - F_{11}v_{3,1111} - \\ &2(F_{12} + 2F_{66})v_{3,1122} - F_{22}v_{3,2222} + d_1a(\eta_{1,1} + av_{3,11}) + d_2a(\eta_{2,2} + av_{3,22}) + q_3 = 0 \end{aligned}$$

Within the mixed formulation, eqs (4.4) and (4.5a-c) constitute the governing system of equations. To facilitate the solution process of this governing system of equations, the expression for the transverse deflection for simply supported boundary conditions satisfying the boundary condition $v_3 = 0$ can be assumed in the following form

$$v_3(x_1, x_2) = w_{mn} \sin\lambda_m x_1 \sin\mu_n x_2 \tag{4.6}$$

where $\lambda_m = m\pi/L_1$, $\mu_n = n\pi/L_2$, w_{mn} are the modal amplitudes, and L_1 and L_2 are the panel side

edges. The representation of the initial geometric imperfection for the most critical postbuckling conditions can be expressed as

$$v_3^{\circ}(x_1, x_2) = w_{mn}^{\circ} \sin \lambda_m x_1 \sin \mu_n x_2 \tag{4.7}$$

where w_{mn}° are the modal amplitudes of the initial geometric imperfection shape. As in the Navier type solution, the transversal load q_3 can be represented as

$$q_3(x_1, x_2) = q_{mn} \sin \lambda_m x_1 \sin \mu_n x_2 \tag{4.8}$$

Moreover, the Airy's potential function can be expressed as [54,55]

$$\phi(x_\alpha) = \phi_1(x_\alpha) - \frac{1}{2}(\tilde{N}_{11} x_2^2 + \tilde{N}_{22} x_1^2 - 2\tilde{N}_{12} x_1 x_2) \tag{4.9}$$

where $\tilde{N}_{11}$, $\tilde{N}_{22}$, and $\tilde{N}_{12}$ represent the average compressive and shear edge loads and ϕ_1 represents a particular solution of Eq (4.4). From this point forward, $\tilde{N}_{12}$ will be excluded from any further analysis since the primary concern is uniaxial and biaxial compressive edge loadings. Substituting Eqs. (4.6), (4.7), and (4.9) into Eq (4.4), and solving the non-homogeneous partial differential equation, following a similar procedure as presented in [55,58], yields the expression for ϕ_1 as

$$\phi_1(x_\alpha) = A_1 \cos 2\lambda_m x_1 + A_2 \cos 2\mu_n x_2 + A_3 \sin \lambda_m x_1 \sin \mu_n x_2 \tag{4.10}$$

where the coefficients A_α and A_3 are determined as

$$A_\alpha = \tilde{A}_\alpha (w_{mn}^2 + 2 w_{mn} w_{mn}^{\circ}), \quad A_3 = \tilde{A}_3 w_{mn} \qquad (\alpha = 1,2) \tag{4.11a,b}$$

The constants $\tilde{A}_\alpha$, $\tilde{A}_3$ are displayed in Appendix 3. It can be readily seen that the particular solution ϕ_1 satisfies the following conditions

(4.12a-d)

$$\int_0^{L_1} \phi_{1,11}\Big|_{x_2=0,L_2} dx_1 = 0, \quad \int_0^{L_2} \phi_{1,22}\Big|_{x_1=0,L_1} dx_2 = 0, \quad \int_0^{L_1} \phi_{1,12}\Big|_{x_2=0,L_2} dx_1 = 0, \quad \int_0^{L_2} \phi_{1,12}\Big|_{x_1=0,L_1} dx_2 = 0$$

This reveals that $\tilde{N}_{11}$ and $\tilde{N}_{22}$ acquire the meaning of average in plane compressive edge loads, expressed mathematically as

$$\int_0^{L_2} \phi_{,22}\Big|_{x_1=0,L_1} dx_2 = -\tilde{N}_{11} L_2, \quad \int_0^{L_1} \phi_{,11}\Big|_{x_2=0,L_2} dx_1 = -\tilde{N}_{22} L_1 \qquad (4.13a,b)$$

Proceeding in the same manner as for the compatibility equation and adopting the established properties that $(A_{16} = A_{26} = F_{16} = F_{26} = 0)$ for cross-ply laminated faces the coupled equilibrium equations, Eqs. (4.5a,b) can be fulfilled by assuming η_1 and η_2 in the following form

$$\eta_1(x_\alpha) = B_1 \cos\lambda_m x_1 \sin\mu_n x_2, \quad \eta_2(x_\alpha) = C_1 \sin\lambda_m x_1 \cos\mu_n x_2 \qquad (4.14a,b)$$

where the coefficients B_1 and C_1 can be expressed as

$$B_1 = \tilde{B}_1 w_{mn}, \qquad C_1 = \tilde{C}_1 w_{mn} \qquad (4.15a,b)$$

The constants $\tilde{B}_1$ and $\tilde{C}_1$ are displayed in Appendix 3.

Currently, three of the governing system of equations are fulfilled. In addition the expressions for the functions ϕ, η_1, η_2, v_3, and v_3° are known. There yet remains to determine the expressions for ξ_1 and ξ_2. These can be established from the following relationships

(4.16a,b)

$$N_{11} = \phi_{,22} = A_{11}\xi_{1,1} + A_{12}\xi_{2,2} + A_{11}(1/2)v_{3,1}^2 + A_{11}v_{3,1}^{\circ}v_{3,1} - A_{11}(v_3/R_1) + A_{12}(1/2)v_{3,2}^2 + A_{12}v_{3,2}^{\circ}v_{3,2} - A_{12}(v_3/R_2)$$

$$N_{12} = -\phi_{,12} = A_{66}\xi_{1,2} + A_{66}\xi_{2,1} + A_{66}v_{3,1}^{\circ}v_{3,2} + A_{66}v_{3,1}v_{3,2}^{\circ} + A_{66}v_{3,1}v_{3,2} \qquad (1 \overset{\rightarrow}{\leftarrow} 2)$$

Knowing the expressions for ϕ, v_3, and v_3°, ξ_1 and ξ_2 can be determined from Eqs. (4.16a,b). The expressions for $\xi_1(x_1, x_2)$ and $\xi_2(x_1, x_2)$ are given here as

(4.17a,b)

$$\xi_1 = D_1 x_1 + D_2 \sin 2\lambda_m x_1 + D_3 \sin 2\lambda_m x_1 \cos 2\mu_n x_2 + D_4 \cos \lambda_m x_1 \sin \mu_n x_2 + \left(D_5 \tilde{N}_{11} + D_6 \tilde{N}_{22}\right) x_1$$

$$\xi_2 = E_1 x_2 + E_2 \sin 2\mu_n x_2 + E_3 \cos 2\lambda_m x_1 \sin 2\mu_n x_2 + E_4 \sin \lambda_m x_1 \cos \mu_n x_2 + \left(E_5 \tilde{N}_{11} + E_6 \tilde{N}_{22}\right) x_2$$

where

$$(D_i, E_i) = (\tilde{D}_i, \tilde{E}_i)(w_{mn}^2 + 2w_{mn}w_{mn}^{\circ}), \quad D_4 = \tilde{D}_4 w_{mn}, \quad E_4 = \tilde{E}_4 w_{mn} \quad (i = 1,2,3) \qquad (4.18a\text{-}c)$$

The expressions for $\tilde{D}_i$, $\tilde{E}_i (i = \overline{1,4})$ and D_5, D_6, E_5, and E_6 are supplied in Appendix 3.

One of the methods allowing for the formulation of postbuckling equations in terms of the modal amplitudes consists of the discretization of eq. (4.5c) via the Galerkin method [55,58]. However, a more inclusive way permitting among others to compensate for the non-fulfillment of certain boundary conditions (non essential ones) is by the use of the Extended Galerkin Method [26]. Replacement of the expressions of ϕ, v_3, v_3°, η_1, η_2, ξ_1, and ξ_2 into Hamilton's variational equation, Eq. (3.1), and carrying out the indicated integrations, results in the following nonlinear algebraic equation expressed in terms of the modal amplitudes w_{mn} as:

(4.19)

$$P_1\left[w_{mn}, w_{mn}^{\circ}, \tilde{N}_{11}, \tilde{N}_{22}\right] + P_2\left[w_{mn}^2, w_{mn}, w_{mn}^{\circ}\right] + P_3\left[w_{mn}^3, w_{mn}^2, w_{mn}, w_{mn}^{\circ}\right] + P_{mn}\left(\frac{\tilde{N}_{22}}{R_1} + \frac{\tilde{N}_{11}}{R_2}\right) + q_{mn} = 0 \qquad \begin{pmatrix} m = 1,\ldots, M \\ n = 1,\ldots, N \end{pmatrix}$$

In these equations, P_1, P_2, and P_3 are linear, quadratic and cubic polynomials of the unknown modal amplitudes. P_{mn} are constants that depend on the material and geometric properties of the panel. $\tilde{N}_{11}$ and $\tilde{N}_{22}$ are the compressive edge loads, w_{mn}° are the modal imperfection amplitudes, while q_{mn} denotes the amplitude of the lateral load. The equilibrium configurations for a given flat or curved panel are determined by solving the nonlinear algebraic Eqs (4.19) via Newton's Method. As a by-product, the values of $\tilde{N}_{11}$ and $\tilde{N}_{22}$ fulfilling the linearized counterpart of Eq. (4.19) corresponding to $w_{mn} \neq 0$ can be obtained. These values correspond to the buckling bifurcation solution.

4.2 Displacement Formulation

In contrast to the mixed representation of the governing equations, the displacement method proves to be an efficient method, allowing more of the general structural attributes to be accounted for theoretically. Equations (3.32a-e) which represent the governing equations in terms of displacements will be utilized to determine the thermomechanical postbuckling behavior for a sandwich panel comprised of symmetrically laminated faces with respect to their local and global mid-surfaces featuring a strong core type behavior with a linear antisymmetric temperature profile distributed through the panel thickness. Just as with the stress potential method, the Extended Galerkin Method will be adopted to determine the postbuckling behavior, with the unfulfilled expressions retained as residual terms in the energy functional.

A linear antisymmetric temperature profile distributed throughout the panel thickness can be represented as

$$T(x_1, x_2, x_3) = x_3 \overset{1}{T}(x_1, x_2) \tag{4.20}$$

where

$$\overset{1}{T} = \frac{2T_u}{H} = -\frac{2T_b}{H} \tag{4.21}$$

Such a temperature field can arise during the accelerated flight of a space vehicle. Herein, $T_u\{\equiv T_u(x_1,x_2)\}$ and $T_b\{\equiv T_b(x_1,x_2)\}$ denote the temperature distributions at the surfaces $x_3=-H/2$ and $x_3=H/2$, respectively. As concerns the problem at hand, $\overset{1}{T}$ can be represented as

$$\overset{1}{T}(x_1,x_2)=\overset{1}{T}_{mn}\sin\lambda_m x_1\sin\mu_n x_2 \tag{4.22}$$

Adopting this representation for $\overset{1}{T}(x_\alpha)$ and utilizing Eqs. (4.6), (4.7), (4.22), and (3.37a,b) in conjunction with Eqs. (3.32a,b), ξ_1 and ξ_2 can be assumed in the following form

(4.23a,b)

$$\begin{Bmatrix}\xi_1\\ \xi_2\end{Bmatrix}=\begin{Bmatrix}F_1\\ G_1\end{Bmatrix}\sin 2\lambda_m x_1+\begin{Bmatrix}F_2\\ G_2\end{Bmatrix}\sin 2\mu_n x_2+\begin{Bmatrix}F_3\\ G_3\end{Bmatrix}\sin\lambda_m x_1\cos\mu_n x_2+\begin{Bmatrix}F_4\\ G_4\end{Bmatrix}\cos\lambda_m x_1\sin\mu_n x_2$$
$$+\begin{Bmatrix}F_5\\ G_5\end{Bmatrix}\sin 2\lambda_m x_1\cos 2\mu_n x_2+\begin{Bmatrix}F_6\\ G_6\end{Bmatrix}\cos 2\lambda_m x_1\sin 2\mu_n x_2+\begin{Bmatrix}F_7\\ G_7\end{Bmatrix}x_1+\begin{Bmatrix}F_8\\ G_8\end{Bmatrix}x_2$$

where

(4.24a-c)

$$(F_i,G_i,F_5,G_6)=(\tilde{\tilde{F}}_i,\tilde{\tilde{G}}_i,F_5,G_6)(w_{mn}^2+2w_{mn}\overset{\circ}{w}_{mn}),\qquad (F_j,G_j)=(\tilde{\tilde{F}}_j,\tilde{\tilde{G}}_j)w_{mn},\qquad F_6=G_5=0$$
$$\begin{Bmatrix}\mathrm{i}=1,2\\ \mathrm{j}=3,4\end{Bmatrix}$$

The expressions for F_i, G_i, F_j, G_j, $\tilde{\tilde{F}}_5$, and $\tilde{\tilde{G}}_6$ are provided in Appendix 3. As concerns the coefficients F_7, F_8, G_7, and G_8, these are determined from the in-plane static boundary counditions, Eqs. (3.42a,b) with the aid of Eqs. (4.6), (4.7), and (4.16a,b). These coefficients have been determined and are expressed as

$$F_7 = -\frac{\lambda_m^2}{8}(w_{mn}^2 + 2w_{mn}w_{mn}^{\circ}) + \frac{A_{26}^2 - \Lambda_{22}\Lambda_{66}}{\Omega}\tilde{N}_{11} + \frac{\Lambda_{12}\Lambda_{66} - A_{16}A_{26}}{\Omega}\tilde{N}_{22} \qquad (4.25a,b)$$

$$G_8 = -\frac{\mu_n^2}{8}(w_{mn}^2 + 2w_{mn}w_{mn}^{\circ}) + \frac{\Lambda_{12}\Lambda_{66} - A_{16}A_{26}}{\Omega}\tilde{N}_{11} + \frac{A_{16}^2 - \Lambda_{11}\Lambda_{66}}{\Omega}\tilde{N}_{22}$$

where

$$\Omega = \Lambda_{11}\Lambda_{22}\Lambda_{66} - \Lambda_{12}^2\Lambda_{66} + 2\Lambda_{12}A_{16}A_{26} - \Lambda_{11}A_{26}^2 - \Lambda_{22}A_{16}^2 \qquad (4.26)$$

It turns out that F_8 and G_7 are arbitrary and do not have an effect on the final postbuckling solution. The equilibrium equations, Eqs. (3.32a,b) are now fulfilled with the expressions for ξ_1 and ξ_2 now known. To fulfill the equilibrium equations, Eqs. (3.32c,d). η_1 and η_2 can be assumed in the following form

$$\begin{Bmatrix}\eta_1(x_1,x_2)\\ \eta_2(x_1,x_2)\end{Bmatrix} = \begin{Bmatrix}H_1\\ I_1\end{Bmatrix}\cos\lambda_m x_1 \sin\mu_n x_2 + \begin{Bmatrix}H_2\\ I_2\end{Bmatrix}\sin\lambda_m x_1 \cos\mu_n x_2 \qquad (4.27a,b)$$

where

$$(H_i, I_i) = (\tilde{H}_i, \tilde{I}_i)w_{mn} + (\tilde{\tilde{H}}_i^T, \tilde{\tilde{I}}_i^T)T_{mn}^1 \qquad (i = 1,2) \qquad (4.28)$$

The expressions for $\tilde{H}_i$, $\tilde{I}_i$, $\tilde{\tilde{H}}_i^T$, and $\tilde{\tilde{I}}_i^T$ are provided in Appendix 3. Having determined the expressions for η_1 and η_2, the equilibrium equations, Eqs. (3.32c,d) are now fulfilled. With the fulfillment of the four equilibrium equations Eqs. (3.32a-d), there remains unfulfilled the fifth equilibrium equation, Eq. (3.32e). This unfulfilled equilibrium equation will be retained within the energy functional. Retainment of the unfulfilled equilibrium equation, the unfulfilled

boundary terms, and replacement of the expressions for v_3, $\overset{\circ}{v_3}$, ξ_1, ξ_2, η_1, η_2, q_3, and $\overset{1}{T}$ within variational equation, Eq. (3.1), and carrying out the indicated integrations following in the same manner as within the mixed formulation results in the following nonlinear algebraic equation governing the postbuckling response expressed as

(4.29)

$$P_1\left[w_{mn}, \overset{\circ}{w_{mn}}, \tilde{N}_{11}, \tilde{N}_{22}\right] + P_2\left[w_{mn}^2, w_{mn}, \overset{\circ}{w_{mn}}\right] + P_3\left[w_{mn}^3, w_{mn}^2, w_{mn}\overset{\circ}{w_{mn}}\right] + \left(\frac{\tilde{N}_{22}}{R_2} + \frac{\tilde{N}_{11}}{R_1}\right) + Q_1 \overset{1}{T}_{mn}$$
$$+ Q_2 q_{mn} = 0$$

Within this nonlinear algebraic equation, R_1 and R_2 denote the principal radii of curvature. P_1, P_2, and P_3 are linear, quadratic, and cubic polynomials of the unknown modal amplitudes, w_{mn}. Q_1 and Q_2 are coefficients containing geometrical and thermomechanical properties of the sandwich structure.

4.3 Immovability of The Edges

If the tangential motion of any pair of opposite edges is prevented (immovable edges), the effects of the immovability of the edges needs to be incorporated into the thermomechanical postbuckling equation. This can be accomplished by determining the fictitious edge loads obtained from the immovability conditions, Eq. (3.41).

If two edges are immovable along $(x_1 = 0,\ L_1)$ the condition

$$\int_0^{L_2}\int_0^{L_1} \left(\partial \xi_1 / \partial x_1\right) dx_1 dx_2 = 0 \tag{4.30}$$

needs to be fulfilled. Incorporating the expression for ξ_1 from Eq. (4.23a) results in

(4.31)

$$\int_0^{L_2}\int_0^{L_1}\{2\lambda_m F_1\cos 2\lambda_m x_1+\lambda_m F_3\cos\lambda_m x_1\cos\mu_n x_2-\lambda_m F_4\sin\lambda_m x_1\sin\mu_n x_2+$$
$$+2\lambda_m F_5\cos 2\lambda_m x_1\cos 2\mu_n x_2+F_7\}dx_1dx_2=0$$

Utilizing the expressions for the coefficients from Eqs. (4.24a-c) and Eqs. (4.25a,b), the expression for the fictitious edge load $\tilde{N}_{11}$ can be determined. This expression for $\tilde{N}_{11}$ can be incorporated into the postbuckling equation. This expression for $\tilde{N}_{11}$ is not provided here.

If the two edges are immovable along $(x_2=0,\ L_2)$, the condition

$$\int_0^{L_2}\int_0^{L_1}(\partial\xi_2/\partial x_2)dx_1dx_2=0 \tag{4.32}$$

needs to be fulfilled. Incorporating the expression for ξ_2 from Eq. (4.23b) results in

(4.33)

$$\int_0^{L_2}\int_0^{L_1}\{2\mu_n G_2\cos 2\mu_n x_2-\mu_n G_3\sin\lambda_m x_1\sin\mu_n x_2+\mu_n G_4\cos\lambda_m x_1\cos\mu_n x_2+$$
$$+2\mu_n G_6\cos 2\lambda_m x_1\cos 2\mu_n x_2+G_8\}dx_1dx_2=0$$

Utilizing the expressions for the coefficients from Eqs. (4.24a-c) and Eqs. (4.25a,b), the expression for the ficticious edge load $\tilde{N}_{22}$ can be determined. This expression for $\tilde{N}_{22}$ can be incorporated into the postbuckling equation. The expression for $\tilde{N}_{22}$ is not provided here. A number of results for two immovable edges along $(x_2=0, L_2)$ have been presented in the results and conclusions section.

4.4 The End-shortening of the Edges

During uniaxial compression, the edges have a tendency to displace inwardly. A measure of this end-shortening in the x_1-direction can be determined from the following integral expression.

$$\Delta_1 = -\frac{1}{L_1 L_2}\int_0^{L_2}\int_0^{L_1}(\partial\xi_1/\partial x_1)dx_1 dx_2 \tag{4.34}$$

Similiarly the amount of end- shortening in the x_2-direction can be determined from the following integral expression.

$$\Delta_2 = -\frac{1}{L_1 L_2}\int_0^{L_2}\int_0^{L_1}(\partial\xi_2/\partial x_2)dx_1 dx_2 \tag{4.35}$$

Incorporating the expressions for ξ_1 and ξ_2 from Eqs. (4.23a,b) gives the expressions for the amount of end-shortening during compression. These expressions are not provided here. Results for end-shortening are provided in the results and discussion section.

5 Stress/Strain Analysis

5.1 Stress/Strain Formulation

The determination of the stresses and the strains at each point within the structure can be determined with the use of the stress/strain equations, eqs. (2.14a,b), the strain displacement equations, eqs. (2.9a-e), (2.10a-e), (2.11a-e), and the displacement functions ξ_1, ξ_2, η_1, and η_2. With the use of the extended Galerkin Method, the deflection at each point within the structure can be determined per each fixed load. Knowing the deflection at each point within the structure, allows the evaluation of the strains at each point within the structure which then allows the evaluation of the stresses at each point within the structure.

The stress/strain equations were presented in section 2.4. Neglecting the thermal and moisture effects and considering only the 2-D stress conditions, within the facings, they are

$$\begin{Bmatrix} {}'S_{11} \\ {}'S_{22} \\ {}'S_{12} \end{Bmatrix}_k = \begin{bmatrix} {}'\hat{Q}_{11} & {}'\hat{Q}_{12} & {}'\hat{Q}_{16} \\ {}'\hat{Q}_{12} & {}'\hat{Q}_{22} & {}'\hat{Q}_{26} \\ {}'\hat{Q}_{16} & {}'\hat{Q}_{26} & {}'\hat{Q}_{66} \end{bmatrix}_k \begin{Bmatrix} {}'e_{11} \\ {}'e_{22} \\ 2'e_{12} \end{Bmatrix} \qquad (5.1a,b)$$

$$\begin{Bmatrix} {}'S_{23} \\ {}'S_{13} \end{Bmatrix}_k = {}'K^2 \begin{bmatrix} {}'Q_{44} & {}'Q_{45} \\ {}'Q_{45} & {}'Q_{55} \end{bmatrix}_k \begin{Bmatrix} 2'e_{23} \\ 2'e_{13} \end{Bmatrix}$$

Replacement of single primes with double primes and superposed bars, respectively in Eqs. (5.1) yield the respective equations for the top face and the core respectively. In addition, the core layer is considered as an orthotropic layer with the orthotropic axes coinciding with the geometrical axes. To determine the stresses, the strain relations are needed. The strain relations presented in section 2.3 are presented again here as

Bottom facings

$$\begin{aligned} {}'e_{11} &= {}'\varepsilon_{11} + (x_3 - a')\kappa'_{11} \\ {}'e_{22} &= {}'\varepsilon_{22} + (x_3 - a')\kappa'_{22} \qquad (\bar{h} \le x_3 \le \bar{h} + h') \\ 2'e_{12} &= {}'\gamma_{12} + (x_3 - a')\kappa'_{12} \\ 2'e_{13} &= {}'\gamma_{13}, \quad 2'e_{23} = {}'\gamma_{23} \end{aligned} \qquad (2.9a\text{-}e)$$

Core Layer

$$\begin{aligned} \bar{e}_{11} &= \bar{\varepsilon}_{11} + x_3\bar{\kappa}_{11} \\ \bar{e}_{22} &= \bar{\varepsilon}_{22} + x_3\bar{\kappa}_{22} \qquad \left(-\bar{h} \le x_3 \le \bar{h}\right) \\ 2\bar{e}_{12} &= \bar{\gamma}_{12} + x_3\bar{\kappa}_{12} \\ 2\bar{e}_{13} &= \bar{\gamma}_{13}, \quad 2\bar{e}_{23} = \bar{\gamma}_{23} \end{aligned} \qquad (2.10a\text{-}e)$$

Upper facings

$$
\begin{aligned}
&{}^{//}e_{11} = {}^{//}\varepsilon_{11} + (x_3 + a^{//})\kappa^{//}_{11} \\
&{}^{//}e_{22} = {}^{//}\varepsilon_{22} + (x_3 + a^{//})\kappa^{//}_{22} \qquad \left(-\bar{h} - h^{//} \le x_3 \le -\bar{h}\right) \\
&2^{//}e_{12} = {}^{//}\gamma_{12} + (x_3 + a^{//})\kappa^{//}_{12} \\
&2^{//}e_{13} = {}^{//}\gamma_{13}, \quad 2^{//}e_{23} = {}^{//}\gamma_{23}
\end{aligned}
\tag{2.11a-e}
$$

In order to evaluate the strains within the structure, the strain-displacement relationships are needed. For the most general case, these relationships are presented in Appendix 1. When the Love-Kirchoff assumptions are adopted for the facings, these relationships are simplified and presented as

Bottom Facings

$$
\begin{aligned}
&{}^{/}\varepsilon_{11} = \xi_{1,1} + \eta_{1,1} + (1/2)v_{3,1}^2 + v_{3,1}v^{\circ}_{3,1} - v_3/R_1 \\
&{}^{/}\gamma_{12} = \xi_{1,2} + \xi_{2,1} + \eta_{1,2} + \eta_{2,1} + v_{3,1}v_{3,2} + v^{\circ}_{3,1}v_{3,2} + v_{3,1}v^{\circ}_{3,2} \qquad (1\overrightarrow{\leftarrow}2) \\
&{}^{/}\kappa_{11} = -v_{3,11} \\
&{}^{/}\kappa_{12} = -2v_{3,12}
\end{aligned}
\tag{5.2a-d}
$$

Core Layer

$$
\begin{aligned}
&\bar{\varepsilon}_{11} = \xi_{1,1} + \frac{1}{2}v_{3,1}^2 + v^{\circ}_{3,1}v_{3,1} - v_3/R_1 \\
&\bar{\gamma}_{12} = \xi_{1,2} + \xi_{2,1} + v_{3,1}v_{3,2} + v^{\circ}_{3,1}v_{3,2} + v_{3,1}v^{\circ}_{3,2} \\
&\bar{\kappa}_{11} = \frac{1}{\bar{h}}\left\{\eta_{1,1} - \frac{1}{2}hv_{3,11}\right\} \qquad (1\overrightarrow{\leftarrow}2) \\
&\bar{\kappa}_{12} = \frac{1}{\bar{h}}\left\{\eta_{1,2} + \eta_{2,1} + hv_{3,12}\right\} \\
&\bar{\gamma}_{13} = \frac{1}{\bar{h}}\left\{\eta_1 - \frac{1}{2}hv_{3,1}\right\} + v_{3,1}
\end{aligned}
\tag{5.3a-e}
$$

Upper Facings

$$
\begin{aligned}
^{//}\varepsilon_{11} &= \xi_{1,1} - \eta_{1,1} + (1/2)v_{3,1}^2 + v_{3,1}\overset{\circ}{v}_{3,1} - v_3/R_1 \\
^{//}\gamma_{12} &= \xi_{1,2} + \xi_{2,1} - \eta_{1,2} - \eta_{2,1} + v_{3,1}v_{3,2} + \overset{\circ}{v}_{3,1}v_{3,2} + v_{3,1}\overset{\circ}{v}_{3,2} \qquad (1\overset{\rightarrow}{\leftarrow}2) \\
^{//}\kappa_{11} &= -v_{3,11} \\
^{//}\kappa_{12} &= -2v_{3,12}
\end{aligned}
\tag{5.4a-d}
$$

Replacement of the expressions for ξ_1, ξ_2, η_1, η_2, $\overset{\circ}{v}_3$, and v_3 as obtained from Eqs. (4.23a,b), (4.27a,b), (4.6), and (4.7) into the strain-displacement relationships, Eqs. (5.2a-d), (5.3a-e), and (5.4a-d) provides the strain-displacment relationships as a function of deflection in terms of the geometrical and material properties of the sandwich structure. Knowing the deflections for each applied load and the material and geometrical properties of the structure, allows for the determination of the strains and the stresses at each point within the structure. These strain-displacement relationships are expressed as

Bottom Facings

$$
\begin{aligned}
^{/}\overset{\circ}{\varepsilon}_{11} = &\left[\lambda_m\left(\tilde{F}_3 + \tilde{H}_2\right)\cos\lambda_m x_1 \cos\mu_n x_2 - \left\{\lambda_m\left(\tilde{F}_4 + \tilde{H}_1\right) + 1/R_1\right\}\sin\lambda_m x_1 \sin\mu_n x_2\right]w_{mn} + \\
&+\left\{2\lambda_m \tilde{F}_1 \cos 2\lambda_m x_1 + 2\lambda_m \tilde{F}_5 \cos 2\lambda_m x_1 \cos 2\mu_n x_2 + \left(\lambda_m^2/2\right)\cos^2\lambda_m x_1 \sin^2\mu_n x_2 + \right. \\
&\left.\tilde{F}_7\right\}\left(w_{mn}^2 + 2\overset{\circ}{w}_{mn} w_{mn}\right) + \frac{A_{26}^2 - \Lambda_{22}\Lambda_{66}}{\Omega}\tilde{N}_{11} + \frac{\Lambda_{12}\Lambda_{66} - A_{16}A_{26}}{\Omega}\tilde{N}_{22}
\end{aligned}
\tag{5.5a}
$$

$$
\begin{aligned}
^{/}\overset{\circ}{\varepsilon}_{22} = &\left[\mu_n\left(\tilde{G}_4 + \tilde{I}_1\right)\cos\lambda_m x_1 \cos\mu_n x_2 - \left\{\mu_n\left(\tilde{G}_3 + \tilde{I}_2\right) + 1/R_2\right\}\sin\lambda_m x_1 \sin\mu_n x_2\right]w_{mn} + \\
&+\left\{2\mu_n \tilde{G}_2 \cos 2\mu_n x_2 + 2\mu_n \tilde{G}_6 \cos 2\lambda_m x_1 \cos 2\mu_n x_2 + \left(\mu_n^2/2\right)\sin^2\lambda_m x_1 \cos^2\mu_n x_2 + \right. \\
&\left.\tilde{G}_8\right\}\left(w_{mn}^2 + 2\overset{\circ}{w}_{mn} w_{mn}\right) + \frac{\Lambda_{12}\Lambda_{66} - A_{16}A_{26}}{\Omega}\tilde{N}_{11} + \frac{A_{16}^2 - \Lambda_{11}\Lambda_{66}}{\Omega}\tilde{N}_{22}
\end{aligned}
\tag{5.5b}
$$

(5.5c)

$$\gamma^{\circ}_{12} = \left[-\left\{\mu_n\left(\tilde{F}_3 + \tilde{H}_2\right) + \lambda_m\left(\tilde{G}_4 + \tilde{I}_1\right)\right\}\sin\lambda_m x_1 \sin\mu_n x_2 + \left\{\mu_n\left(\tilde{H}_1 + \tilde{F}_4\right) + \lambda_m\left(\tilde{G}_3 + \right.\right.\right.$$
$$\left.\left.\left. + \tilde{I}_2\right)\right\}\cos\lambda_m x_1 \cos\mu_n x_2\right] w_{mn} + \left\{2\lambda_m \tilde{G}_1 \cos 2\lambda_m x_1 + 2\mu_n \tilde{F}_2 \cos 2\mu_n x_2 - 2\left(\mu_n \tilde{F}_5 + \right.\right.$$
$$\left.\left. \lambda_m \tilde{G}_6\right)\sin 2\lambda_m x_1 \sin 2\mu_n x_2 + \lambda_m \mu_n \cos\lambda_m x_1 \sin\lambda_m x_1 \cos\mu_n x_2 \sin\mu_n x_2\right\}\left(w_{mn}^2 + 2w^{\circ}_{mn} w_{mn}\right)$$
$$+ \frac{\Lambda_{22} A_{16} - \Lambda_{12} A_{26}}{\Omega} \tilde{N}_{11} + \frac{\Lambda_{11} A_{26} - \Lambda_{12} A_{16}}{\Omega} \tilde{N}_{22}$$

$$\kappa^{/}_{11} = \lambda_m^2 w_{mn} \sin\lambda_m x_1 \sin\mu_n x_2 \tag{5.5d}$$

$$\kappa^{/}_{22} = \mu_n^2 w_{mn} \sin\lambda_m x_1 \sin\mu_n x_2 \tag{5.5e}$$

$$\kappa^{/}_{12} = -2\lambda_m \mu_n w_{mn} \cos\lambda_m x_1 \cos\mu_n x_2 \tag{5.5f}$$

Core Layer

(5.6a)

$$\bar{\varepsilon}^{\circ}_{11} = \left\{\lambda_m \tilde{F}_3 \cos\lambda_m x_1 \cos\mu_n x_2 - \left(\lambda_m \tilde{F}_4 + 1/R_1\right)\sin\lambda_m x_1 \sin\mu_n x_2\right\} w_{mn} + \left\{2\lambda_m \tilde{F}_1 \cos 2\lambda_m x_1 + \right.$$
$$\left. + 2\lambda_m \tilde{F}_5 \cos 2\lambda_m x_1 \cos 2\mu_n x_2 + \left(\lambda_m^2/2\right)\cos^2\lambda_m x_1 \sin^2\mu_n x_2 + \tilde{F}_7\right\}\left(w_{mn}^2 + 2w^{\circ}_{mn} w_{mn}\right) +$$
$$+ \frac{A_{26}^2 - \Lambda_{22}\Lambda_{66}}{\Omega} \tilde{N}_{11} + \frac{\Lambda_{12}\Lambda_{66} - A_{16} A_{26}}{\Omega} \tilde{N}_{22}$$

(5.6b)

$$\bar{\varepsilon}^{\circ}_{22} = \left\{-\left(\mu_n \tilde{G}_3 + 1/R_2\right)\sin\lambda_m x_1 \sin\mu_n x_2 + \mu_n \tilde{G}_4 \cos\lambda_m x_1 \cos\mu_n x_2\right\} w_{mn} + \left\{2\mu_n \tilde{G}_2 \cos 2\mu_n x_2 + \right.$$
$$\left. + 2\mu_n \tilde{G}_6 \cos 2\lambda_m x_1 \cos 2\mu_n x_2 + \left(\mu_n^2/2\right)\sin^2\lambda_m x_1 \cos^2\mu_n x_2 + \tilde{G}_8\right\}\left(w_{mn}^2 + 2w^{\circ}_{mn} w_{mn}\right) +$$
$$+ \frac{\Lambda_{12}\Lambda_{66} - A_{16} A_{26}}{\Omega} \tilde{N}_{11} + \frac{A_{16}^2 - \Lambda_{11}\Lambda_{66}}{\Omega} \tilde{N}_{22}$$

(5.6c)

$$\bar{\gamma}_{12}^{\circ} = \left\{-\left(\mu_n \tilde{F}_3 + \lambda_m \tilde{G}_4\right)\sin\lambda_m x_1 \sin\mu_n x_2 + \left(\mu_n \tilde{F}_4 + \lambda_m \tilde{G}_3\right)\cos\lambda_m x_1 \cos\mu_n x_2\right\} w_{mn} +$$
$$\left\{2\mu_n \tilde{F}_2 \cos 2\mu_n x_2 + 2\lambda_m \tilde{G}_1 \cos 2\lambda_m x_1 - 2\left(\mu_n \tilde{F}_5 + \lambda_m \tilde{G}_6\right)\sin 2\lambda_m x_1 \sin 2\mu_n x_2 +\right.$$
$$\left. + \lambda_m \mu_n \cos\lambda_m x_1 \sin\lambda_m x_1 \cos\mu_n x_2 \sin\mu_n x_2\right\}\left(w_{mn}^2 + 2w_{mn}^{\circ} w_{mn}\right) + \frac{\Lambda_{22} A_{16} - \Lambda_{12} A_{26}}{\Omega} \tilde{N}_{11}$$
$$+ \frac{\Lambda_{11} A_{26} - \Lambda_{12} A_{16}}{\Omega} \tilde{N}_{22}$$

$$\bar{\kappa}_{11} = \frac{1}{\bar{h}}\left\{-\lambda_m\left(\tilde{H}_1 + \lambda_m h/2\right)\sin\lambda_m x_1 \sin\mu_n x_2 + \lambda_m \tilde{H}_2 \cos\lambda_m x_1 \cos\mu_n x_2\right\} w_{mn} \tag{5.6d}$$

$$\bar{\kappa}_{22} = \frac{1}{\bar{h}}\left\{-\mu_n\left(\tilde{I}_2 + \mu_n h/2\right)\sin\lambda_m x_1 \sin\mu_n x_2 + \mu_n \tilde{I}_1 \cos\lambda_m x_1 \cos\mu_n x_2\right\} w_{mn} \tag{5.6e}$$

(5.6f)

$$\bar{\kappa}_{12} = \frac{1}{\bar{h}}\left\{\left(\mu_n \tilde{H}_1 + \lambda_m \tilde{I}_2 + \lambda_m \mu_n h\right)\cos\lambda_m x_1 \cos\mu_n x_2 - \left(\mu_n \tilde{H}_2 + \lambda_m \tilde{I}_1\right)\sin\lambda_m x_1 \sin\mu_n x_2\right\} w_{mn}$$

$$\bar{\gamma}_{13} = \frac{1}{\bar{h}}\left\{\left(\tilde{H}_1 + a\lambda_m\right)\cos\lambda_m x_1 \sin\mu_n x_2 + \tilde{H}_2 \sin\lambda_m x_1 \cos\mu_n x_2\right\} w_{mn} \tag{5.6g}$$

$$\bar{\gamma}_{23} = \frac{1}{\bar{h}}\left\{\left(\tilde{I}_2 + a\mu_n\right)\sin\lambda_m x_1 \cos\mu_n x_2 + \tilde{I}_1 \cos\lambda_m x_1 \sin\mu_n x_2\right\} w_{mn} \tag{5.6h}$$

Upper Facings

$$^{//}\varepsilon_{11}^{\circ} = \left[\lambda_m\left(\tilde{F}_3 - \tilde{H}_2\right)\cos\lambda_m x_1 \cos\mu_n x_2 + \left\{\lambda_m\left(\tilde{H}_1 - \tilde{F}_4\right) - 1/R_1\right\}\sin\lambda_m x_1 \sin\mu_n x_2\right] w_{mn} +$$
$$+ \left\{2\lambda_m \tilde{F}_1 \cos 2\lambda_m x_1 + 2\lambda_m \tilde{F}_5 \cos 2\lambda_m x_1 \cos 2\mu_n x_2 + \left(\lambda_m^2/2\right)\cos^2\lambda_m x_1 \sin^2\mu_n x_2 + \right. \tag{5.7a}$$
$$\left. \tilde{F}_7\right\}\left(w_{mn}^2 + 2w_{mn}^{\circ} w_{mn}\right) + \frac{A_{26}^2 - \Lambda_{22}\Lambda_{66}}{\Omega} \tilde{N}_{11} + \frac{\Lambda_{12}\Lambda_{66} - A_{16} A_{26}}{\Omega} \tilde{N}_{22}$$

$$^{//}\varepsilon^{\circ}_{22} = \left[\mu_n\left(\tilde{G}_4 - \tilde{I}_1\right)\cos\lambda_m x_1 \cos\mu_n x_2 + \left\{\mu_n\left(\tilde{I}_2 - \tilde{G}_3\right) - 1/R_2\right\}\sin\lambda_m x_1 \sin\mu_n x_2\right]w_{mn} +$$
$$+\left\{2\mu_n\tilde{G}_2\cos 2\mu_n x_2 + 2\mu_n\tilde{G}_6\cos 2\lambda_m x_1\cos 2\mu_n x_2 + \left(\mu_n^2/2\right)\sin^2\lambda_m x_1\cos^2\mu_n x_2 + \right. \quad (5.7b)$$
$$\left.\tilde{G}_8\right\}\left(w_{mn}^2 + 2w^{\circ}_{mn}w_{mn}\right) + \frac{\Lambda_{12}\Lambda_{66} - A_{16}A_{26}}{\Omega}\tilde{N}_{11} + \frac{A_{16}^2 - \Lambda_{11}\Lambda_{66}}{\Omega}\tilde{N}_{22}$$

(5.7c)

$$^{//}\gamma^{\circ}_{12} = \left[-\left\{\mu_n\left(\tilde{H}_2 - \tilde{F}_3\right) + \lambda_m\left(\tilde{I}_1 - \tilde{G}_4\right)\right\}\sin\lambda_m x_1\sin\mu_n x_2 + \left\{\mu_n\left(\tilde{F}_4 - \tilde{H}_1\right) + \lambda_m\left(\tilde{G}_3 - \right.\right.\right.$$
$$\left.\left.\left.-\tilde{I}_2\right)\right\}\cos\lambda_m x_1\cos\mu_n x_2\right]w_{mn} + \left\{2\lambda_m\tilde{G}_1\cos 2\lambda_m x_1 + 2\mu_n\tilde{F}_2\cos 2\mu_n x_2 - 2\left(\mu_n\tilde{F}_5 + \right.\right.$$
$$\left.\left.\lambda_m\tilde{G}_6\right)\sin 2\lambda_m x_1\sin 2\mu_n x_2 + \lambda_m\mu_n\cos\lambda_m x_1\sin\lambda_m x_1\cos\mu_n x_2\sin\mu_n x_2\right\}\left(w_{mn}^2 + 2w^{\circ}_{mn}w_{mn}\right)$$
$$+\frac{\Lambda_{22}A_{16} - \Lambda_{12}A_{26}}{\Omega}\tilde{N}_{11} + \frac{\Lambda_{11}A_{26} - \Lambda_{12}A_{16}}{\Omega}\tilde{N}_{22}$$

$$\kappa^{//}_{11} = \lambda_m^2 w_{mn}\sin\lambda_m x_1\sin\mu_n x_2 \quad (5.7d)$$

$$\kappa^{//}_{22} = \mu_n^2 w_{mn}\sin\lambda_m x_1\sin\mu_n x_2 \quad (5.7e)$$

$$\kappa^{//}_{12} = -2\lambda_m\mu_n w_{mn}\cos\lambda_m x_1\cos\mu_n x_2 \quad (5.7f)$$

6 Results and Discussion

6.1 Buckling of Flat and Curved Anisotropic Sandwich Panels

Theoretical data developed from the linear counterpart of the postbuckling equation have been developed and compared with experimental data [5,39]. In Table 6.1, data concerning a three-layer symmetric flat sandwich panel with isotropic facings (Comprised of Dura-Aluminum $E = 6.96 \times 10^6$ kg / cm^2, $\nu = 0.3,$) and a transversely isotropic weak core (of Penoplast) uniaxially compressed is considered. In Table 6.2, data concerning a flat sandwich panel with isotropic facings and a weak orthotropic core uniaxially compressed is considered. In Table 6.3, data concerning a circular cylindrical sandwich panel, with isotropic facings and a transversely isotropic weak core, uniaxially compressed and comprised of the same materials, as for the case, in Table 6.1, is considered.

Table 6.1. Comparisons of theoretical and experimental buckling predictions for a flat sandwich panel with isotropic facings and a transversely-isotropic core with simply supported edge conditions.

	L_1(cm)	L_2(cm)	h(cm)	$\bar{h}$(cm)	$\overline{G}$(kg / cm^2)	Theory*	Exp*	% Error
1	60	40	0.05	0.425	99.4	3.79	3.6	+5.28
2	60	40	0.10	0.650	149.6	9.03	8.25	+9.45
3	40	60	0.10	0.700	117.1	11.3	12.3	-8.13
4	40	60	0.10	1.400	96.5	17.4	16.00	+8.75
5	80	60	0.05	0.450	73.5	4.21	4.00	+5.25
6	80	60	0.05	0.450	74.1	4.24	4.10	+3.41

(*$\tilde{N}_{11} L_2 \times 10^3$ kg)

Table 6.2. Comparisons of theoretical and experimental buckling predictions for a flat sandwich panel with isotropic facings and an orthotropic core with simply supported edge conditions.

	L_1(cm)	L_2(cm)	h(cm)	$\bar{h}$(cm)	$\overline{G}_{13}$**	$\overline{G}_{23}$**	Theory*	Exp*	% Error
1	60	40	0.05	0.45	140.4	100.8	5.29	5.85	-9.57
2	60	40	0.25	1.25	390.0	103.0	47.22	46.7	+1.11
3	60	40	0.25	1.15	337.0	97.0	38.2	36.5	+4.66
4	80	60	0.10	0.95	138.1	78.6	17.34	15.25	+13.7

$(*\tilde{N}_{11}L_2 \times 10^3 \text{ kg}), (** \text{kg/cm}^2)$

Table 6.3. Comparisons of theoretical and experimental buckling predictions for a circular cylindrical sandwich panel with isotropic facings and a transversely-isotropic core with simply supported edge conditions.($L_1 = 60$ cm, $L_2 = 40$ cm, $h = 0.1$ cm, $R_1 = \infty$, $R_2 = 100$ cm)

	$\bar{h}$(cm)	$\bar{G}$(kg/cm^2)	Theory*	Exp*	% Error
1	0.750	81.3	9.114	8.2	+11.4
2	0.750	84	9.3	7.8	+19.23
3	0.475	150	10.49	8.9	+17.865
4	0.200	127	6.643	6.28	+5.78
5	0.200	566	16.35	14.6	+11.99
6	0.225	92	5.965	5.0	+19.3
7	0.500	32.6	5.087	4.4	+15.61
8	0.475	40	5.369	4.62	+16.212
9	0.500	141	10.36	9.25	+12.00
10	0.700	104	10.26	8.55	+20.00

$(*\tilde{N}_{11}L_2 \times 10^3 \text{ kg})$

The results, in Tables 6.1 and 6.2, reveal a reasonable agreement between theory and experiment. It is also revealed that the theoretical results slightly overpredict the experimental results. The results presented in Table 6.3 reveal overpredictions as high as 20%. One possible interpretation of these discrepancies are given to the disregard of the geometrical imperfections. Another explanation for this discrepancy is given to the fact that nothing is mentioned about the conditions under which these experimental results were obtained. In addition, nothing is mentioned about what type of simply supported edge conditions were used to obtain the experimental results. All of these factors play a role in the discrepancy between the theoretical and experimental results.

The data, appearing in Table 6.4, contain comparisons between theory and experimental buckling results [77] of uniaxially compressed sandwich plates with anisotropic laminated facings. These comparisons concern a sandwich panel with the following geometrical and material properties listed below.

Facings(Carbon Fiber Reinforced Plastic)

$L_1 = L_2 = 228$ mm, $h^{/} = h^{//} = 0.375$ mm(*0.5mm), $\bar{h} = 2.5$ mm

$E_1 = 14200 \text{ N/mm}^2$, $E_2 = 9800 \text{ N/mm}^2$, $G_{12} = 4300 \text{ N/mm}^2$, $\nu_{12} = 0.34$

Core layer*(non-metallic honeycomb core)*

$G_{13} = 60\ \text{N/mm}^2,\ G_{23} = 35.2\ \text{N/mm}^2$

Table 6.4. Comparisons of theoretical and experimental buckling loads for anisotropic laminated flat sandwich panels (simply supported edge conditions).

Facing Layup	[0/90°/0]	[45°/0/45°]	[45°/0*/45°]
Experimental (N/mm)	185	161	262
Present (N/mm)	137	161	200
% Error	-25.95	0	-23.66

(* indicates a 0.250 mm thick ply)

In Table 6.4, the comparisons show that buckling predictions for the [45°/0/45°] lay-up agrees perfectly with those obtaind via experimental results. In contrast, the [0/90°/0] and [45°/0*/45°] lay-ups, for the present theoretical results, reveal a slightly conservative nature compared with the experimental values.

In addition to the comparisons of theory and experiment, several results have been developed based on the theory presented. The following materials with their properties and designations, displayed in the following tables, were used to generate the results.

Table 6.5. Material properties for the facesheets.

Type	Material	E_1(psi)	E_2 (psi)	G_{12} (psi)	ν_{12}	α_1 (in/in/°F)	α_2 (in/in/°F)
F1	HS Graphite Epoxy	26.25	1.5	1.05	0.28	6.3	20.5
F2	IM7/977-2	11.6	10.9	1.4	0.06	0.9	0.93
F3	SCS-6/Ti-15-3	27.72	18.09	8.15	0.30	-----	-----
F4	IM7/K3BR-4	22.0	1.2	0.6	0.30	-----	-----
F5	CFRP	33.22	1.936	0.761	0.32	-----	-----

[Note: Multiply $(E_1, E_2, G_{12}) \times 10^6$; $(\alpha_1, \alpha_2) \times 10^{-6}$]

Table 6.6. Material properties for the core.

Type	Core Type	G_{13} (psi)	G_{23} (psi)
C1	Titanium Honeycomb	2.0835×10^5	0.9435×10^5
C2	Aluminum Honeycomb	21177	13112.1
C3	Aluminum Honeycomb	14200	8600

In Figs. 6.1 and 6.2, the buckling load as a function of the panel face thickness for a flat sandwich panel with 3 ply facings for various values of the parameter a (the distance between the midsurface of the core and the midsurface of the facings) is depicted. Fig. 6.1 is depicted for all four edges being movable, while Fig. 6.2 is depicted for the two unloaded edges being immovable. In both cases, the results reveal that with an increase in both the panel face thickness and the parameter a, a continuous increase of the buckling load is experienced. In contrast to the movability of all four edges, the immovability of the edges reveals lower buckling loads. Similar results to the ones in Fig. 6.1 have been provided in Pearce and webber [76]. Their results have been depicted for $\pm 45^{\circ}$ angle ply facings. Several approximate data points have been taken from their results and plotted against the present results. The present results reveal close agreement.

In Fig. 6.3, the buckling load as a function of ply angle for a flat sandwich panel with 4 ply facings consisting of metal matrix composite facings (Material F3) and a C1 type core has been depicted. This figure has been presented to show very close agreement between the present theory and the theory where similar results have been developed in Ko and Jackson [41]. Several approximate data points have been taken from their results and plotted against the present results. Very close agreement is revealed between their results and the present results. In this figure, the low sensitivity to the variation in the ply angle is revealed. This is attributed to the low orthotropicity ratio of the material used within the facings. In addition, it can be seen that at a panel aspect ratio of $\psi = 0.9$, the peak buckling load occurs approximately at a ply angle of $\theta = 50^{\circ}$. For a panel aspect ratio of $\psi = 1$, the peak buckling load appears to occur approximately at a ply angle of $\theta = 45^{\circ}$. From this, a trend can be observed such that as the panel aspect ratio ψ increases, the ply angle θ at which the peak buckling load occurs, decreases.

In Fig. 6.4 and Fig. 6.5, the buckling load as a function of ply angle for a flat sandwich panel for various aspect ratios is depicted. In both cases, the facings consist of a F1 (HS Graphite Epoxy) material in conjunction with an aluminum honeycomb core. The sandwich panel depicted in Fig. 6.4 consists of facings with one ply in contrast to the panel depicted in Fig. 6.5 which consists of facings with four plies. The results for the panel depicted in Fig. 6.4 reveal that the peak buckling load occurs at greater ply angles up to panel aspect ratios of $\psi = 1$. For aspect ratios greater than one, the peak buckling load occurs at ply angles of $\theta = 0^{\circ}$. In addition, the discontinuities which reveal changes in the mode shape of deflection seem to occur at larger ply angles up to panel aspect ratios of $\psi = 1$. Beyond aspect ratio values of one, there does not appear to be any discontinuities which reveals that beyond this value the panel deflects with the same mode shape.

In contrast to the panel depicted in Fig. 6.4, the panel depicted in Fig. 6.5 with four ply facings appears to be more sensitive to mode shape of deflection changes. In addition, up to aspect ratios of $\psi = 1.2$, the peak buckling load occurs at larger ply angles beyond which the ply angles seem to decrease at the point where the peak buckling loads occur. By comparing Fig. 6.5 to the other figures, again it can be seen that there appears to be more discontinuities revealing the sensitivity of mode shape of deflection changes to ply angle. This is being attributed to a soft aluminum honeycomb core.

In Figs. 6.6, 6.8, and 6.9, the buckling load as a function of ply angle at various aspect ratios for a flat sandwich panel are depicted. All of the geometrical and material properties are consistent for the panels depicted in all three figures. The difference exists in the number of plies embedded within the facings. With a face thickness of $h_f = 0.02$ in, Fig. 6.6, 6.8, and 6.9 depict a panel with one, three, and five ply facings, respectively. It is revealed that a flat sandwich panel with 3 ply facings having the same thickness as a flat sandwich panel with one ply facings exhibits higher buckling loads within a small margin at lower aspect ratios and between ply angles of $\theta = 30^\circ$ and $\theta = 60^\circ$. At higher aspect ratios and small and large ply angles there appears to be very little difference. Comparisons of the panels with three and five ply facings reveals a very small difference. In conclusion, it appears that for a flat sandwich panel with a constant face thickness that increasing the number of plies within the facings is only beneficial to increasing the buckling load capacity up to a point.

Fig. 6.10 and Fig. 6.12 depict a flat sandwich panel as a function of ply angle for various aspect ratios where the difference exists in the number of plies within the facings and the face thickness. In contrast to Fig. 6.6 as discussed earlier which depicts a flat sandwich panel with one ply facings with a face thickness of $h = 0.02$ in, Fig. 6.10 and Fig. 6.12 depict a panel containing three and five ply facings with face thicknesses of $h = 0.06$ in and 0.08 in, respectively. By comparing the three cases it is revealed that proportionately increasing the face thickness in conjunction with the number of plies within the facings, increases the buckling load capacity at all ply angles and aspect ratios. It is also revealed that as the aspect ratio increases the peak buckling load decreases and the ply angle at which the peak buckling load occurs decreases.

In Fig. 6.7, the counterpart of Fig. 6.6 for two immovable edges is depicted. It is seen that for two immovable edges that the buckling loads are lower. It is also revealed that at small and large ply angles that the margin between the buckling loads appears to be small. Between ply angles of $\theta = 35^\circ$ and $\theta = 60^\circ$ the margin appears to be much greater.

In Fig. 6.11 which is the counterpart of Fig. 6.10 for two immovable edges with three ply facings, the buckling loads appear to be smaller. Noticeable differences appear in the peak buckling loads which occur at smaller ply angles than its counterpart for all four edges being movable. Another noticeable difference is that discontinuities appear at larger ply angles. It can be seen that prior to the discontinuity there is a rise in the buckling load capacity with a decrease afterwards. In Fig. 6.13, which is the counterpart of Fig. 6.12 for the case of two immovable edges with four ply facings the same trend at larger buckling loads seems to be exhibited as in Fig. 6.11.

In Figs. 6.14, 6.15, and 6.16 the buckling load as a function of ply angle for a circular cylindrical sandwich panel with various aspect ratios is depicted for one, three, and four ply facings. As seen with the case of the flat sandwich panel as the number of plies and the face thickness increase proportionately the buckling load increases. In addition it is seen that at smaller aspect ratios the buckling load ply angle interaction seems to behave in the same manner as its flat panel counterpart. At larger aspect ratios this behavior seems to depart from the flat panel counterpart. At these larger aspect ratios there appears to be a decrease in the buckling load capacity followed by an increase and then a final decrease in the buckling loads with mode shape of deflection changes.

In Fig. 6.17, the buckling load as a function of the panel aspect ratio is depicted for a flat sandwich panel with five ply facings for three different lay-ups. All three lay-ups reveal a decrease in the buckling load with an increase in the aspect ratio. The [90°/-90°/90°/-90°/90°] lay-up appears to exhibit the lowest buckling loads up to an aspect ratio of $\psi = 2.4$, beyond which the [45°/-45°/45°/-45°/45°] lay-up exhibits the lowest buckling loads . This latter lay-up also exhibits the largest buckling loads of the three lay-ups up to an aspect ratio of $\psi \cong 2.4$. For aspect ratios greater than $\psi \cong 2.4$ the [0/0/0/0/0] lay-up yields the largest buckling loads.

In Fig. 6.18, which is the counterpart of Fig. 6.17 for the case of two immovable edges, the buckling loads appear to occur at smaller values than for the case of all four edges being movable. This difference appears to be more pronounced at smaller aspect ratios as opposed to the larger aspect ratios. In addition, the [0/0/0/0/0] and [90°/-90°/90°/-90°/90°] lay-ups relative to one another seem to reveal the same trend as in the case of all four edges being movable. The [45°/-45°/45°/-45°/45°] lay-up seems to reveal the lowest buckling load capacity of the three lay-ups up to aspect ratios of $\psi \cong 1$ beyond which this lay-up exhibits the largest buckling load capacity to an aspect ratio of $\psi \cong 1.75$. Finally from an aspect ratio of $\psi \cong 2.1$ or greater this lay-up exhibits the lowest buckling load capacity.

In Fig. 6.19, the counterpart of Fig. 6.17 for the case of a circular cylindrical sandwich panel is depicted. Clearly it is seen that the buckling loads occur at larger values than in the case of its flat panel counterpart. Another difference can be seen in the [45°/-45°/45°/-45°/45°] and [90°/-90°/90°/-90°/90°] layups where instead of the buckling loads decreasing with increasing aspect ratios, they appear to increase beyond an aspect ratio of $\psi \cong 1.6$. The [0/0/0/0/0] lay-up appears to exhibit the same trend as in the case of the flat sandwich panel but at larger values of the buckling load.

In Figs. 6.20 and 6.21, the buckling load as a function of aspect ratio for a circular cylindrical sandwich panel for various curvatures is depicted. Fig. 6.20 is depicted for a lay-up of [0/0/0/0/0] and Fig. 6.21 is depicted for a lay-up of [45°/-45°/45°/-45°/45°]. The [0/0/0/0/0] lay-up appears to reveal that the buckling load decreases with an increase in the panel aspect ratio at smaller curvatures. At larger values of the curvature, the buckling loads decrease to aspect ratios of $\psi \cong 1.3$ to $\psi \cong 1.75$, between curvatures of 0.0075 and 0.0150 in magnitude. For the [45°/-45°/45°/-45°/45°] lay-up, depicted in Fig. 6.21, the buckling load decreases with an increase in the aspect ratio. In contrast to the [0/0/0/0/0] lay-up, discontinuities are revealed at larger curvatures indicating that mode shape of deflection changes are occuring.

6.2 Thermomechanical Postbuckling of Anisotropic Sandwich Panels

In Figs. 6.22 and 6.23, the amplitude of pressure as a function of amplitude of deflection is depicted, for four ply facings. Figure 6.22 depicts these interactions for all four edges being movable while Fig. 6.23 depicts these interactions for two immovable edges along the unloaded

edges. It is revealed that beyond ply angles of 45^o that the load capacity of the panel decreases. It is also revealed that by the comparison of the two cases, that for the case of two immovable edges between ply angles of 60^o-90^o that the load capacity of the panel is greater than for the case of all four edges being movable.

In Fig. 6.25, the compressive edge load deflection interaction is depicted for one ply facings with all four edges movable for the geometrical and material properties specified. It is revealed that the buckling bifurcation increases to ply angles of 30^o after which the buckling bifurcation decreases. In addition, within the deep postbuckling range, it can be seen that the load carrying capacity decreases as the ply angles increase.

In Fig. 6.26, the same interactions are depicted as in Fig. 6.25 but for a different set of materials and a smaller face thickness. Here it is revealed that the buckling bifurcation increases to ply angles of 45^o after which, as the ply angles increase, the buckling bifurcation decreases. The same type of behavior can be seen where, as the ply angles increase, the load carrying capacity of the panel decreases, within the deep postbuckling range. In Fig. 6.24, the same trend can be seen as in Fig. 6.26.

In Fig. 6.27, the same conditions are depicted as in Fig. 6.26 but for three ply facings. The same type of behavior can be seen for the deep postbuckling range but differs at the buckling bifurcation. It is revealed that at the smaller ply angles the buckling bifurcation is a little larger in magnitude as opposed to the conditions depicted in Fig. 6.26.

In contrast to Fig. 6.27, Fig. 6.28 depicts the same conditions and interactions but at a larger face thickness. Here it is seen that the buckling bifurcation points are much higher with the familiar behavior that as the ply angles increase in the deep postbuckling range, the load carrying capacity of the panel decreases. The counterpart of Fig. 6.28 is depicted in Fig. 6.29, where the compressive edge loading as a function of the end-shortening is depicted. Here it is seen that as the ply angles increase, the end-shortening capacity increases. At smaller ply angles, the end-shortening capacity is much smaller.

In contrast to Fig. 6.28, Fig. 6.30 depicts the same conditions and interactions but at a proportionately larger face thickness. Here it is seen that the same type of behavior exists but at a much higher load carrying capacity. The counterpart of Fig. 6.30 is depicted in Fig. 6.31 where the same type of behavior can be seen as in Fig. 6.29.

In Fig. 6.32, the counterpart of Fig. 6.28 is depicted for the case of two immovable edges along the unloaded edges. Here it is revealed that the onset of buckling occurs at much smaller ply angles for all ply angle configurations. In addition, it is apparent that the maximum buckling bifurcation occurs at a ply angle of 30^o as opposed to 45^o as previously seen with the case of all four edges being movable. In Fig. 6.33, which is the counterpart of Fig. 6.32, again it is seen that at larger ply angles the end-shortening is greater for a given compressive edge load. In addition, it is also revealed that the buckling bifurcation occurs at smaller magnitudes of the end-shortening as opposed to the case of all four edges being movable.

In Fig. 6.34. which is the counterpart of Fig. 6.30, for the case of two immovable edges, it is revealed that the same type of behavior is seen as depicted for the case in Fig. 6.32. Where the maximum buckling bifurcation is reached at around ply angles of 30^o. Without being repetitive, the counterpart of Fig. 6.34 which is depicted in Fig. 6.35, reveals the same type of behavior as depicted in Fig. 6.33.

In Fig. 6.36, for a fixed biaxial load ratio, the uniaxially compressive edge load as a function of deflection is depicted for a flat sandwich panel with three ply facings. The biaxial load ratio which is defined as $L_R = \tilde{N}_{22} / \tilde{N}_{11}$ is fixed at a ratio of 0.25. This implies that $\tilde{N}_{22}$ is smaller in magnitude than $\tilde{N}_{11}$. With all four edges being loaded , in contrast to Fig. 6.27 where $\tilde{N}_{22} = 0$, it is seen that the buckling load capacity is much smaller and that the load carrying capacity of the panel beyond buckling is reduced.

In Fig. 6.38, which is an extension of Fig. 6.37 for various fixed biaxial load ratios with the uniaxial compressive edge load $\tilde{N}_{11}$ as a function of the amplitude of deflection, for the given lay-up depicted, it is revealed that as the biaxial load ratio increases the onset of buckling decreases. In addition, at larger ratios, on the negative scale, which implies two edges are in tension while the other two edges are in compression, the load carrying capacity of the panel appears to increase in the deep postbuckling range. Also, the onset of buckling occurs at much larger load magnitudes.

In Fig. 6.39, the influence of geometrical imperfections on the compressive edge load-deflection interaction of a flat sandwich panel with simply supported edge conditions consisting of a fixed lay-up in the facings is depicted. It is revealed that buckling bifurcation occurs in the absence of geometrical imperfections. In addition, if positive imperfections exist, it is revealed that a monotonous increase of the deflection with the compressive edge load occurs in the positive direction. The influence of geometrical imperfections on the compressive edge load-deflection interaction reveals the same type of behavior, in the case of a circular cylindrical sandwich panel, as depicted in Fig. 6.40. In the case of a circular cylindrical sandwich panel, it is apparent that buckling bifurcation occurs without imperfections, as in the previous case, but at a higher compressive edge load. In addition, the same type of monotonous behavior is seen with positive imperfections attributed to positive deflections and negative imperfections attributed to negative dflections.

In Fig. 6.41, for the given combinations of loadings and geometrical and material properties, with three ply facings, exposed to positive bottom surface temperatures it is revealed that the snap-through type behavior appears to be suppresed at ply angles of 45^o. In contrast to Fig. 6.41, In Fig. 6.42, for the given conditions it appears that the snap-through behavior is suppresed at ply angles of 30^o, 45^o, and 60^o . In Fig. 6.43, where positive temperatures appear on the upper surface, it appears again that the snap-through behavior can be suppressed at ply angles of 30^o, 45^o, and 60^o.

6.3 Stress/Strain of Anisotropic Sandwich Panels

In Fig. 6.44, the inplane strain ε_{11} is plotted as a function of ply angle, in the geometrical and material coordinate systems, at the onset of buckling bifurcation, for a flat sandwich panel with one ply facings. These relationships have been depicted for both movable and two immovable edges. It is revealed that the inplane strain ε_{11}, in the geometrical coordinate system, is very sensitive to the variation in the ply angles, for both movable and immovables edges. In contrast, ε_{11}, in the geometrical coordinate system, appears to be slighlty lower, in magnitude, for the case of two immovable edges. The trend reveals a substantial decrease from ply angles of 0^o to ply angles of aproximately 55^o beyond which a substantial increase to ply angles of 90^o is revealed. The inplane strain ε_{11}, in the material coordinate system for both cases of the tangential boundary conditions, reveals a very small sensitivity to the variation in the ply angles. In addition, the inplane strain ε_{11}, within the material coordinate system, reveals only a slight difference between the cases of movable and two immovable edges.

In Fig. 6.45, the inplane strain ε_{22} is depicted for the same relationships as depicted in Fig. 6.44. It is revealed that the trends seen in Fig. 6.44 for both the geometrical and material coordinate systems are reversed, in Fig. 6.45. In addition, the inplane strain ε_{22} appears to reveal a larger margin between both types of tangential boundary conditions, within the geometrical coordinate system. With $\varepsilon_{22} = 0$, for two immovable edges, in the geometrical coordinate system, ε_{22} for all four edges being movable, reveals a slightly larger sensitivity to the variation in the ply angles, in contrast to the trend revealed in Fig. 6.44, for the inplane strain ε_{11}.

In Fig. 6.46, The inplane shear strain γ_{12} as a function of ply angle, with one ply facings for a flat sandwich panel, in the geometrical and material coordinate systems, at the onset of buckling bifurcation, is depicted. The trends in both coordinate systems for both movable and two immovable edges reveal a very large sensitivity to the variation in ply angles. The largest magnitude of the inplane shear strain γ_{12} is revealed in the material coordinate system for the case of all four edges being movable.

In Fig. 6.47, the inplane stress σ_{11} as a function of ply angle for a flat sandwich panel with one ply facings, at the onset of buckling bifurcation, is depicted. The trends reveal a sudden dip followed by an uphill type increase for both cases of tangential boundary conditions and in both coordinate systems. The majority of the largest magnitude of the inplane stress σ_{11} exists for the case of movable edges in the material coordinate system. The lowest values are seen in the geometrical coordinate system for the case of movable edges.

In Fig. 6.48, the inplane stress σ_{22} is depicted for the same relationships as depicted in Fig. 6.47. The inplane stress σ_{22} in the material coordinate system for the both types of edge conditions reveals a large sensitivity to the variation in the ply angles with a fall and rise type of trend. In contrast, the trend exhibited, within the geometrical coordinate system, reveals a much smaller sensitivity to the variation in the ply angles.

The inplane shear stress σ_{12} as a function of the ply angle for a flat sandwich panel, at the onset of buckling bifurcation, is depicted in Fig. 6.49. Here the same type of trend for σ_{12} in the material coordinate system can be seen as was seen in Fig. 6.46, where the relationship of shear strain to the variation in the ply angle was depicted. It is also revealed, within the geometrical coordinate system, that the inplane shear stress $\sigma_{12} = 0$ for both types of edge conditions.

The inplane stresses σ_{11}, σ_{22}, σ_{12} as a function of ply angle for circular cylindrical sandwich panel with one ply facings, at the onset of buckling bifurcation, in the geometrical and material coordinate systems for movable edges is depicted in Fig. 6.50. The trends revealed by these three inplane stresses show similar trends as seen for the flat sandwich panel counterpart but at slightly larger magnitudes of stress.

The counterpart of Fig. 6.50 for the inplane strains ε_{11}, ε_{22}, γ_{12} is depicted in Fig. 6.51. In comparison to the flat sandwich panel counterpart, the inplane strains ε_{11}, ε_{22}, γ_{12} appear to be slightly larger.

6.4 Buckling, Postbuckling, and Stress/Strain Figures

Buckling Results

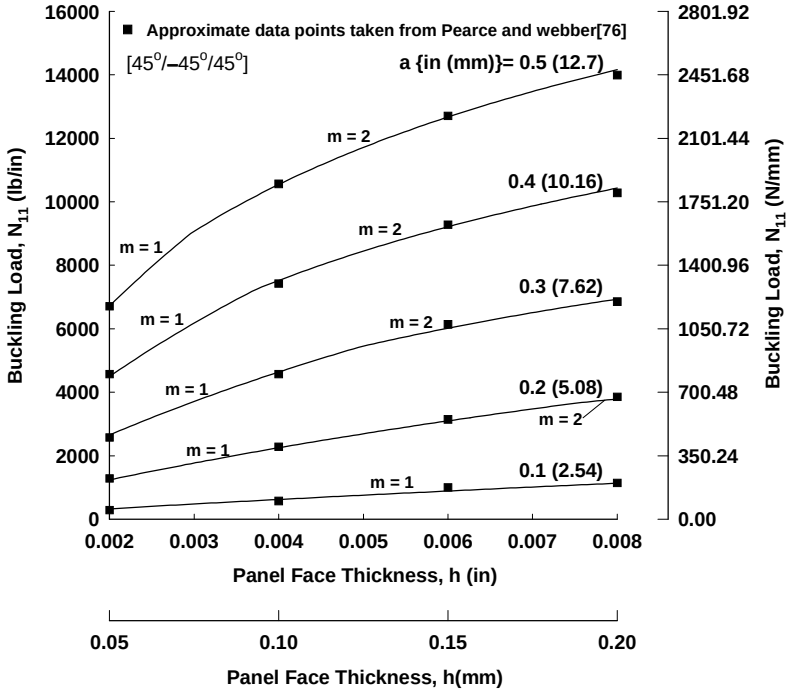

Fig 6.1. The effect of the distance between the local midsurface of the faces and the midsurface of the core upon the buckling load and the panel face thickness interaction for a flat panel. All four edges are movable and simply supported. (Note: n = 1 is fixed ; $L_1 = L_2 = 9$ in, Materials F5:C2)

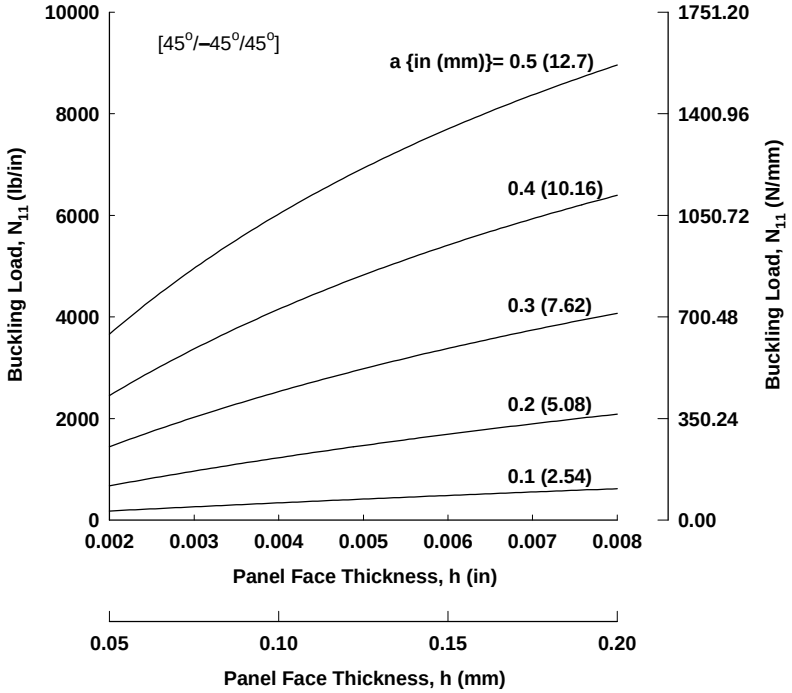

Fig. 6.2. The counterpart of Fig. 6.1. for the case of two immovable edges along ($x_2 = 0$, L_2). (Note: m = n = 1)

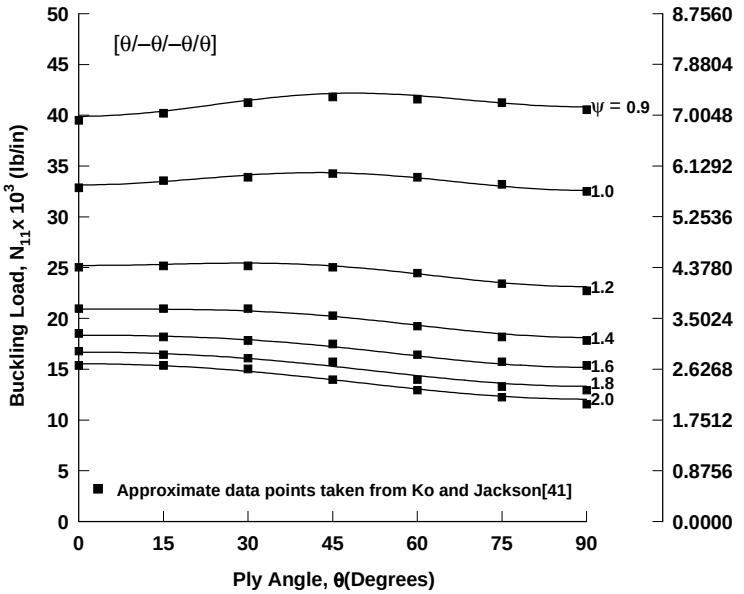

Fig. 6.3. The influence of the fiber orientation,in the facings, on the compressive buckling strengths of a flat sandwich panel with four layered facings. All four edges are movable and simply supported. (Note: m = n =1)

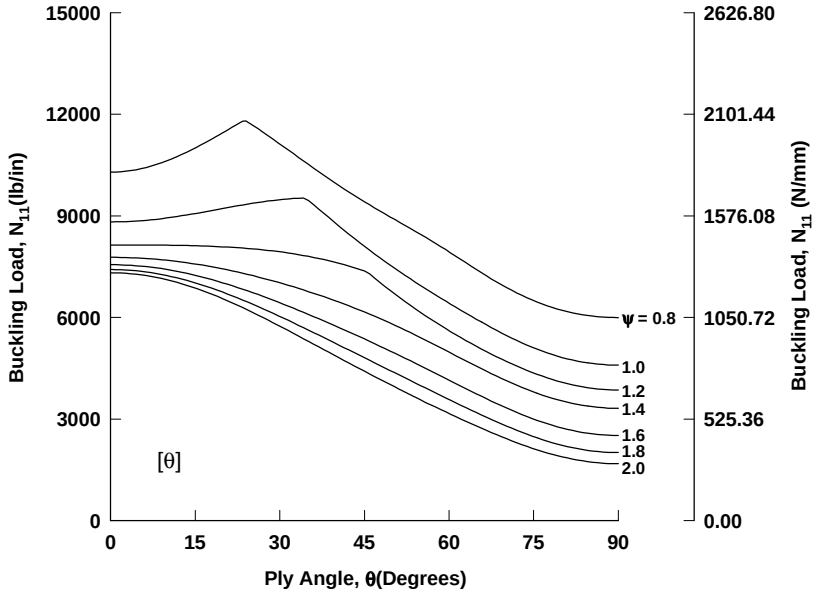

Fig. 6.4. The influence of the fiber orientation,in the facings, on the compressive buckling strengths of a flat sandwich panel with single layered facings. All four edges are movable and simply supported. (Note: prior to the first discontinuities, m = n = 1 beyond which n = 1, m = 2 ; L_1 = 24 in, h_f = 0.05 in, h_c = 0.5 in, Materials F1:C3)

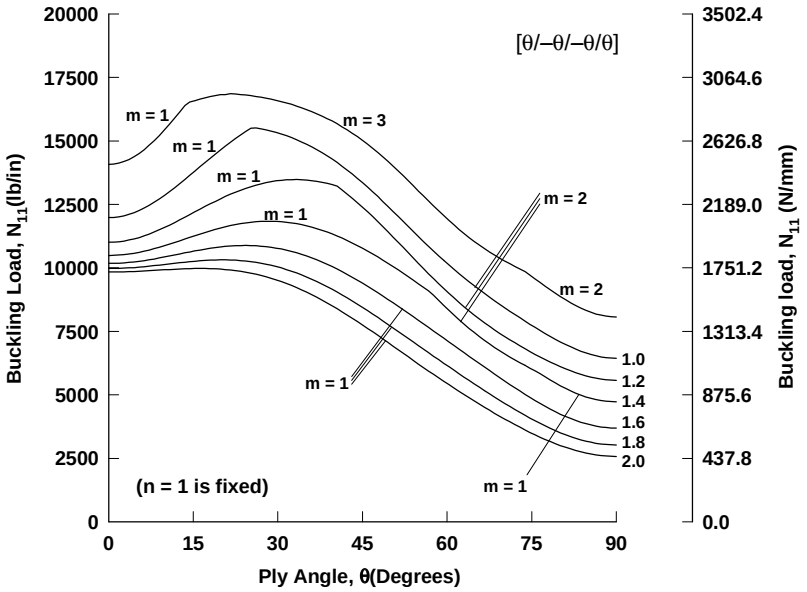

Fig. 6.5. The influence of the fiber orientation,in the facings, on the compressive buckling strengths of a flat sandwich panel with four layered facings. All four edges are movable and simply supported. (L_1 = 24 in, h_f = 0.08 in, h_c = 0.5 in, Materials F1:C3)

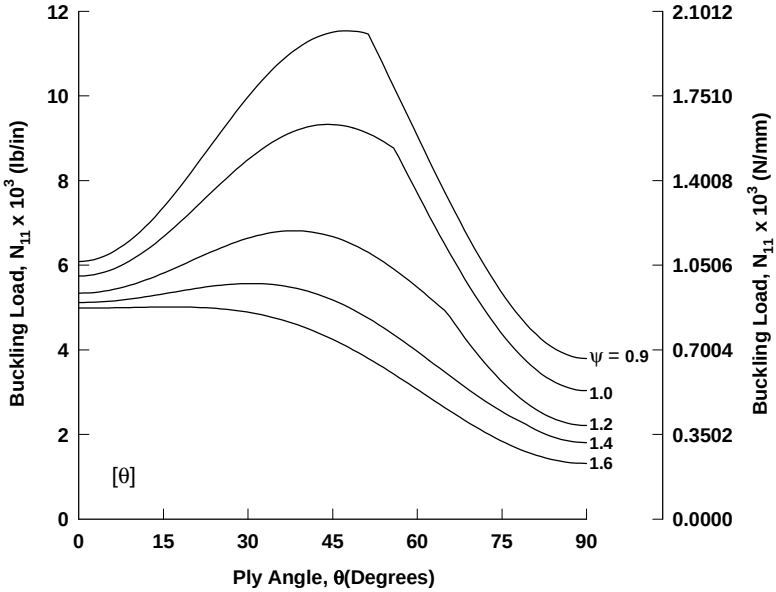

Fig. 6.6. The influence of the fiber orientation,in the facings, on the compressive buckling strengths of a flat sandwich panel with single layered facings. All four edges are movable and simply supported. (Note: prior to the first discontinuities, m = n = 1 beyond which n = 1, m = 2 ; L_1 = 24 in, h_f = 0.02 in, h_c = 0.5 in, Materials F1:C1)

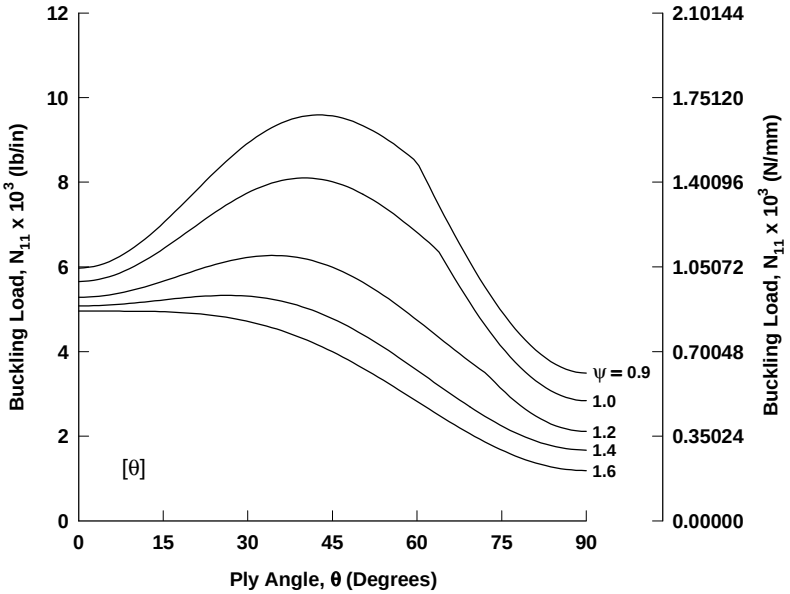

Fig. 6.7. The counterpart of Fig. 6.6. for the case of two immovable edges along (x_2 = 0, L_2).(Note: prior to the first discontinuities, m = n = 1 beyond which n = 1, m = 2)

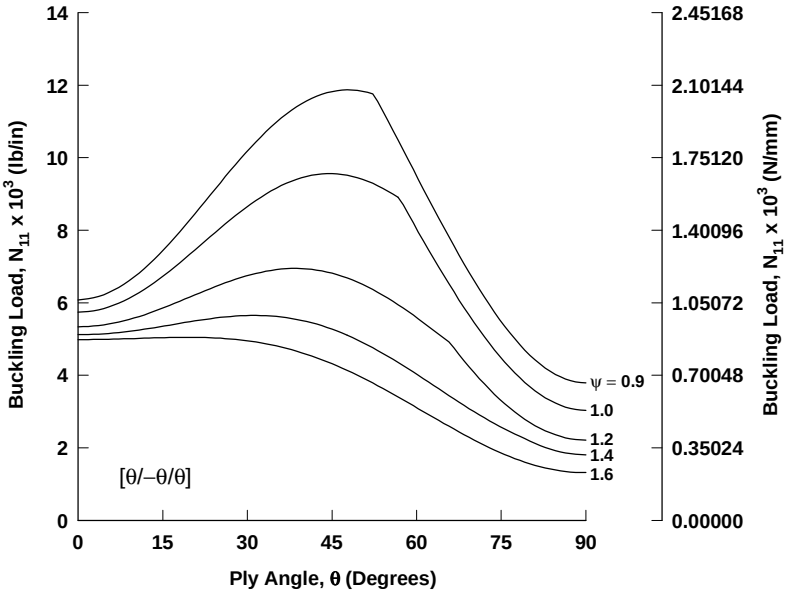

Fig. 6.8. The influence of the fiber orientation,in the facings, on the compressive buckling strengths of a flat sandwich panel with three layered facings. All four edges are movable and simply supported. (Note: prior to the first discontinuities, m = n = 1, beyond which n = 1, m = 2 ; L_1 = 24 in, h_f = 0.02, h_c = 0.5 in, Materials F1:C1)

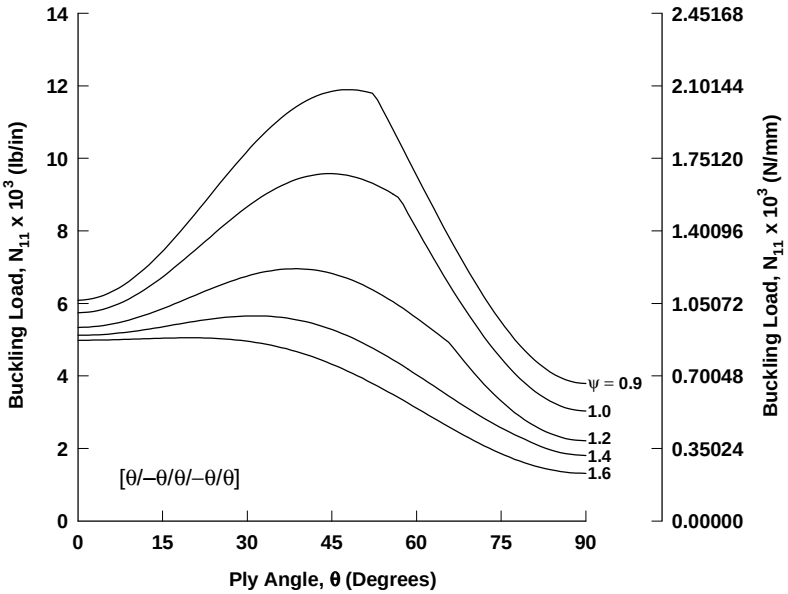

Fig. 6.9. The influence of the fiber orientation,in the facings, on the compressive buckling strengths of a flat sandwich panel with five layered facings. All four edges are movable and simply supported. (Note: prior to the first discontinuities, m = n = 1 beyond which n = 1, m = 2 ; L_1 = 24 in, h_f = 0.02 in, h_c = 0.5 in, Materials F1:C1)

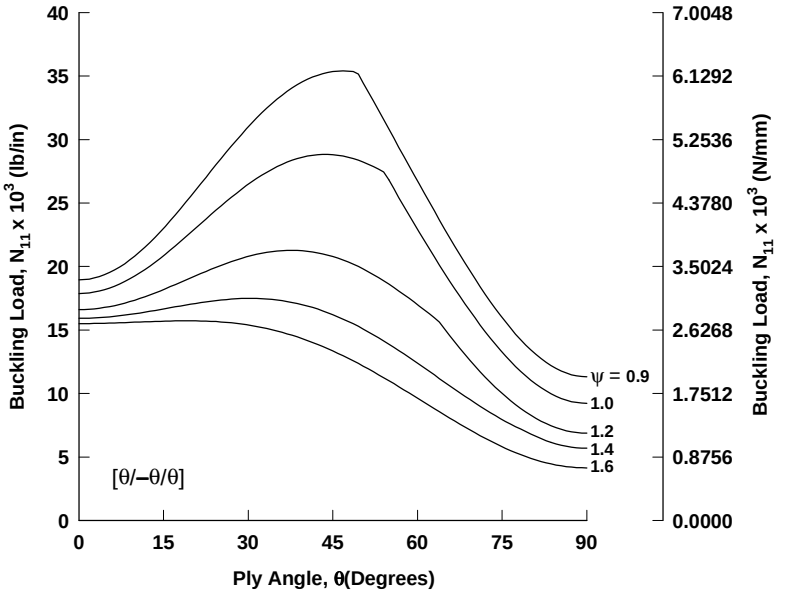

Fig. 6.10. The influence of the fiber orientation,in the facings, on the compressive buckling strengths of a flat sandwich panel with three layered facings. All four edges are movable and simply supported. (Note: prior to the first discontinuities, m = n = 1 beyond which n = 1, m = 2 ; L_1 = 24 in, h_f = 0.06 in, h_c = 0.5 in, Materials F1:C1)

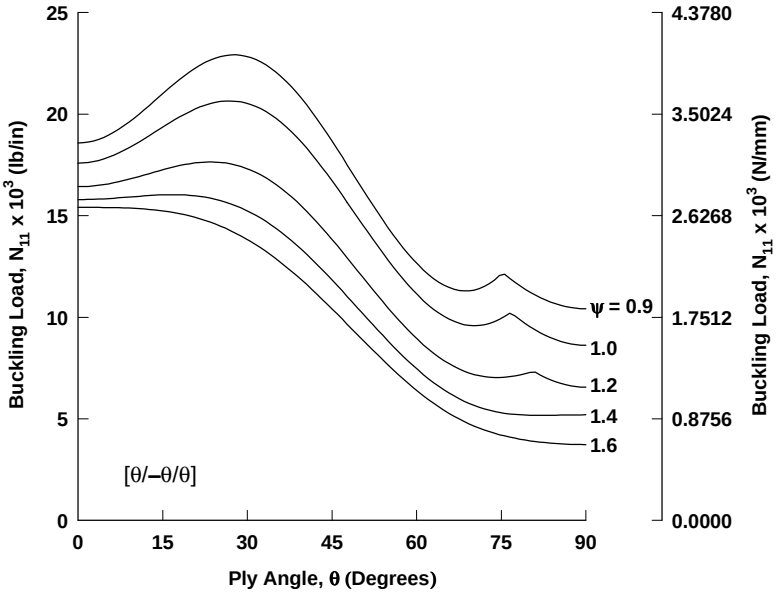

Fig. 6.11. The counterpart of Fig. 6.10. for the case of two immovable edges along (x_2 = 0, L_2). (Note: prior to the first discontinuities, m = n = 1 beyond which n = 1, m = 2)

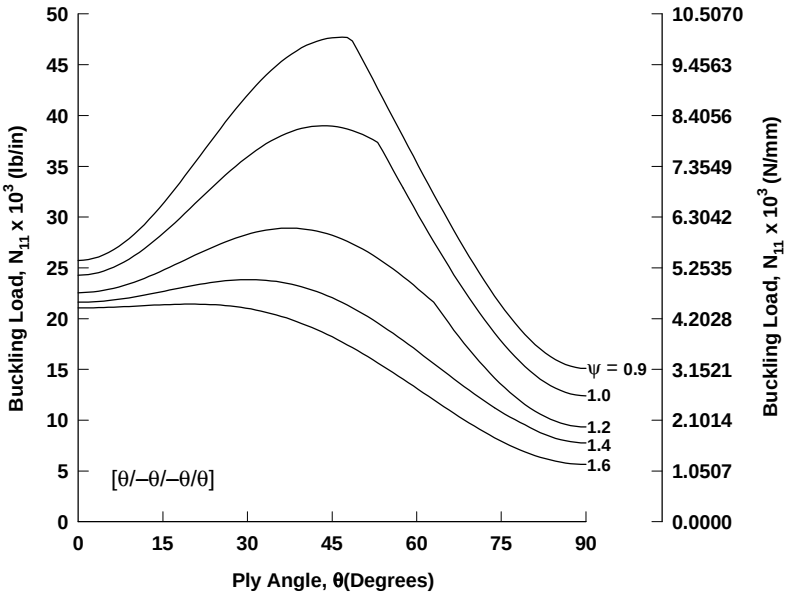

Fig. 6.12. The influence of the fiber orientation,in the facings, on the compressive buckling strengths of a flat sandwich panel with four layered facings. All four edges are movable and simply supported. (Note: prior to the first discontinuities, m = n = 1 beyond which n = 1, m = 2 ; L_1 = 24 in, h_f = 0.08 in, h_c = 0.5 in, Materials F1:C1)

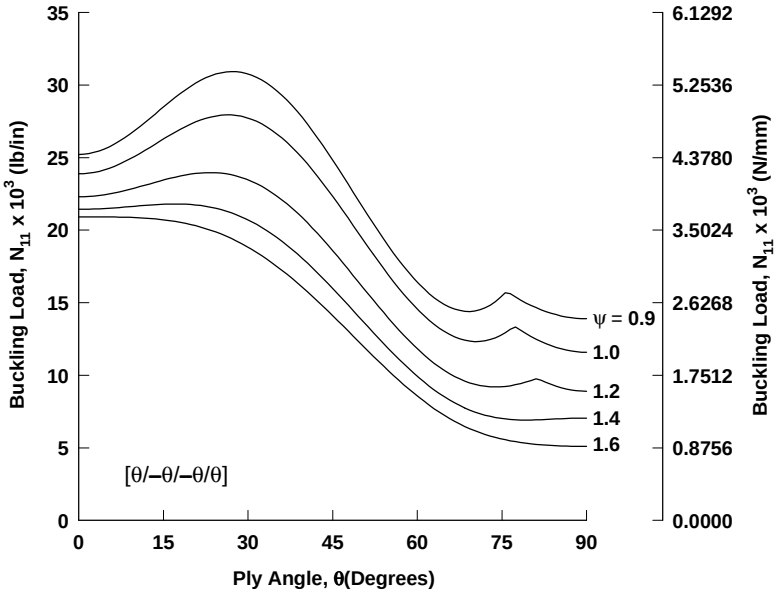

Fig. 6.13. The counterpart of Fig. 6.12. for the case of two immovable edges along (x_2 = 0, L_2).(Note: prior to the first discontinuities, m = n = 1 beyond which n = 1, m = 2)

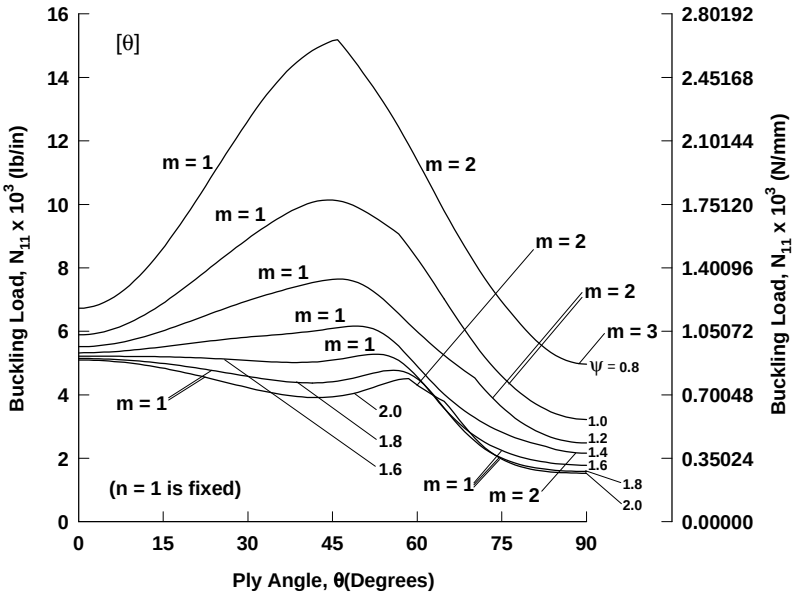

Fig. 6.14. The influence of the fiber orientation,in the facings, on the compressive buckling strengths of a circular cylindrical sandwich panel with single layered facings. All four edges are movable and simply supported. (L_1 = 24 in, h_f = 0.02 in, h_c = 0.5 in, R_2 = 100 in, Materials F1:C1)

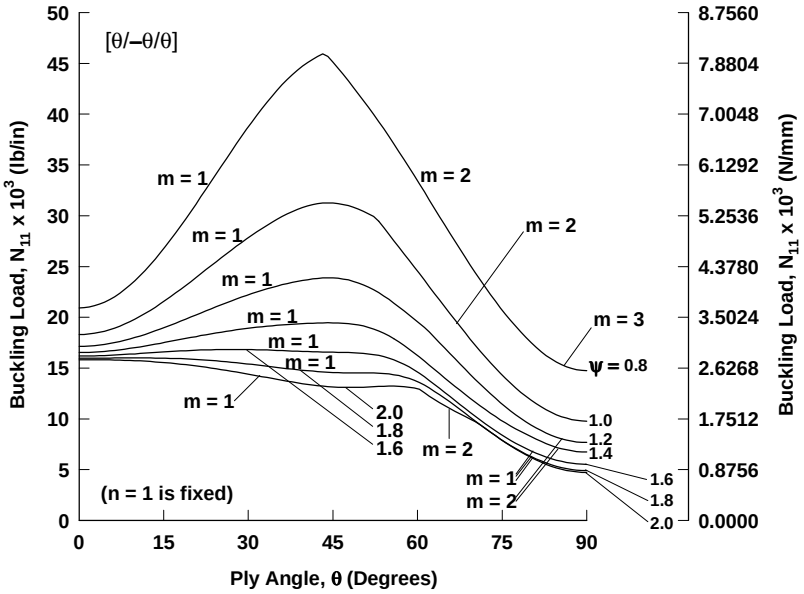

Fig. 6.15. The influence of the fiber orientation,in the facings, on the compressive buckling strengths of a circular cylindrical sandwich panel with three layered facings. All four edges are movable and simply supported. (L_1 = 24 in, h_f = 0.06 in, h_c = 0.5 in, R_2 = 100 in, Materials F1:C1)

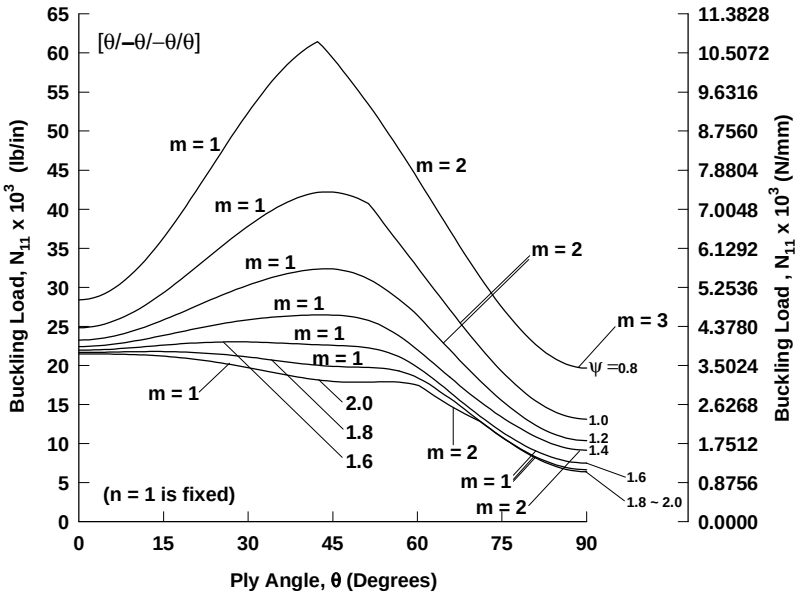

Fig. 6.16. The influence of the fiber orientation,in the facings, on the compressive buckling strengths of a circular cylindrical sandwich panel with four layered facings. All four edges are movable and simply supported. (L_1 = 24 in, h_f = 0.08 in, h_c = 0.5 in, R_2 = 100 in, Materials F1:C1)

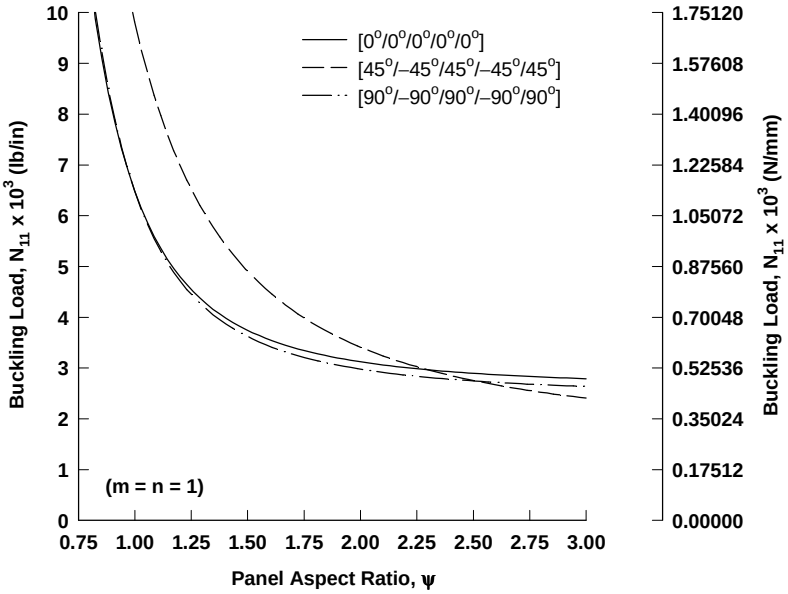

Fig. 6.17. The Buckling Load vs the panel aspect ratio ψ for a flat sandwich panel with five layered facings for three different fiber orientations. All four edges are movable and simply supported. (L_1 = 24 in, h_f = 0.025 in, h_c = 0.5 in, Materials F2:C1)

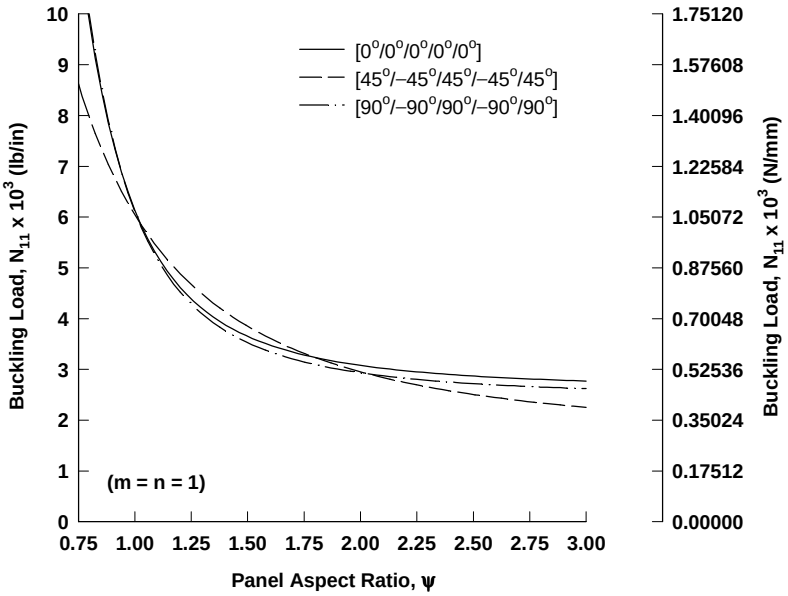

Fig. 6.18. The counterpart of Fig. 6.17. for the case of two immovable edges along (x_2 = 0, L_2).

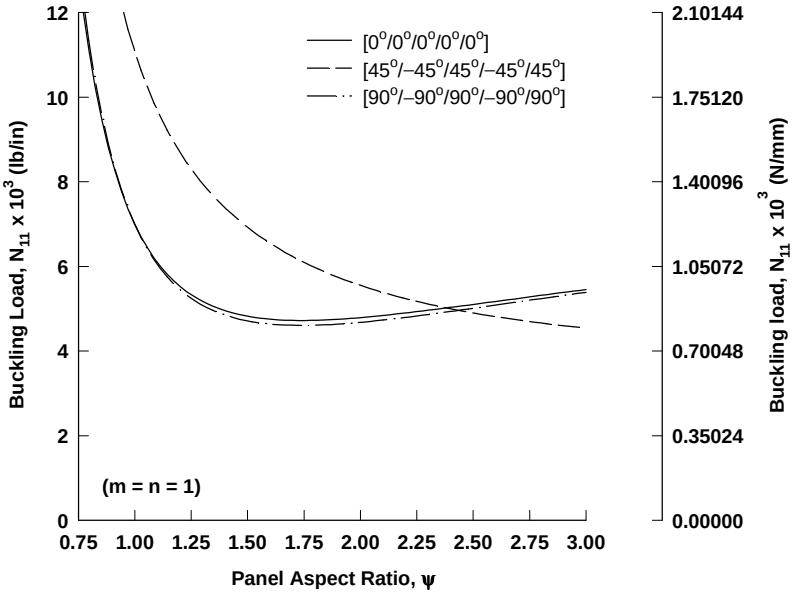

Fig. 6.19. The Buckling Load vs the panel aspect ratio ψ for a circular cylindrical sandwich panel with five layered facings for three different fiber orientations. All four edges are movable and simply supported. (L_1 = 24 in, h_f = 0.025 in, h_c = 0.5 in, R_2 = 80 in Materials F2:C1)

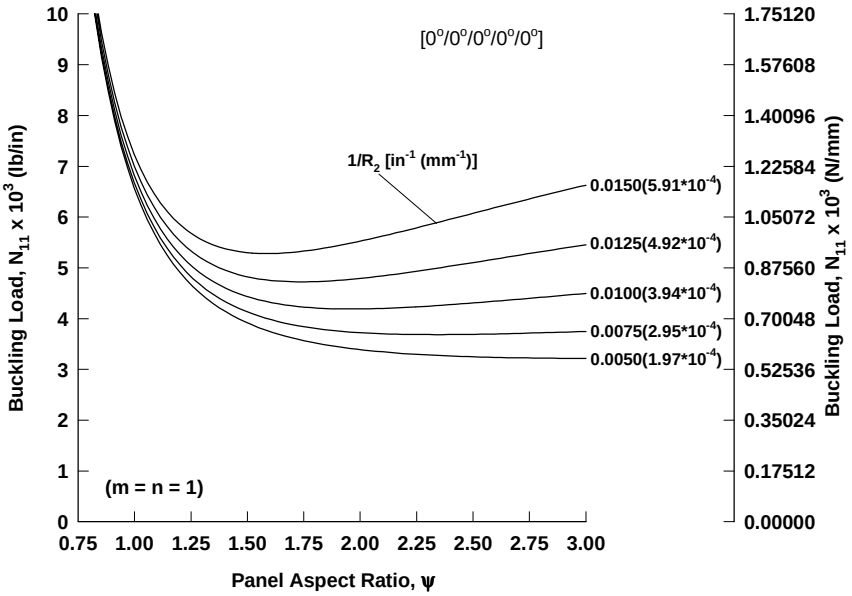

Fig. 6.20. The effect of the curvature on the buckling load and aspect ratio interaction for a fixed fiber orientation in the facings comprised of five layers for a circular cylindrical sandwich panel. All four edges are movable and simply supported. (L_1 = 24 in, h_f = 0.025 in, h_c = 0.5 in, Materials F2:C1)

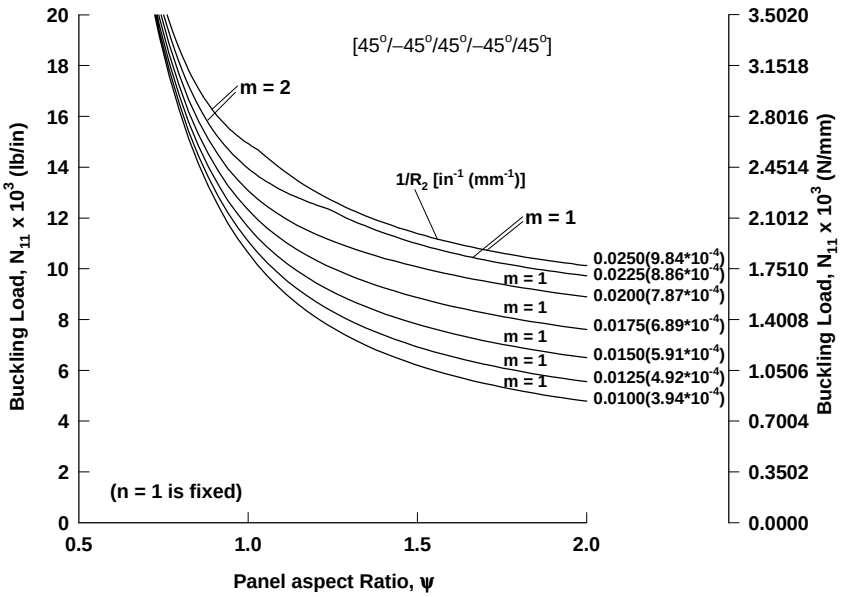

Fig. 6.21. The effect of the curvature on the buckling load and aspect ratio interaction for a fixed fiber orientation in the facings comprised of five layers for a circular cylindrical sandwich panel. All four edges are movable and simply supported. (L_1 = 24 in, h_f = 0.025 in, h_c = 0.5 in, Materials F2:C1)

Postbuckling Results

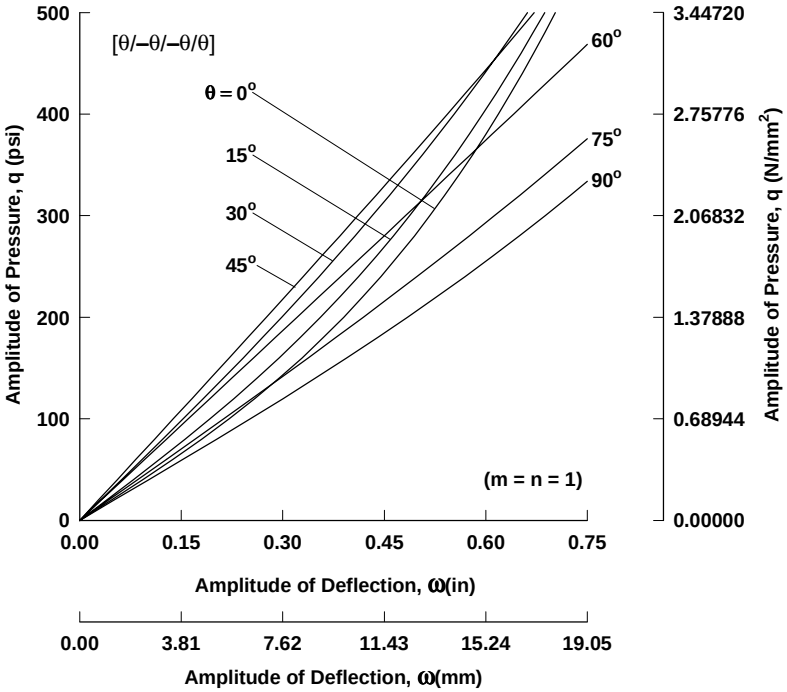

Fig. 6.22. The influence of the fiber orientation, in the facings, on the pressure deflection interaction of a circular cylindrical sandwich panel with four layered facings. All four edges are movable and simply supported. ($L_1 = L_2$ = 24 in, h_f = 0.08 in, h_c = 0.5 in, R_2 = 100 in, Materials F1:C1)

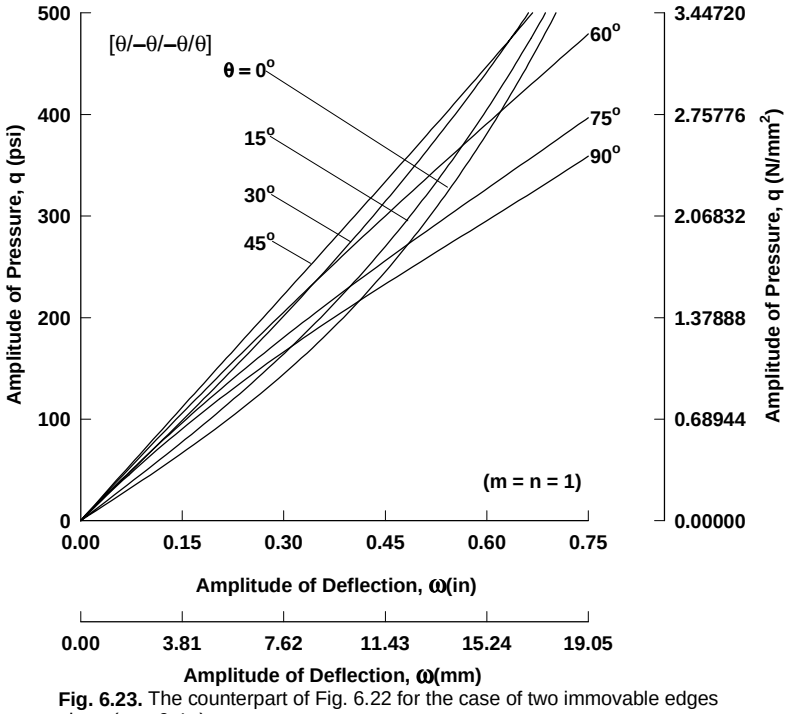

Fig. 6.23. The counterpart of Fig. 6.22 for the case of two immovable edges along (x_2 = 0, L_2).

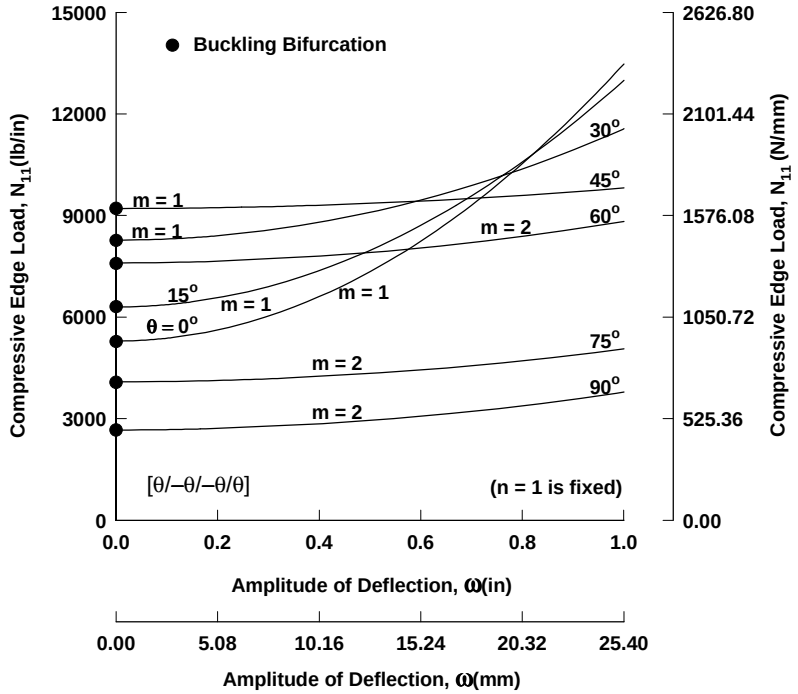

Fig. 6.24. The influence of the fiber orientation, in the facings, on the compressive load deflection interaction of a flat sandwich panel with four layered facings. All four edges are movable and simply supported. (L_1 = L_2 = 24 in, h_f = 0.0228 in , h_c = 0.5 in, Materials F4:C1)

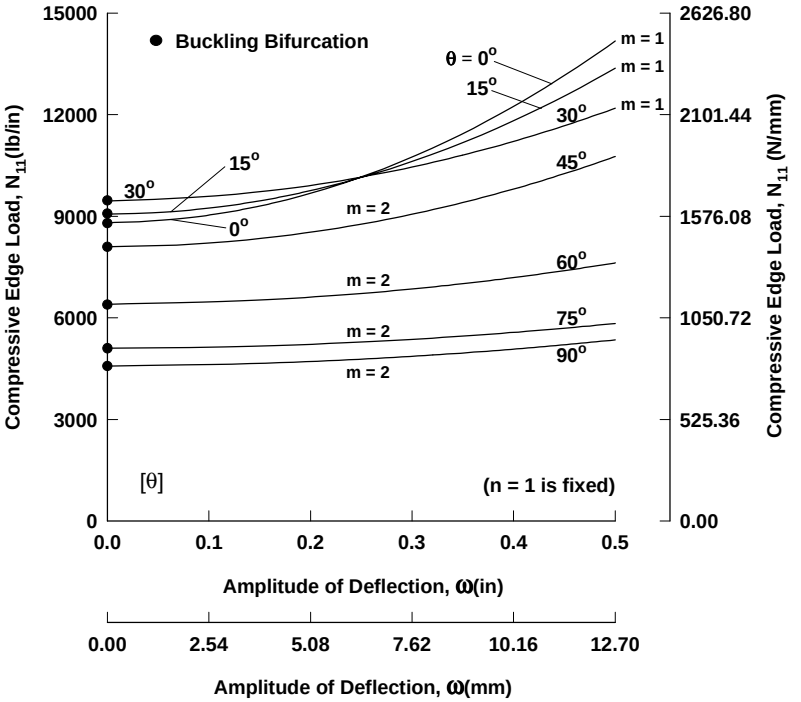

Fig. 6.25. The influence of the fiber orientation, in the facings, on the compressive load deflection interaction of a flat sandwich panel with one layered facings. All four edges are movable and simply supported. ($L_1 = L_2 = 24$ in, $h_f = 0.05$ in, $h_c = 0.5$ in, Materials F1:C3)

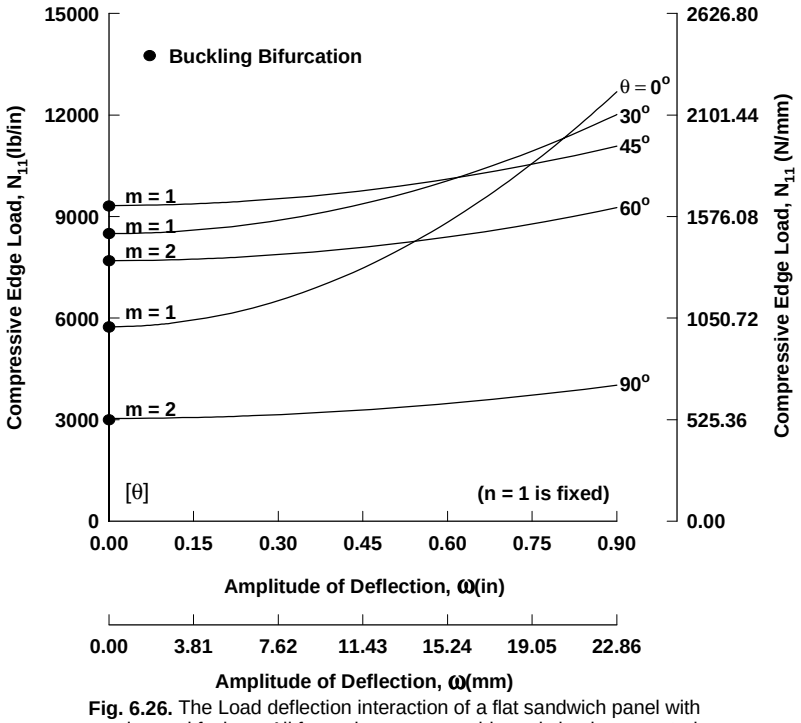

Fig. 6.26. The Load deflection interaction of a flat sandwich panel with one layered facings. All four edges are movable and simply supported. ($L_1 = L_2 = 24$ in, $h_f = 0.02$ in, $h_c = 0.5$ in, Materials F1:C1)

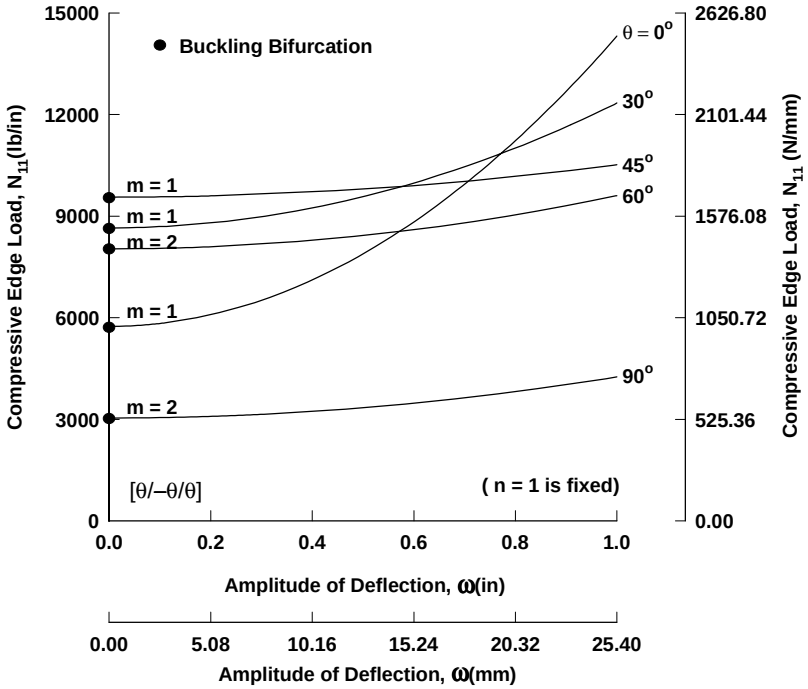

Fig. 6.27. The Load deflection interaction of a flat sandwich panel with three layered facings. All four edges are movable and simply supported. ($L_1 = L_2 = 24$ in, $h_f = 0.02$ in, $h_c = 0.5$ in, Materials F1:C1)

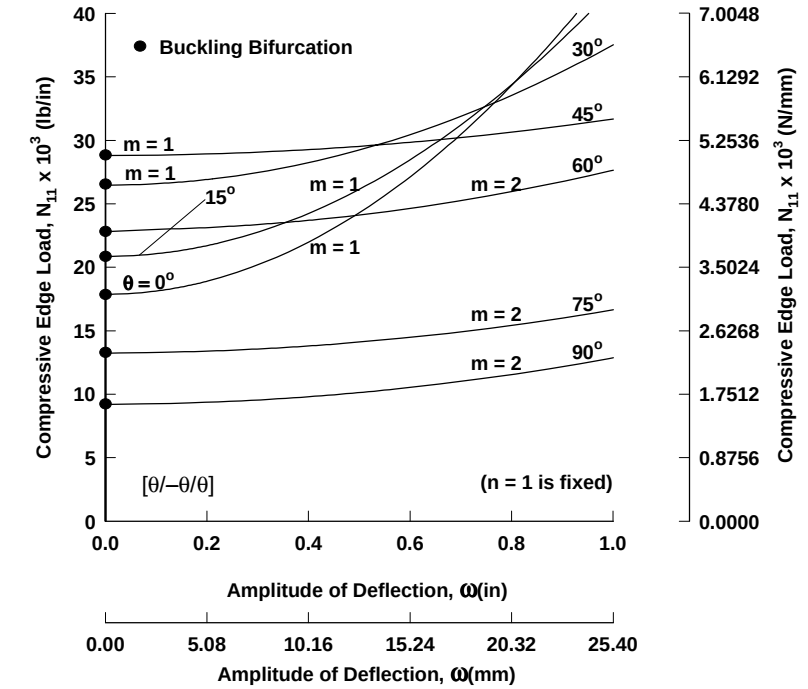

Fig. 6.28. The influence of the fiber orientation, in the facings, on the compressive load deflection interaction of a flat sandwich panel with three layered facings. All four edges are movable and simply supported. ($L_1 = L_2 = 24$ in, $h_f = 0.06$ in, $h_c = 0.5$ in, Materials F1:C1)

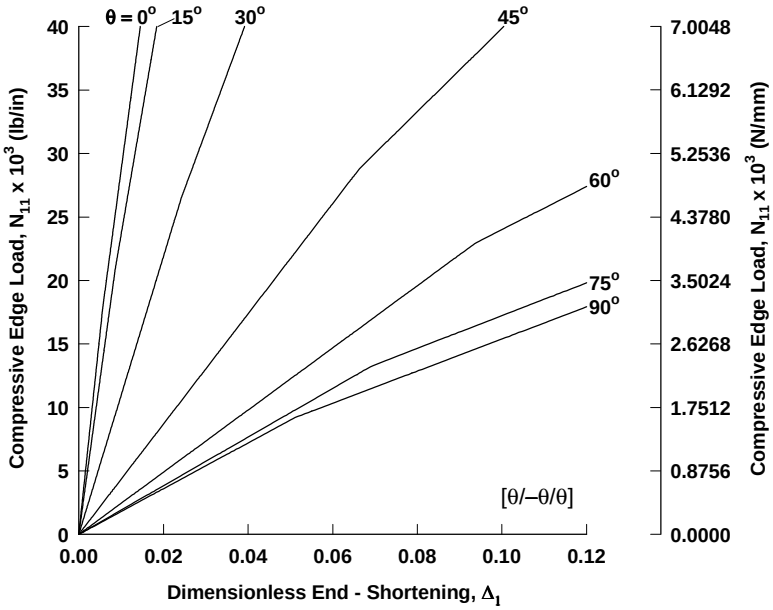

Fig. 6.29. The counterpart of Fig. 6.28., in the (N_{11}, Δ_1) plane. (see Fig. 6.28. for m, n values)

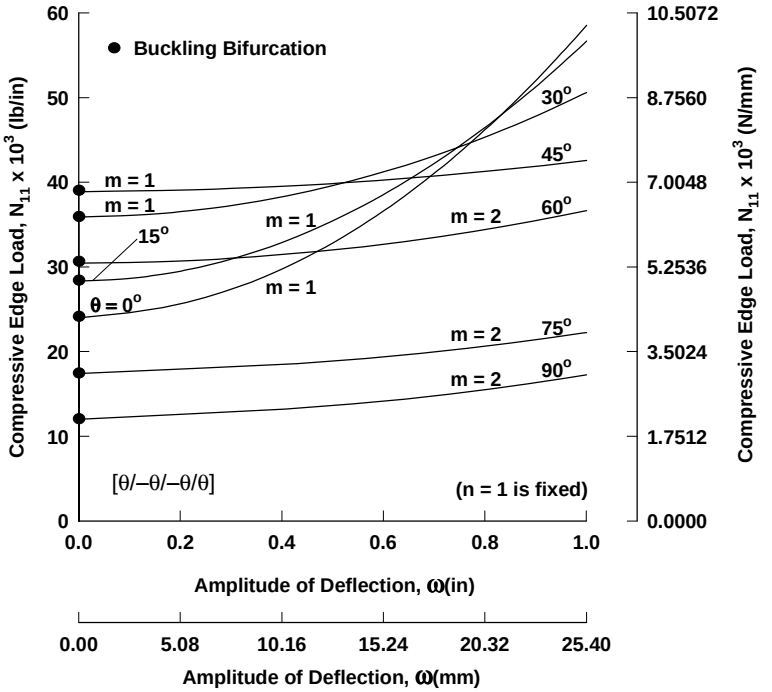

Fig. 6.30. The influence of the fiber orientation, in the facings, on the compressive load deflection interaction of a flat sandwich panel with four layered facings. All four edges are movable and simply supported. ($L_1 = L_2 = 24$ in, $h_f = 0.08$ in, $h_c = 0.5$ in, Materials F1:C1)

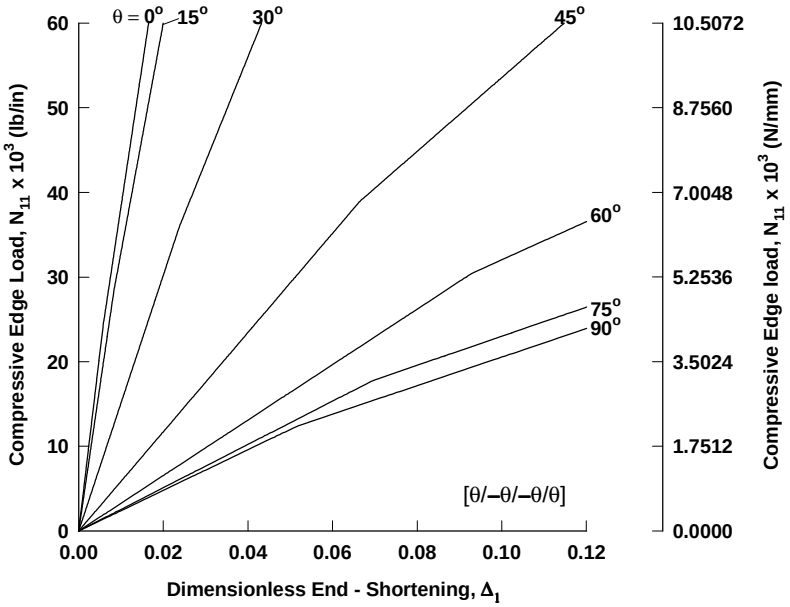

Fig. 6.31. The counterpart of Fig. 6.30., in the (N_{11}, Δ_l) plane. (see Fig. 6.30. for m, n values)

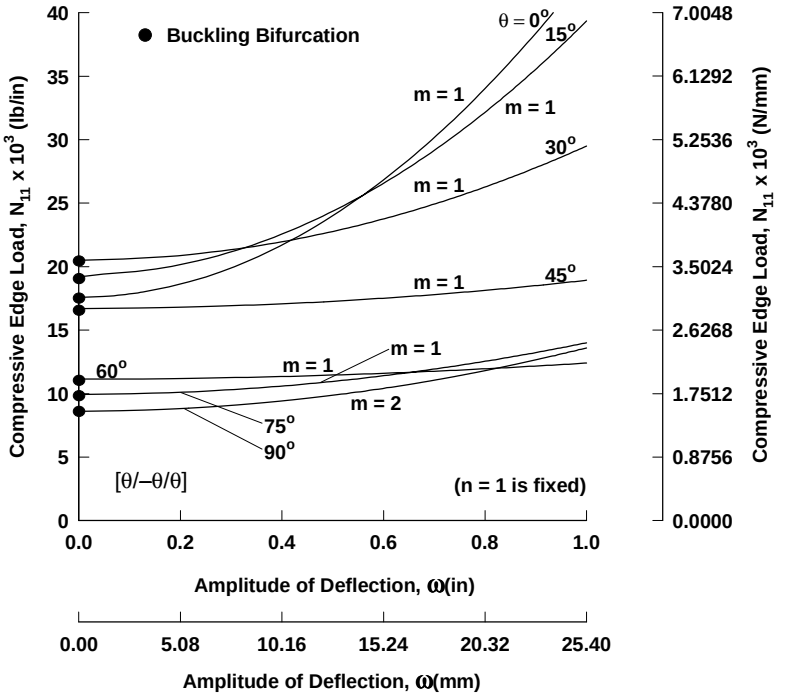

Fig. 6.32. The counterpart of Fig. 6.28. for the case of two immovable edges along ($x_2 = 0$, L_2).

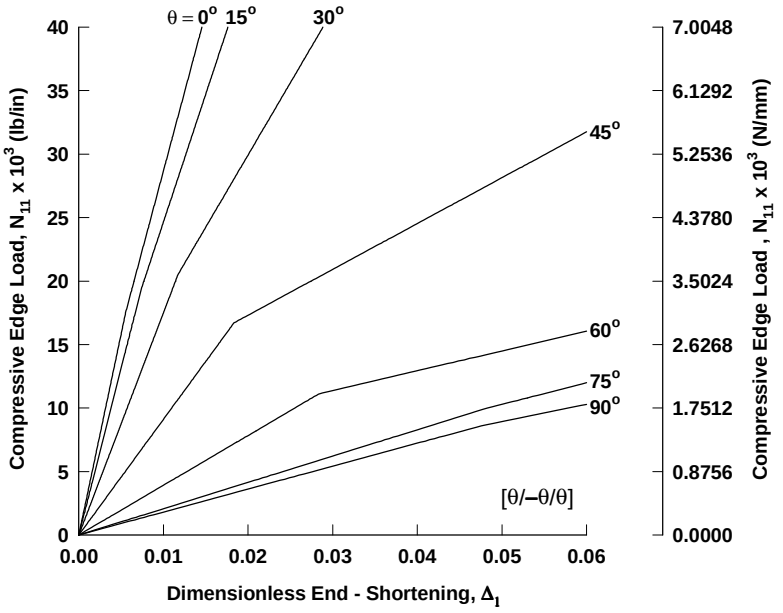

Fig. 6.33. The counterpart of Fig. 6.32., in the (N_{11}, Δ_1) plane. (see Fig. 6.32. for m, n values)

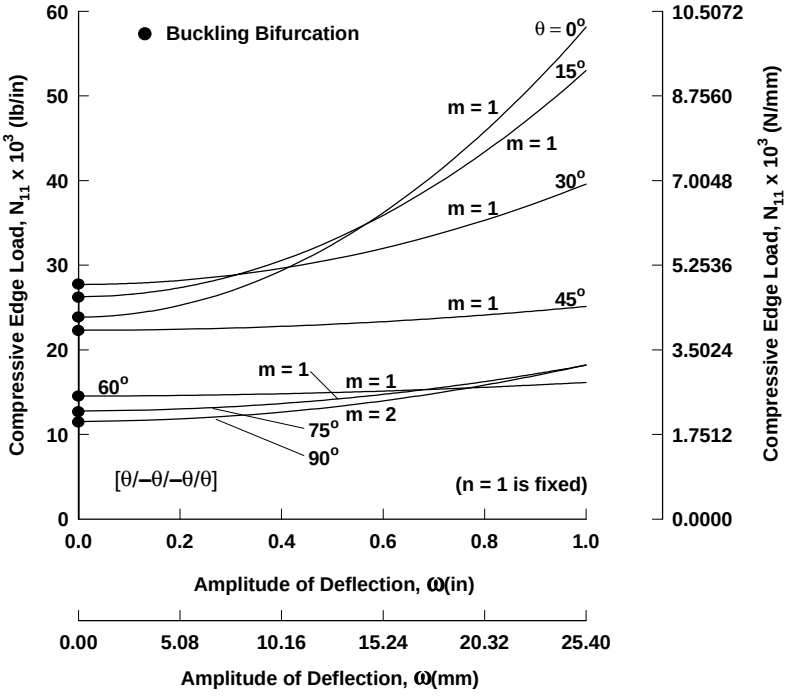

Fig. 6.34. The counterpart of Fig. 6.30. for the case of two immovable edges along ($x_2 = 0$, L_2).

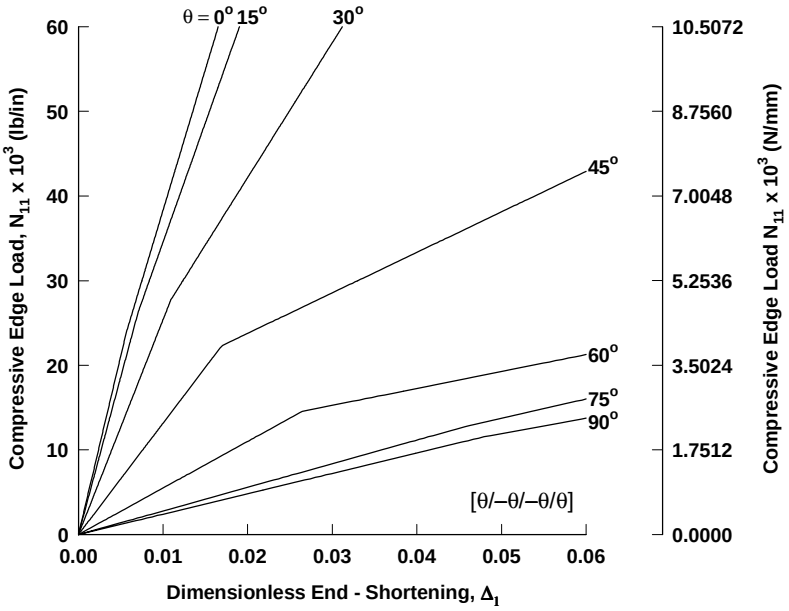

Fig. 6.35. The counterpart of Fig. 6.34., in the (N_{11}, Δ_1) plane. (see Fig. 6.34 for m, n values)

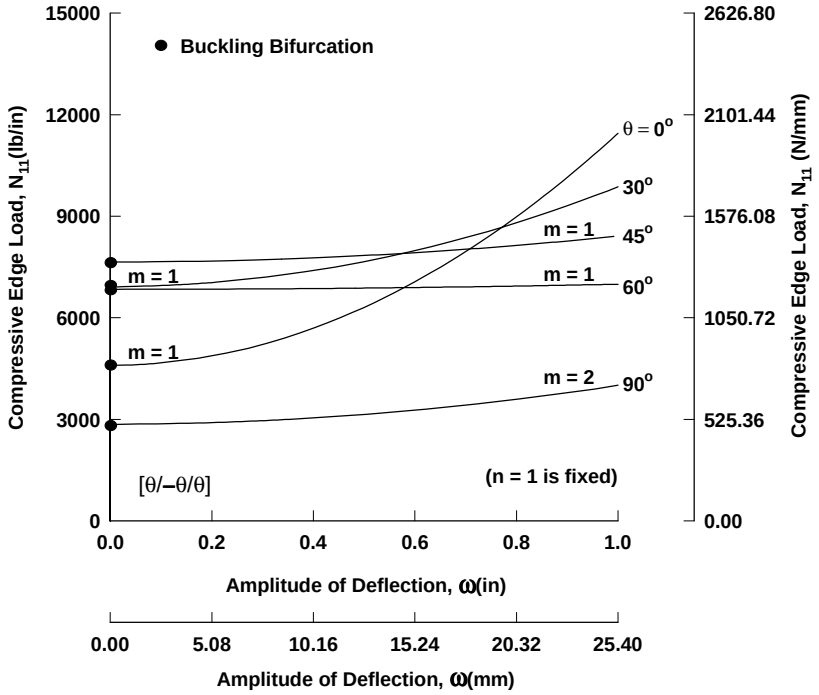

Fig. 6.36. A flat sandwich panel with three layered facings subjected to a fixed biaxial edge loading L_R. All four edges are movable and simply supported. ($L_1 = L_2 = 24$ in, $h_f = 0.02$ in, $h_c = 0.5$ in, $L_R = 0.25$ Materials F1:C1)

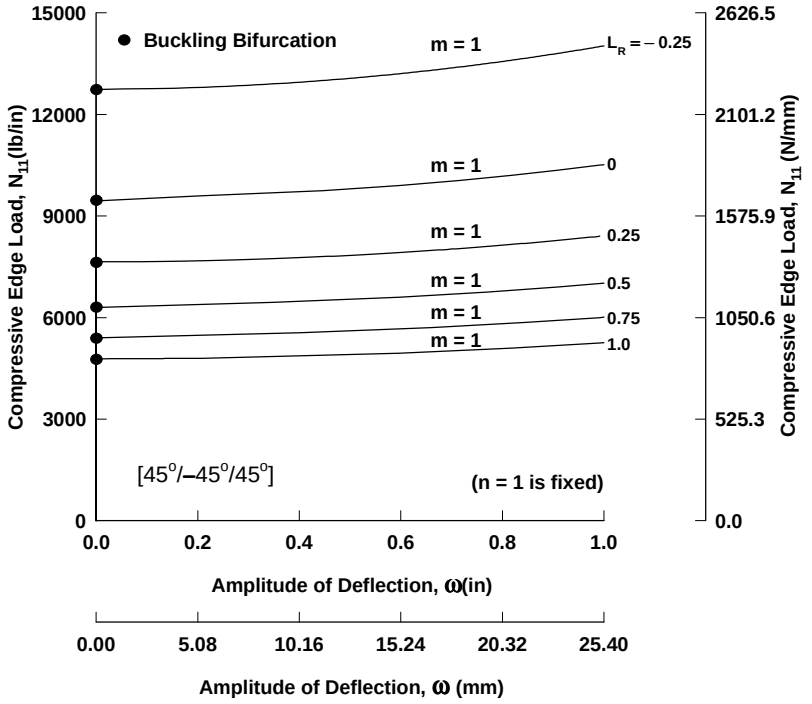

Fig. 6.37. A flat sandwich panel with three layered facings subjected to prescribed biaxial edge loadings L_R. All four edges are movable and simply supported. ($L_1 = L_2 = 24$ in, $h_f = 0.02$ in, $h_c = 0.5$ in, Materials F1:C1).

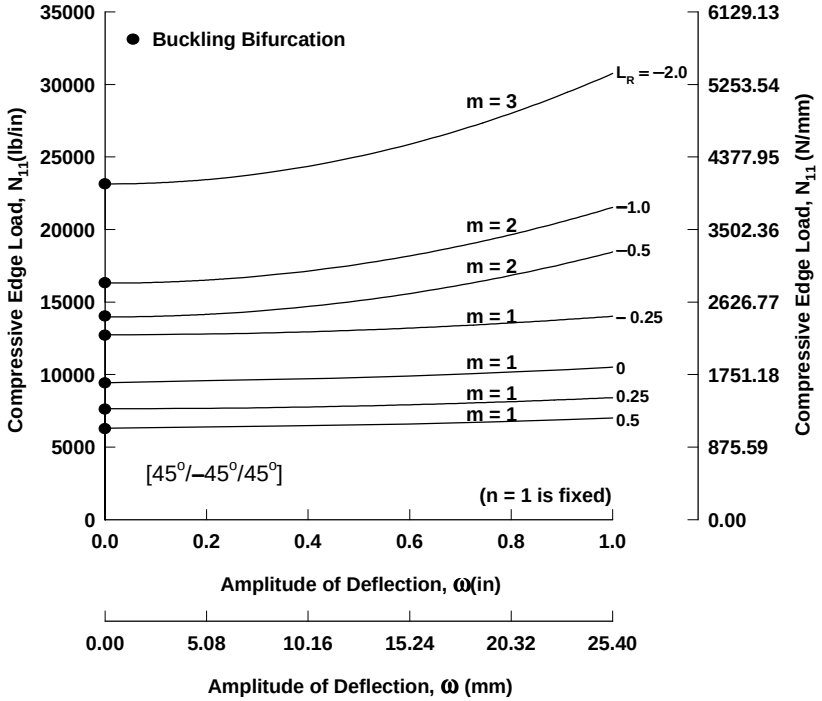

Fig. 6.38. A flat sandwich panel with three layered facings subjected to prescribed biaxial edge loadings L_R. All four edges are movable and simply supported. ($L_1 = L_2 = 24$ in, $h_f = 0.02$ in, $h_c = 0.5$ in, Materials F1:C1)

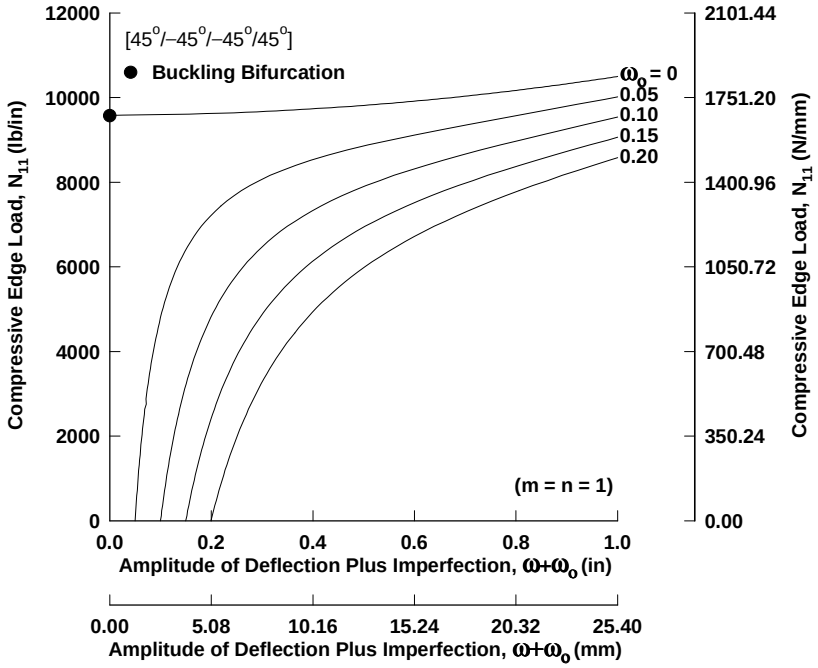

Fig. 6.39. The influence of the initial geometric imperfection on the compressive edge load-deflection interaction of a flat sandwich panel consisting of four layered facings with a fixed lay-up. All four edges are movable and simply supported. ($L_1 = L_2 = 24$ in, $h_f = 0.02$ in, $h_c = 0.5$ in, Materials F1:C1).

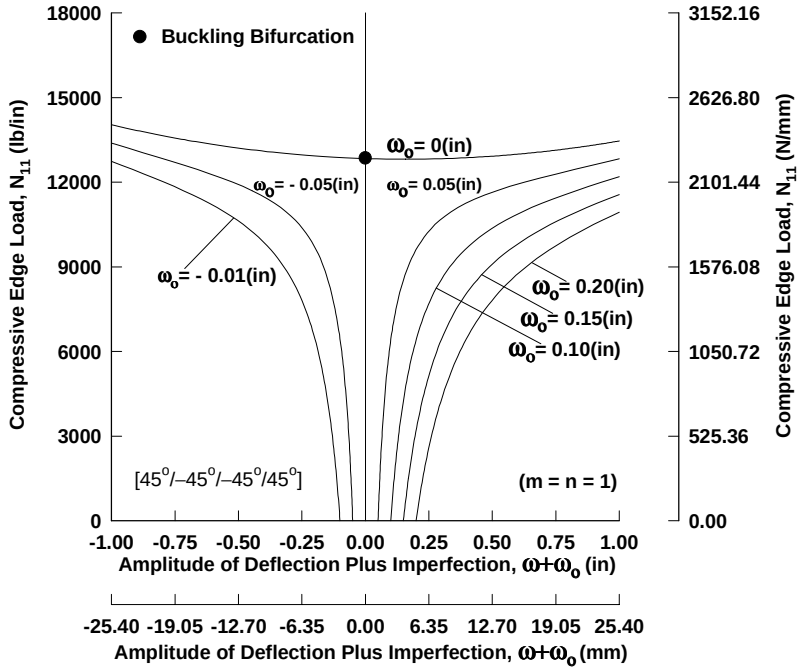

Fig. 6.40. The influence of the initial geometric imperfection on the compressive edge load-deflection interaction of a circular cylindrical sandwich panel consisting of four layered facings with a fixed lay-up. All four edges are movable and simply supported. ($L_1 = L_2 = 24$ in, $h_f = 0.02$ in, $h_c = 0.5$ in, $R_2 = 50$ in, Materials F1:C1).

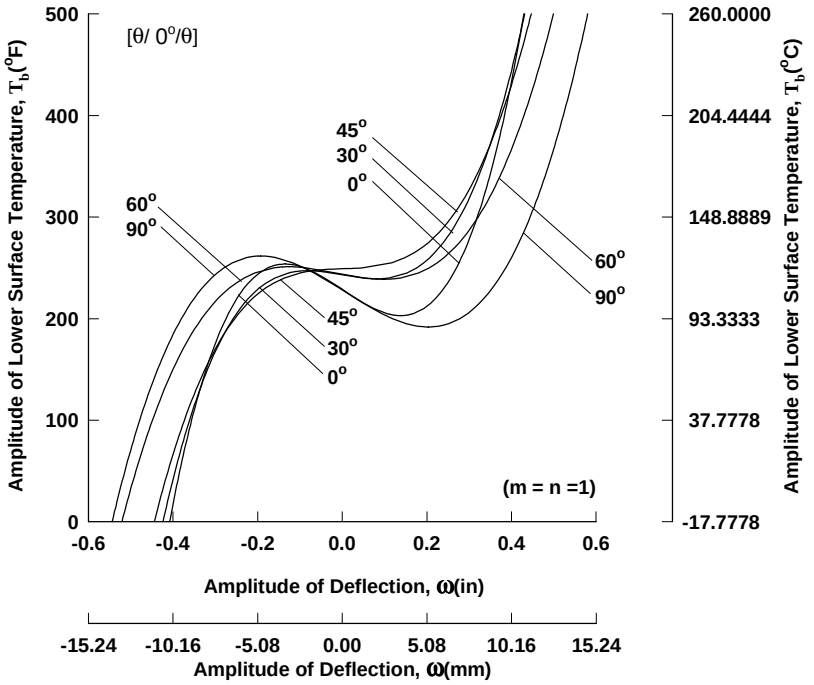

Fig. 6.41. A double curved sandwich panel with three layered facings subjected to a fixed compressive edge load and a temperature rise T_b. All four edges are movable and simply supported. ($L_1 = L_2 = 24$ in, $h_f = 0.045$ in, $h_c = 0.25$ in, $R_1 = R_2 = 450$ in, $N_{11} = 4200$ lb/in, Materials F1:C3)

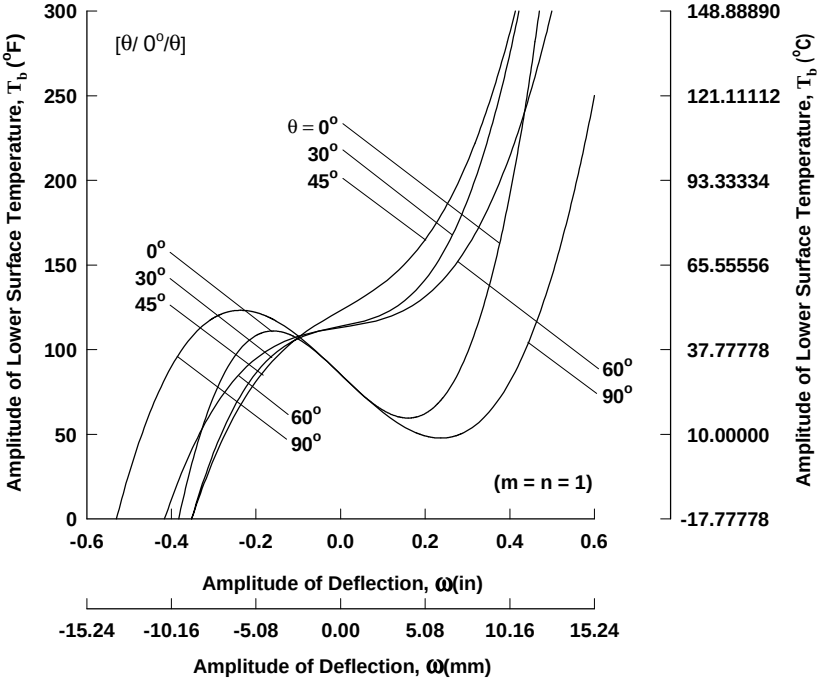

Fig. 6.42. A flat sandwich panel with three layered facings subjected to a fixed compressive edge load with an initial imperfection and a temperature rise T_b. All four edges are movable and simply supported. ($L_1 = L_2 = 24$ in, $h_f = 0.01125$ in, $h_c = 0.35$ in, $\omega_o = -0.0875$ in, $N_{11} = 1850$ lb/in, Materials F1:C3)

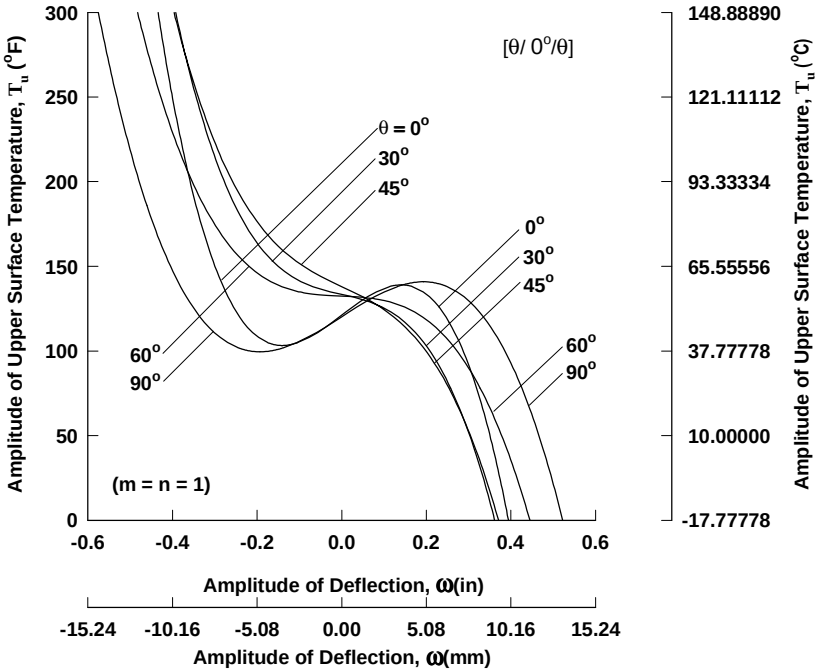

Fig. 6.43. A flat sandwich panel with three layered facings subjected to a fixed compressive edge load, A fixed pressure, and a temperature rise T_u. All four edges are movable and simply supported. ($L_1 = L_2 = 24$ in, $h_f = 0.054$ in, $h_c = 0.485$ in, $N_{11} = 11750$ lb/in, q = 15 psi, Materials F1:C3)

Stress/Strain

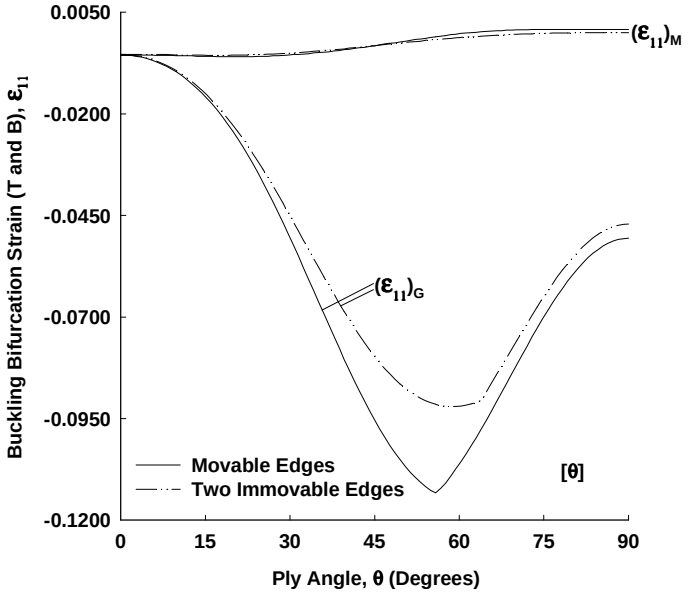

Fig. 6.44. The influence of the fiber orientation on the inplane strain ε_{11} at buckling bifurcation for a flat sandwich panel with single layered facings. (Note: prior to the first discontinuities, m = n = 1beyond which n = 1, m = 2; $L_1 = L_2 = 24$ in, $h_f = 0.02$ in, $h_c = 0.5$ in, Materials F1:C1)

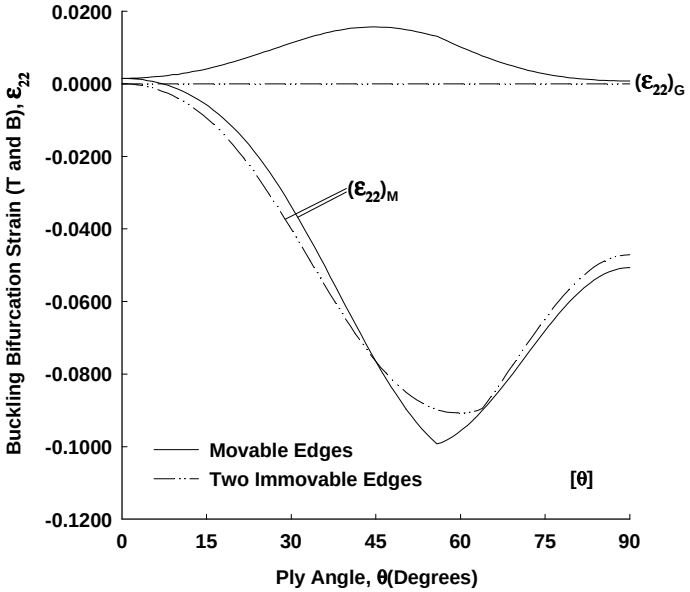

Fig. 6.45. The influence of the fiber orientation on the inplane strain ε_{22} at buckling bifurcation for a flat sandwich panel with single layered facings. (Note: prior to the first discontinuities, m = n = 1 beyond which n = 1, m = 2 ; $L_1 = L_2$ =24 in, h_f = 0.02 in, h_c = 0.5 in, Materials F1:C1)

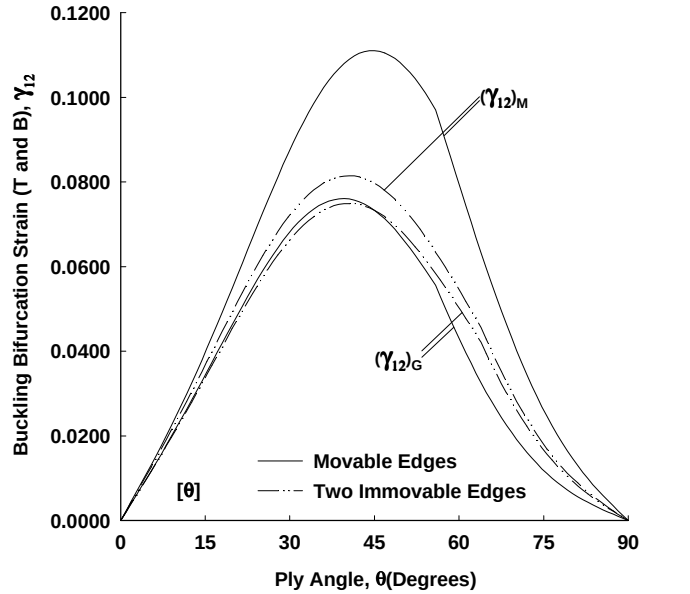

Fig. 6.46. The influence of the fiber orientation on the inplane strain γ_{12} at buckling bifurcation for a flat sandwich panel with single layered facings. (Note: prior to the first discontinuities, m = n = 1 beyond which n = 1, m = 2 ; $L_1 = L_2$ =24 in, h_f = 0.02 in, h_c = 0.5 in, Materials F1:C1)

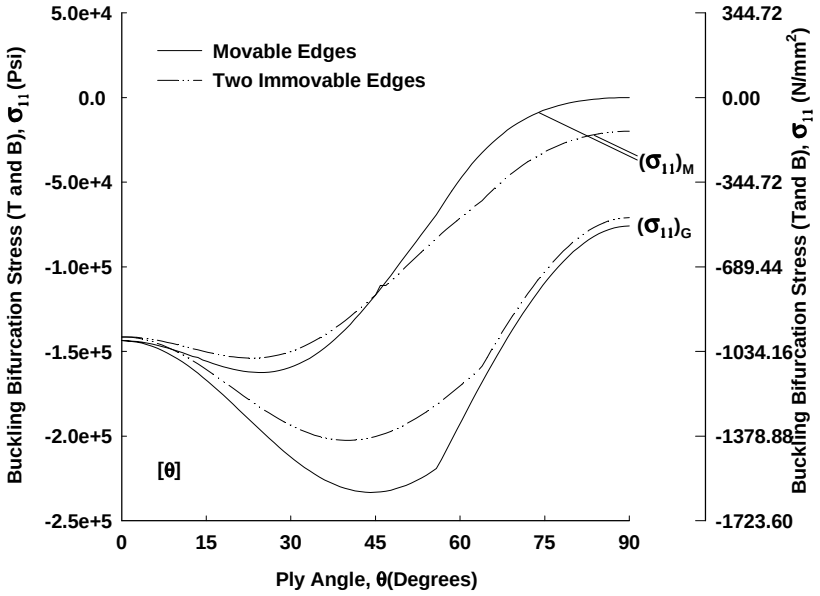

Fig. 6.47. The influence of the fiber orientation on the inplane stress σ_{11} at buckling bifurcation for a flat sandwich panel with single layered facings. (Note: prior to the first discontinuities, m = n = 1beyond which n = 1, m = 2 ; $L_1 = L_2$ = 24 in, h_f = 0.02 in, h_c = 0.5 in, Materials F1:C1)

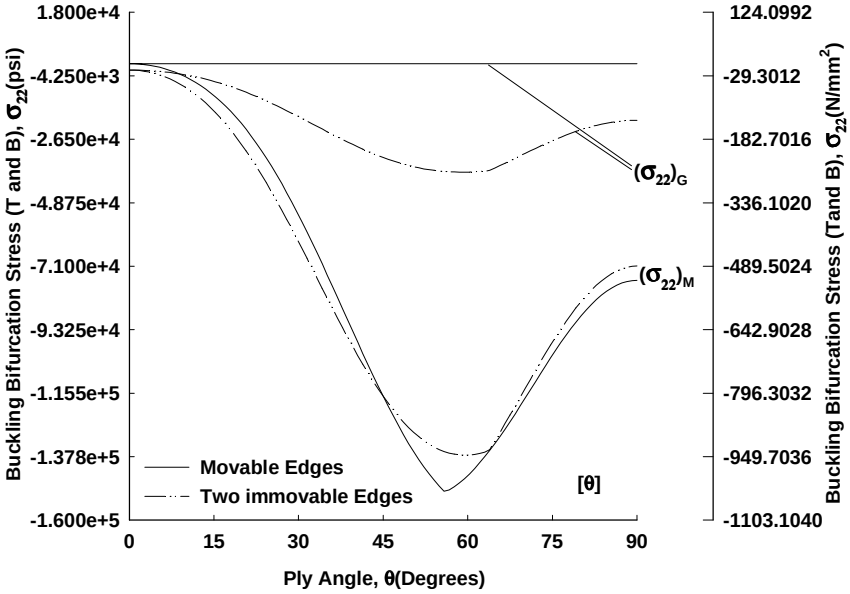

Fig. 6.48. The influence of the fiber orientation on the inplane stress σ_{22} at buckling bifurcation for a flat sandwich panel with single layered facings. (Note: prior to the first discontinuities, m = n = 1 beyond which n = 1, m = 2 ; $L_1 = L_2$ =24 in, h_f = 0.02 in, h_c = 0.5 in, Materials F1:C1)

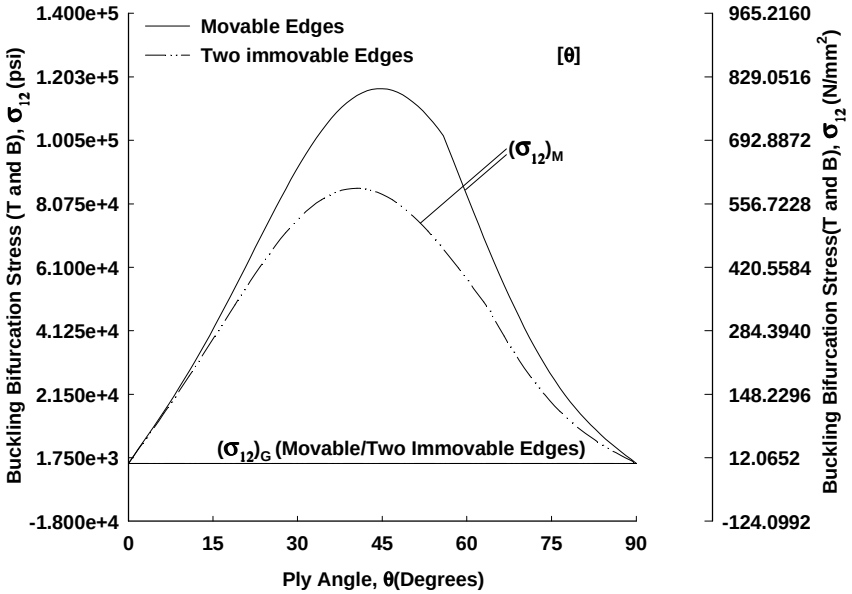

Fig. 6.49. The influence of the fiber orientation on the inplane stress σ_{12} at buckling bifurcation for a flat sandwich panel with single layered facings. (Note: prior to the first discontinuities, m = n = 1 beyond which n = 1, m = 2 ; $L_1 = L_2$ =24 in, h_f = 0.02 in, h_c = 0.5 in, Materials F1:C1)

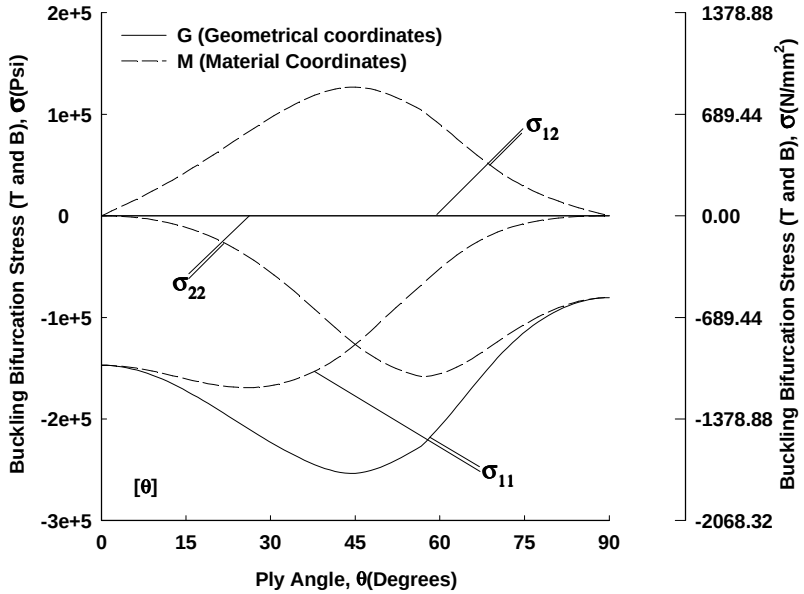

Fig. 6.50. The influence of the fiber orientation on the inplane stresses at buckling bifurcation for a circular cylindrical sandwich panel with single layered facings. All four edges are movable and simply supported. (Note: prior to the first discontinuities, m = n = 1 beyond which n = 1, m = 2 ; $L_1 = L_2$ =24 in, h_f = 0.02 in, h_c = 0.5 in, R_2 = 100 in, Materials F1:C1)

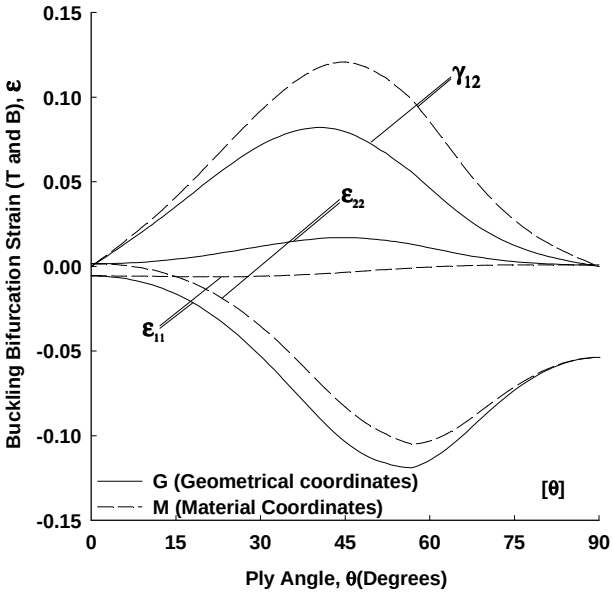

Fig. 6.51. The influence of the fiber orientation on the inplane strains at buckling bifurcation for a circular cylindrical sandwich panel with single layered facings. All four edges are movable and simply supported. (Note: prior to the first discontinuities, m = n = 1 beyond which n = 1, m = 2 ; L_1 = L_2 =24 in, h_f = 0.02 in, h_c = 0.5 in, R_2 = 100 in, Materials F1:C1)

7 Summary, Conclusions, and Future Developments

As a brief overview, a comprehensive geometrically non-linear theory of doubly-curved sandwich structures constructed of anisotropic laminated facings with an orthotropic core under various loading conditions for simply supported boundary conditions has been developed for a symmetric sandwich structure with an orthotropic weak core. As an application of the theory, several results were compared with experimental results found in the literature which were found to agree reasonably well. In addition, results which encompassed buckling, postbuckling, and stress/strain analysis have been obtained. These results were developed utilizing various types of advanced materials, under various loading conditions, which encompassed uniaxial compressive edge loads, biaxial edge loads (tensile and compressive), thermal loads, lateral pressure, and imperfections.

The results showed that the load carrying capacity of the sandwich structure can be enhanced via the use of the structural tailoring technique. The results also showed that the sandwich structure is capable of sustaining large compressive edge loads in the deep postbuckling range. It was also revealed that buckling bifurcation can be increased by the appropriate lay-up. In addition, it was found that sandwich structures are imperfection insensitive. It was also revealed that for the case of two immovable edges the buckling bifurcation occurs at lower compressive edge loads. The phenomenon of the snap-through type behavior occurred only under special loading conditions. Finally, large stresses and strains were found to exist under compressive edge loads (both uniaxial and biaxial).

Future developments of the associated work, presented here, should include the buckling and thermomechanical postbuckling response of doubly curved sandwich panels comprised of anisotropic laminated facings with weak core behavior, under various loading conditions with the effect of the inplane temperature profile integrated into the theory, for both simply supported and clamped edges. Some additional complexities could be integrated into the theory such as the temperature dependent material properties, the effect of the antisymmetry with respect to the local and global midsurfaces for both simply supported and clamped edges under various loading conditions, the modeling of a compressible core with all of the above mentioned complexities, and several other effects involving e.g. the physical nonlinearities which will act as a catalyst in the evolutionary process of the knowledge base of sandwich structures and will enable one to search further for an optimal design of sandwich constructions.

References

1. Adi Murphy, N. K., and Alwar, R. S., "Nonlinear Dynamic Buckling of sandwich Panels", *Journal of Applied Mechanics*, 43, pp. 459-463, Sept 1976.

2. Akkas, N., and Bauld Jr, N. R., "Buckling and Initial Postbuckling Behavior of Clamped Shallow Spherical Sandwich Shells", *International Journal of Solids and Structures*, 7, pp. 1237-1259, 1971.

3. Akkas, N., "Classical and Nonlinear Buckling Analysis of Spherical Sandwich Shells", *International Journal of Solids and Structures*, 8, pp. 1373-1387, 1972.

4. Akkas, N., "On the Buckling and Initial Postbuckling Behavior of Shallow Spherical and Conical Sandwich Shells", *Journal of Applied Mechanics*, 39, pp. 163-171, march 1972.

5. Alexandrov, A. I., Briuker, L. E., Kurshin, L. M., and Prusakov, A. P., *Research on three Layered Panels*,(in Russian), Oboronghiz, Moskow, 1960.

6. Amato, A. J., and Ebcioglu, I. K., "Axisymmetric Buckling of Annular Sandwich Panels", *AIAA Journal*, 10(10), pp. 1351-1353, 1972.

7. Azar, J. J., "Bending Theory for Multilayered Orthotropic Sandwich Plates", *AIAA Journal*, 6(11), pp. 2166-2169, 1968.

8. Baker. E. H., and Herrmann, G., "Vibrations of Orthotropic Cylindrical Sandwich Shells Under Initial Stress", *AIAA Journal*, 4, 1063, 1966.

9. Bauld Jr, N. R., "Imperfection Sensitivity of Axially Compressed Stringer Reinforced Cylindrical Sandwich Panels", International Journal of Solids and Structures, 10, pp. 883-902, Aug 1974.

10. Bert, C. W., and Cho, K. N., "Uniaxial Compressed and Shear Buckling in Orthotropic Sandwich Plates by an Improved Theory", *Mech Struct Machines*, 17(3), pp. 283-302, 1989.

11. Bert, C. W., and Egle, D. M., "Dynamics of Composite sandwich and Stiffened Shell-Type Structures", *Journal of Spacecraft and Rockets*, 6(12), 1345-1361, 1969.

12. Bert, C. W., and Francis, O. H., "Composite Material Mechanics:Structural Mechanics", *AIAA Journal*, 12(9), pp. 1173-1186, 1974.

13. Bert, C. W., Crisman, W. C., and Nordby, G. M., "Buckling of Cylindrical and Conical Sandwich Shells With Orthotropic Facings", *AIAA Journal*, 7(2), pp. 250-257, 1969.

14. Chang, M. Y., and Librescu, L., "Postbuckling of Shear-Deformable Flat and Curved Panels Under Combined Loading Conditions", *Int. J. Mech. Sci*., Vol. 37, No. 2, pp. 121-143, 1995.

15. Cheng, Z-Q., Wang, X-X., and Huang, M-G., "Large Deflections of Rectangular Hoff Sandwich plates", *International Journal of Solids and Structures*, Vol. 30, No. 17, pp. 2335-2346, 1993.

16. Chong, K. P., Cheung, Y. K., and Tham, L. G., "Free Vibration of Formed Sandwich Panel", *Journal of Sound and Vibration*, 81, pp. 575-582, 1982.

17. Davenport, O. B., and Bert, C. W., "Buckling of Orthotropic curved sandwich Panels in Shear and Axial Compression", *Journal of Aircraft*, 10(100), pp. 632-634, 1973.

18. Davenport, O. B., and Bert, C. W., Buckling of Orthotropic Curved Sandwich Panels Subjected to Edge Shear Loads", *Journal of Aircraft*, 9(7), pp. 477-480, 1972.

19. Doxsee, L. E., Lee Jr, W. I., Springer, G. S., and Chang, S. S., "Temperature and moisture Induced Deformations in Composite Sandwich Panels", *Journal of Reinforced Plastics and Composites*, 4, pp. 326-353, 1985.

20. Ebcioglu, I. K., "A general Theory of Sandwich Panels", *International Journal of Engineering Science*, Vol. 27, No. 8, pp. 865-878, 1989.

21. Ebcioglu, I. K., "Nonlinear Theory of Sandwich Panels", *Developments in theoretical and Applied Mechanics*, Vol. 4, Ed. Daniel frederick, Pergamon Press, Oxford and New York, pp. 611-637, 1970.

22. EI-Senussi, A. K., and Webber, J. P. H., "The Buckling of Honeycomb Sandwich Circular Rings", *Aeronautical J*., 88, pp. 249-256, 1984.

23. Eslami, H., and Maerz, S., "Thermally Induced Vibration of a Symmetric Cross-Ply Plate with Hygrothermal Effects", *AIAA Journal*, Vol. 33, No. 10:Technical Notes.

24. Evans, K. E., "The Design of Doubly Curved Sandwich Panels with Honeycomb Cores", *Composite Structures*, 17, pp. 95-111, 1991.

25. Evans, K. E., "The Design of Doubly Curved Sandwich Panels With Honeycomb Cores", *Composite Structures*, 17(2), pp. 95-111, 1991.

26. Fulton, R. E., "Non-Linear Equations for a Shallow Unsymmetrical Sandwich Shell of Double Curvature", *Developments in Mechanics. Proceedings of 7th Midwestern Mech. Conf.*, Plenum Press. New York, N.Y., pp. 365-380, 1961.

27. Grigoliuk, E. I., "Large Deflection Sandwich Shells with Strong Core", *Investia. Acad. Nauk SSSR, OTN*, 1, pp. 26-34, 1958.

28. Grigoliuk, E. I., and Chulkov, P. P., "General Large Deflection Theory of Elastic Sandwich Shallow Shells", *Archiwum Mechaniki Stosowanej*, 1, 16, pp. 123-133, 1964.

29. Grigolyuk, E. I., and Kiryukhin, Y. P., "Linear Theory of Three Layered Shells With a Stiff Core", *AIAA Journal*, Vol. 1, No. 10, pp. 2438-2445, October 1963.

30. Guangyu S., and Pin T., "Equivalent Transverse Shear Stiffness of Honeycomb Cores", *International Journal of Solids and Structures*, Vol. 32, No. 10, pp. 1383-1393, 1995.

31. Gutierrez, A. J., and Webber, J. P. H., "Flexural Wrinkling of Honeycomb Sandwich Beams With Laminated Faces", *International Journal of Solids and Structures*, 16(7), pp. 645-651, 1980.

32. Hause, T., Librescu, L., and Camarda, C. J., "Postbuckling of Anisotropic Flat and Doubly-Curved Sandwich Panels Under Complex Loading Conditions",*11th DOD/NASA/FAA Conference on Fibrous Composites in Structural Design*, Fortworth, TX, pp. IV-41-IV-60, August 26-29, 1996.

33. Hause, T., Librescu, L., and Camarda, C. J., "Postbuckling of Anisotropic Flat and Doubly-Curved Sandwich Panels under Complex Loading Conditions", *International Journal of Solids and Structures*, Vol. 35/31, July 1998.

34. Hause, T., Librescu, L., and Johnson, T. F., "Thermomechanical Postbuckling of Geometrically Imperfect Flat and Curved Sandwich Panels", *Proceedings of the 38th AIAA/ASME/ASCE/AHS/ASC Structures, Structural Dynamics, Materials Conference and Exhibition and AIAA/ASME/AHS/Adaptive Structures Forum*, Paper AIAA 97-1248, part 4, pp. 2481-2491, Kissimmee, Florida, April 7-10, 1997.

35. Hause, T., Librescu, L., and Johnson, T. F., "Non-Linear Response of Sandwich Flat Panels Under Thermomechanical Loading Systems", Thermal Stresses, 97 *Proceedings of the Second International Symposium on Thermal Stresses and Related Topics*, pp. 33-36, June 8-11, 1997, Rochester Institute. of Technology, Rochester, N.Y.

36. Hwu, C., and Hu, J. S., "Buckling and Postbuckling of Delaminated Composite Sandwich Beams, *AIAA Journal*, 30(7), pp. 1901-1909, 1992.

37. Jeusette, J. P., and Laschet, G., "Pre and Postbuckling Finite Element Analysis of Curved Composite and Sandwich Panels", *AIAA Journal*, 28(7), 1233-1239, 1990.

38. Kan, H-P., and Huang, J-C., "Large deflection of Rectangular Sandwich Plates", *AIAA Journal*, Vol. 5, No. 9, 1967.

39. Karavanov, V. F., "Stability of Three-Layer Shallow Cylindrical Panels With Soft Core", *Izvestia Vishish Ukebnich Zavedenia-Aviatsionaia Technika* 2, 50-60 (in Russian), 1960.

40. Kim, C. G., and Hong, C. S., "Buckling of Unbalanced Anisotropic Sandwich Plates with Finite Bonding Stiffness", *AIAA Journal,* Vol. 26, No. 8, 1988.

41. Ko, W. L., and Jackson, R. H., "Compressive and Shear Buckling Analysis of Metal Matrix Composite Sandwich Panels Under Different Thermal Environments", *Composite Structures*, 25, 227-239, 1993.

42. Ko, W. L., and Jackson, R. H., "Combined Compressive and Shear Buckling Analysis of Hypersonic Aircraft Structural Sandwich Panels, *NASA TM-4290*, 1991.

43. Ko, W. L., and Jackson, R. H., "Combined Load Buckling Behavior of Metal Matrix Composite Sandwich Panels Under Different Thermal Environments", *NASA TM-4321*, 1991.

44. Ko, W. L., and Jackson, R. H., "Compressive and Shear Buckling Analysis of Metal Matrix Composite Sandwich Panels Under Different Thermal Environments", *Composite Structures*, 25(1-4), pp. 227-239, 1993.

45. Ko, W. L., and Jackson, R. H., "Thermal Behavior of Titanium Honeycomb Core Sandwich Panel", *NASA TM-101732*, 1991.

46. Kuhhorn, A., and Schoop, H., "A Nonlinear Theory for Sandwich Shells Including The Wrinkling Phenomenon", *Archive Applied Mech*, 62(6), pp. 413-427, 1992.

47. Kurshin, L. M., "Large Deflection of Sandwich Cylindrical Shells", in Research of Aeronautical Structures-Sandwich Plates and Shells in Russian Ed. A. Ia. Alexandrov, Obornghiz, Moskow, pp. 39-50, 1959.

48. Kutylowski, R., and Myslecki, K., "Geometrically Nonlinear FEM Analysis of Sandwich Shells", *Zeitschrift fur Angewandte Math and Mech*, 72(4), T260-T264, 1992.

49. Kutylowski, R., and Myslecki, K., "Nonlinear Theory of Sandwich Shells With Distinctly Soft Core", *Zeitschrift fur Angewandte Math and Mech*, 71(4), pp. 302-305, 1991.

50. Lam, K. Y., and Chun, L., "Dynamics Response of a Simply Supported Sandwich Beam Subjected to Impulse Loading", *Composite Structures*, 27, pp. 331-337, 1994.

51. Lee, L. J., and Fan, Y. J., "Bending and Vibration Analysis of Composite Sandwich Plates", *Computers and Structures*, Vol. 60, No. 1, pp. 103-112, 1996.

52. Leissa, A. W., and Qatu, M. S., "Equations of Elastic Deformation of Laminated Composite Shallow Shells", *Journal of Applied Mechanics*, Vol. 58, No. 1, pp. 181-188, March 1991.

53. Librescu, L., and Chang, M. Y., "Effects of Geometric Imperfections on Vibration of Compressed Shear Deformable Laminated Composite Curved Panels", *Acta Mechanica* 96, pp. 203-224, 1993.

54. Librescu, L., "Aeroelastic Stability of orthotropic Heterogeneous Thin Panels in the Vicinity of the Flutter Critical Boundary",(Part I and Part II), *Journal de Mecanique*, 4, 51-76, 1965 and 6, 132-152, 1967.

55. Librescu, L., "*Elastostatics and Kinetics of Anisotropic and Heterogenious Shell – Type Structures*", Chapters V-VII, pp. 493-540, Noordhoff International Publishers, Leyden, The Netherlands, 1975.

56. Librescu, L., "On a Bending Theory of Elastic Anisotropic Sandwich Type-Plates",*Doklady Akademi Nauk SSR* 182, 1, pp. 60-63, 1967 (in Russian) (Moscow). (Translated into English as *Soviet Physics-Doklady*, Vol. 13, pp. 957-959), 1969.

57. Librescu, L., "On a Geometrically Non-Linear Theory of Elastic Anisotropic Sandwich Type Plates", *Revue Roumaine des Sciences techniques-Mecanique Appliquee*, 15, 2, pp. 323-339, 1970.

58. Librescu, L., "Refined Geometrically Non-Linear Theories of Anisotropic Laminated Shells", *Quarterly of Applied Mathematics*, Vol. 45, No. 1, pp. 1-22, 1987.

59. Librescu, L., and Chang, M. Y., "Postbuckling and Imperfection Sensitivity of Shear Deformable Composite Doubly Curved Panels", *International Journal of Solids and structures*, Vol. 29, No. 9, pp. 1065-1083, 1992.

60. Librescu, L., and Stein, M., "Postbuckling Behavior of Shear Deformable Composite Flat Panels Taking Into Account Geometrical Imperfections",*AIAA Journal*, Vol. 30, pp. 1352-1360, May 1992.

61. Librescu, L., and Stein, M., "A Geometrically Nonlinear Theory of Transversely Isotropic Laminated Composite Plates and its Use in the Postbuckling Analysis", *Thin Walled Structures, Special Aerospace Structures Issue*, 11, pp. 177-201, 1991.

62. Librescu, L., Hause, T., and Camarda, C. J., "Geometrically Nonlinear Models of Initially Imperfect Anisotropic Sandwich Plates and Shells Incorporating Non-Classical Effects",*Proceedings of the 37th AIAA/ASME/ASCE/AHS/ASC Structures, Structural Dynamics and Materials Conference and Exhibit*, Paper AIAA-96-1350, Part 1, pp. 284-299, Salt Lake City, UT, April 15-17, 1996.

63. Librescu, L., Hause, T., and Camarda, C. J., "Geometrically Nonlinear Theory of Initially Imperfect Sandwich Plates and Shells Incorporating Non-classical Effects", *AIAA Journal*, Vol. 35, No. 8, pp. 1393-1403, 1997.

64. Librescu, L., Lin, W., Nemeth, M. P., and Starnes, J.H. Jr., "Classical Versus Non-Classical Postbuckling Behavior of Laminated Composite Panels Under Complex Loading Conditions", *Non-Classical Problems of the Theory and Behavior of Structures Exposed to Complex Environmental Conditions*, AMD-Vol. 164, ASME, Ed. L. Librescu, pp. 169-182, 1993.

65. Lizarev, A. D., and Rostanina, N. B., "Equations of Free Vibration of Spherical Nonshallow Sandwich Shells", *Izv. AN SSSR. Mekhanika Tverdogo tela,* 13(4), pp. 142-148, 1978.

66. Megumi S., and Masuji U., "Deformation and Thermal Stress in a Rectangular Plate Subjected to Aerodynamic Heating", *Aeronautical Research Institute, University of Toko,* Report No. 359, pp. 195-213, December 1960.

67. Mindlin, R. D., "Influence of Rotatory Inertia and Shear on Flexural motions of Isotropic Elastic Plates", *Journal of Applied Mechanics,* 18, pp. 31-38, 1951.

68. Minguet, P., Dugundji, J., and Lagace, P. A., "Buckling and Failure of Sandwich Plates with Graphite-Epoxy Faces and Various Cores", *Proceedings of the 28th AIAA/ASME/ASCE/AHS Structures, Structural* Dynamics *and Materials Conference*, Paper AIAA-87-07, April 6-8, 1987.

69. Monforton, G. R., and Ibrahim, I. M., "Analysis of Sandwich Plates With Unbalanced Cross-ply Faces", *Int. J. Mech. Sci*, Pergamon Press, Vol. 17, pp. 227-238, 1975.

70. Monforton, G. R., and Ibrahim, I. M., "Modified Stiffness Formulation of Unbalanced Anisotropic Sandwich Plates", *Int. J. Mech. Sci*., Vol. 19, pp. 335-343, 1977.

71. Mukhopadhyay, A. K., and Sierakowski, R. L., "On Sandwich Beams With Laminate Facings and Honeycomb Cores Subjected to Hygrothermal Loads:Part I-Analysis", *Journal of Composite Materials*, Vol. 24, pp. 382-400, April 1990

72. Mukhopadhyay, A. K., and Sierakowski, R. L., "On Sandwich Beams With Laminate Facings and Honeycomb Cores Subjected to Hygrothermal Loads: Part II-Analysis", *Journal of Composite Materials*, Vol 24, pp. 401-418, April 1990.

73. Naghdi, P.M., "Foundations of Elastic Shell Theory", *Progress Solid Mechanics*, (edited by I.N. Sneddon and R. Hill), North-Holland Publ., Amsterdam, The Netherlands, 4, 1963.

74. Noor, A. K., Burton, W. S., and Bert, C. W., "Computational Models for Sandwich Panels and Shells", *Applied Mechanics Reviews*, Vol. 4, No. 3, pp. 155-199, March 1996.

75. Palazotto, A. N., and Linneman, I. E., "Vibration and Buckling Characteristics of Composite Cylindrical Panels Incorporating the Effects of a Higher Order Shear Theory", *International Journal of Solids and Structures*, Vol. 28, No. 3, pp. 341-361, 1991.

76. Pearce, T. R. A., and Webber, J. P. H., "Buckling of Sandwich Panels with Laminated Face Plates", *Aeronautical Quarterly*, Vol. 23, pp. 148-160, May 1972.

77. Pearce, T. R. A., and Webber, J. P. H., "Experimental Buckling Loads of Sandwich Panels with Carbon Fiber Face Plates", *Aeronautical Quarterly*, Vol. 24, pp. 295-312, November 1973.

78. Rajagopal, S. V., Singh, G., and Rao, Y. V. K. S., "Non-Linear Vibrations of Sandwich Plates",*Journal of Sound and Vibration*, 110(2), 261-269, 1986.

79. Rajagopal, S. V., Singh, G., Sadasiva Rao, Y. V. K. S., and Narayanan, S., "Nonlinear Vibrations of Sandwich Plates", *Journal of Sound and Vibration*, 110(2), pp. 261-269, 1986.

80. Rao, K. M., and Maeyer-Piening, H. R., "Critical Shear Loading of Curved Sandwich Panels Faced With Fiber-Reinforced Plastic", *AIAA Journal*, Vol. 24, No. 9, pp. 1531- 1536, September 1986.

81. Rao, K. M., and Kaeser, R., "Shear Buckling of Stiff Core Anisotropic Sandwich Plate", *Journal of Engineering Mechanics*, 110(9), pp. 1435-1440, 1984.

82. Rao, K. M., and Meyer-Piening, H. R., "Analysis of Sandwich Plates Using a Hybrid-Stress Finite Element", *AIAA Journal*, 29(9), pp. 1498-1506, 1991.

83. Rao, K. M., and Meyer-Piening, H. R., "Buckling Analysis of FRP Faced Cylindrical Sandwich Panel Under Combined Loading", *Composite Structures*, 14(1), pp. 15-34, 1990.

84. Rao, K. P., "Buckling of Composite Sandwich Rectangular Panels(Grid Core)", *Journal of Reinforced Plastics and Composites*, 7(1), pp. 72-89, 1988.

85. Rao, Y. V. K. S., and Nakra, B. C., "Theory of Vibratory Bending of Unsymmetrical. Sandwich Plates", *Archives of Mechanics*, 25, 2, pp. 213-225, Warszawa, 1973.

86. Schmit Jr, L. A., and Monforton, G. R., "Finite Deflection Discrete Element Analysis of Sandwich Plates and Cylindrical Shells With Laminated Faces", *AIAA Journal*, Vol. 8, No. 8, pp. 1454-1461, August 1970.

87. Seide, P., "A Reexamination of Koiter's Theory of Initial Postbuckling Behavior and Imperfection Sensitivity of Structures", *Thin Shell Structures:Theory, Experiment, and Design*, (Edited by C.Y. Fung and E.E. Sechler), Prentice-Hall, New Jersey, 59-80, 1974.

88. Sinha, P. K., and Rath, A. K., "Frequencies of Free Vibration of Axially Compressed Orthotropic Sandwich Plates", *Journal of Sound and vibration*, 35(4), pp. 541-547, 1974.

89. Tennyson, R. C., and Chan, K. C., "Buckling of Imperfect Sandwich Cylinders Under Axial Compression", *International Journal of Solids and Structures*, Vol. 26, No. 9/10, pp. 1017-1036, 1990.

90. Thompson, J. M. T., "Basic Principles in The General Theoey of Elastic Stability", *J. Mech. Phys. Solids*,Vol. 11, pp. 13-20, 1963.

91. Tsuneyoshi N., and Koji U., "The Secondary Buckling and Post-secondary-Buckling Behaviours of Rectangular Plates", *Int. J. Mech. Sci.*, Vol. 21, pp. 265-286, 1979.

92. Volmir, A. S., "Stability of Sandwich Plates and Shells", *Stability of Deformable S*., Nauka Publ House, Moskow(in Russian), Ch.19, 1967.

93. Wang, C. T., "Principle and Application of Complementary Energy Method for Thin Homogeneous and Sandwich Plates and Shells With Finite Deflections", *NACA TN-2620*, 1952.

94. Wu, H. L., and Jun, C. C., "Nonlinear Buckled States of Rectangular Sandwich Plates and Their Stabilities", *International Journal of Non-Linear Mechanics*, Vol. 27, No. 3, pp. 423-435, 1992.

95. Xia, Z. Q. and Lukasiewicz, S., "Non-Linear, Free Damped Vibrations of Sandwich Plates", *Journal of Sound and Vibration*, 175(2), pp. 219-232, 1994.

96. Yu, Y. Y., "A New Theory of Elastic Sandwich Plates. One Dimensional Case", *Journal of Ap*plied *Mechanics*, 26, pp. 415-421, 1959.

97. Yu, Y. Y., "Nonlinear Flexural Vibrations of Sandwich Plates", *Journal of Acoustical Society of America*, 34, pp. 1176-1183, 1962.

98. Yu, Y. Y., "Simple Thickness-Shear Modes of Vibration of Infinite Sandwich Plates", *Journal of Applied Mechanics*, 26, pp. 679-681, 1959.

Appendix 1

Strain Displacement Relationships

Bottom Face

$$
\begin{aligned}
{}^{/}\varepsilon_{11} &= \xi_{1,1} + \eta_{1,1} + (1/2)v_{3,1}^2 + v_{3,1}v_{3,1}^{\circ} - v_3/R_1 \\
{}^{/}\gamma_{12} &= \xi_{1,2} + \xi_{2,1} + \eta_{1,2} + \eta_{2,1} + v_{3,1}v_{3,2} + v_{3,1}^{\circ}v_{3,2} + v_{3,1}v_{3,2}^{\circ} \\
{}^{/}\gamma_{13} &= {}^{/}\psi_1 + v_{3,1} \qquad (1\overset{\rightarrow}{\leftarrow}2) \qquad \text{(A1.1a – e)} \\
{}^{/}\kappa_{11} &= {}^{/}\psi_{1,1} \\
{}^{/}\kappa_{12} &= {}^{/}\psi_{1,2} + {}^{/}\psi_{2,1}
\end{aligned}
$$

Core Layer

$$
\begin{aligned}
\bar{\varepsilon}_{11} &= \xi_{1,1} - \frac{1}{4}\left(h'\psi'_{1,1} - h''\psi''_{1,1}\right) + \frac{1}{2}v_{3,1}^2 + v_{3,1}^{\circ}v_{3,1} - v_3/R_1 \\
\bar{\gamma}_{12} &= \xi_{1,2} + \xi_{2,1} - \frac{1}{4}\left[h'\left(\psi'_{1,2} + \psi'_{2,1}\right) - h''\left(\psi''_{1,2} + \psi''_{2,1}\right)\right] + v_{3,1}v_{3,2} + v_{3,1}^{\circ}v_{3,2} + v_{3,1}v_{3,2}^{\circ} \\
\bar{\kappa}_{11} &= \frac{1}{\bar{h}}\left\{\eta_{1,1} - \frac{1}{4}\left(h'\psi'_{1,1} + h''\psi''_{1,1}\right)\right\} \qquad (1\overset{\rightarrow}{\leftarrow}2) \qquad \text{(A1.2a – e)} \\
\bar{\kappa}_{12} &= \frac{1}{\bar{h}}\left\{\eta_{1,2} + \eta_{2,1} - \frac{1}{4}\left[h'\left(\psi'_{1,2} + \psi'_{2,1}\right) + h''\left(\psi''_{1,2} + \psi''_{2,1}\right)\right]\right\} \\
\bar{\gamma}_{13} &= \frac{1}{\bar{h}}\left\{\eta_1 - \frac{1}{4}\left(h'\psi'_1 + h''\psi''_1\right)\right\} + v_{3,1}
\end{aligned}
$$

Upper Face

$$
\begin{aligned}
{}^{//}\varepsilon_{11} &= \xi_{1,1} - \eta_{1,1} + (1/2)v_{3,1}^2 + v_{3,1}v_{3,1}^{\circ} - v_3/R_1 \\
{}^{//}\gamma_{12} &= \xi_{1,2} + \xi_{2,1} - \eta_{1,2} - \eta_{2,1} + v_{3,1}v_{3,2} + v_{3,1}^{\circ}v_{3,2} + v_{3,1}v_{3,2}^{\circ} \\
{}^{//}\gamma_{13} &= {}^{//}\psi_1 + v_{3,1} \qquad (1\overset{\rightarrow}{\leftarrow}2) \qquad \text{(A1.3a – e)} \\
{}^{//}\kappa_{11} &= {}^{//}\psi_{1,1} \\
{}^{//}\kappa_{12} &= {}^{//}\psi_{1,2} + {}^{//}\psi_{2,1}
\end{aligned}
$$

Appendix 2

The Reduced Elastic Moduli, Thermal Coefficients, and Moisture Swelling Coefficients as a Function of Ply-Angles for The Respective *kth* Layer of The Respective Face

Bottom Face

$$
\begin{aligned}
{}'\hat{Q}_{11}^{k} &= {}'Q_{11}^{k}\,{}'m_k^4 + 2\,{}'m_k^2\,{}'n_k^2\left({}'Q_{12}^{k} + 2\,{}'Q_{66}^{k}\right) + {}'Q_{22}^{k}\,{}'n_k^4 \qquad (1\overrightarrow{\leftarrow}2)\\
{}'\hat{Q}_{12}^{k} &= \left({}'Q_{11}^{k} + {}'Q_{22}^{k} - 4\,{}'Q_{66}^{k}\right){}'m_k^2\,{}'n_k^2 + {}'Q_{12}^{k}\left({}'m_k^4 + {}'n_k^4\right)\\
{}'\hat{Q}_{16}^{k} &= \left({}'Q_{11}^{k} - {}'Q_{12}^{k} - 2\,{}'Q_{66}^{k}\right){}'m_k^3\,{}'n_k + \left({}'Q_{12}^{k} - {}'Q_{22}^{k} + 2\,{}'Q_{66}^{k}\right){}'m_k\,{}'n_k^3 \qquad \text{(A2.1a – e)}\\
{}'\hat{Q}_{26}^{k} &= \left({}'Q_{11}^{k} - {}'Q_{12}^{k} - 2\,{}'Q_{66}^{k}\right){}'m_k\,{}'n_k^3 + \left({}'Q_{12}^{k} - {}'Q_{22}^{k} + 2\,{}'Q_{66}^{k}\right){}'m_k^3\,{}'n_k\\
{}'\hat{Q}_{66}^{k} &= \left({}'Q_{11}^{k} + {}'Q_{22}^{k} - 2\,{}'Q_{12}^{k} - 2\,{}'Q_{66}^{k}\right){}'m_k^2\,{}'n_k^2 + {}'Q_{66}^{k}\left({}'m_k^4 + {}'n_k^4\right)
\end{aligned}
$$

$$
\begin{aligned}
{}'\hat{\lambda}_{11}^{k} &= {}'\hat{Q}_{11}^{k}\,{}'\hat{\alpha}_{11}^{k} + {}'\hat{Q}_{12}^{k}\,{}'\hat{\alpha}_{22}^{k} + {}'\hat{Q}_{16}^{k}\,{}'\hat{\alpha}_{12}^{k} \qquad (1\overrightarrow{\leftarrow}2) \qquad \text{(A2.2a, b)}\\
{}'\hat{\lambda}_{12}^{k} &= {}'\hat{Q}_{16}^{k}\,{}'\hat{\alpha}_{11}^{k} + {}'\hat{Q}_{26}^{k}\,{}'\hat{\alpha}_{22}^{k} + {}'\hat{Q}_{66}^{k}\,{}'\hat{\alpha}_{12}^{k}
\end{aligned}
$$

$$
\begin{aligned}
{}'\hat{\mu}_{11}^{k} &= {}'\hat{Q}_{11}^{k}\,{}'\hat{\beta}_{11}^{k} + {}'\hat{Q}_{12}^{k}\,{}'\hat{\beta}_{22}^{k} + {}'\hat{Q}_{16}^{k}\,{}'\hat{\beta}_{12}^{k} \qquad (1\overrightarrow{\leftarrow}2) \qquad \text{(A2.3a, b)}\\
{}'\hat{\mu}_{12}^{k} &= {}'\hat{Q}_{16}^{k}\,{}'\hat{\beta}_{11}^{k} + {}'\hat{Q}_{26}^{k}\,{}'\hat{\beta}_{22}^{k} + {}'\hat{Q}_{66}^{k}\,{}'\hat{\beta}_{12}^{k}
\end{aligned}
$$

$$
\begin{aligned}
{}'\hat{\alpha}_{11}^{k} &= {}'\alpha_{11}^{k}\,{}'m_k^2 + {}'\alpha_{22}^{k}\,{}'n_k^2 \qquad (1\overrightarrow{\leftarrow}2) \qquad \text{(A2.4a, b)}\\
{}'\hat{\alpha}_{12}^{k} &= \left({}'\alpha_{11}^{k} - {}'\alpha_{22}^{k}\right){}'m_k\,{}'n_k
\end{aligned}
$$

$$
\begin{aligned}
{}'\hat{\beta}_{11}^{k} &= {}'\beta_{11}^{k}\,{}'m_k^2 + {}'\beta_{22}^{k}\,{}'n_k^2 \qquad (1\overrightarrow{\leftarrow}2) \qquad \text{(A2.5a, b)}\\
{}'\hat{\beta}_{12}^{k} &= \left({}'\beta_{11}^{k} - {}'\beta_{22}^{k}\right){}'m_k\,{}'n_k
\end{aligned}
$$

$$
{}'Q_{11}^{k} = \frac{{}'E_1^{k}}{1 - {}'\nu_{12}^{k}\,{}'\nu_{21}^{k}}, \qquad {}'Q_{22}^{k} = \frac{{}'E_2^{k}}{1 - {}'\nu_{12}^{k}\,{}'\nu_{21}^{k}}, \qquad \text{(A2.6a - d)}
$$

$$
{}'Q_{12}^{k} = \frac{{}'\nu_{21}^{k}\,{}'E_1^{k}}{1 - {}'\nu_{12}^{k}\,{}'\nu_{21}^{k}} = \frac{{}'\nu_{12}^{k}\,{}'E_2^{k}}{1 - {}'\nu_{12}^{k}\,{}'\nu_{21}^{k}}, \qquad {}'Q_{66}^{k} = {}'G_{12}^{k}
$$

$$
{}'m_k = \cos {}'\theta_k, \qquad {}'n_k = \sin {}'\theta_k \qquad \text{(A2.7a, b)}
$$

Note:
For the upper face, replace single primes with double primes and for the core replace single primes with superposed bars and equate $(n_k,\ m_k = 0,\ k = 1)$.

Appendix 3

Coefficients of the displacement functions

$$\tilde{A}_1 = \frac{\left(A_{11}A_{22} - A_{12}^2\right)\mu_n^2}{32\,A_{11}\lambda_m^2}$$

$$\tilde{A}_2 = \frac{\left(A_{11}A_{22} - A_{12}^2\right)\lambda_m^2}{32\,A_{22}\mu_n^2}$$

$$\tilde{A}_3 = \frac{\left(\mu_n^2/R_1 + \lambda_m^2/R_2\right)\left(A_{11}A_{22}A_{66} - A_{66}A_{12}^2\right)}{\hat{\Delta}_{mn}}$$

$$\tilde{B}_1 = \frac{a\left\{\left[\left(A_{12} + A_{66}\right)d_2 - A_{22}d_1\right]\lambda_m\mu_n^2 - d_1A_{66}\lambda_m^3 - d_1d_2\lambda_m\right\}}{\hat{\hat{\Delta}}_{mn}}$$

$$\tilde{C}_1 = \frac{a\left\{\left[\left(A_{12} + A_{66}\right)d_1 - A_{11}d_2\right]\lambda_m^2\mu_n - d_2A_{66}\mu_n^3 - d_1d_2\mu_n\right\}}{\hat{\hat{\Delta}}_{mn}}$$

$$\tilde{D}_1 = \frac{-\lambda_m^2}{8}$$

$$\tilde{D}_2 = \frac{A_{12}\mu_n^2 - A_{11}\lambda_m^2}{16A_{11}\lambda_m}$$

$$\tilde{D}_3 = \frac{\lambda_m}{16}$$

$$\tilde{D}_4 = \frac{\left(A_{12}A_{66} + A_{12}^2 - A_{11}A_{22}\right)\lambda_m\mu_n^2 - A_{11}A_{66}\lambda_m^3}{R_1\hat{\Delta}_{mn}} + \frac{A_{22}A_{66}\lambda_m\mu_n^2 - A_{12}A_{66}\lambda_m^3}{R_2\hat{\Delta}_{mn}}$$

$$D_5 = \frac{-A_{22}}{A_{11}A_{22} - A_{12}^2}$$

$$D_6 = \frac{A_{12}}{A_{11}A_{22} - A_{12}^2}$$

$$\tilde{E}_1 = \frac{-\mu_n^2}{8}$$

$$\tilde{E}_2 = \frac{A_{12}\lambda_m^2 - A_{22}\mu_n^2}{16A_{22}\mu_n}$$

$$\tilde{E}_3 = \frac{\mu_n}{16}$$

$$\tilde{E}_4 = \frac{\left(A_{12}A_{66} + A_{12}^2 - A_{11}A_{22}\right)\lambda_m^2\mu_n - A_{22}A_{66}\mu_n^3}{R_2\hat{\Delta}_{mn}} + \frac{A_{11}A_{66}\lambda_m^2\mu_n - A_{12}A_{66}\mu_n^3}{R_1\hat{\Delta}_{mn}}$$

$$E_5 = \frac{A_{12}}{A_{11}A_{22} - A_{12}^2}$$

$$E_6 = \frac{-A_{11}}{A_{11}A_{22} - A_{12}^2}$$

Where, in these expressions, $\hat{\Delta}_{mn}$ and $\hat{\hat{\Delta}}_{mn}$ are defined as follows

$$\hat{\Delta}_{mn} = A_{11}A_{66}\lambda_m^4 + \left(A_{11}A_{22} - 2A_{12}A_{66} - A_{12}^2\right)\lambda_m^2\mu_n^2 + + A_{22}A_{66}\mu_n^4$$

$$\hat{\tilde{\Delta}}_{mn} = A_{11}A_{66}\lambda_m^4 + \left(d_2 A_{11} + d_1 A_{66}\right)\lambda_m^2 + \left(A_{11}A_{22} - 2A_{12}A_{66} - A_{12}^2\right)\lambda_m^2\mu_n^2 + \left(d_1 A_{22} + d_2 A_{66}\right)\mu_n^2 + A_{22}A_{66}\mu_n^4 + d_1 d_2$$

$$\tilde{F}_1 = \frac{\left(A_{16}^2 - \Lambda_{11}\Lambda_{66}\right)\lambda_m^2 + \left(\Lambda_{12}\Lambda_{66} - A_{16}A_{26}\right)\mu_n^2}{16\lambda_m\left(\Lambda_{11}\Lambda_{66} - A_{16}^2\right)}$$

$$\tilde{F}_2 = \frac{\left(A_{16}\Lambda_{22} - A_{26}\Lambda_{12}\right)\lambda_m^2}{16\left(\Lambda_{22}\Lambda_{66} - A_{26}^2\right)\mu_n}$$

$$\tilde{F}_3 = \frac{\hat{\phi}_{3mn}}{\hat{\Gamma}_{mn}}, \qquad \tilde{F}_4 = \frac{\hat{\phi}_{4mn}}{\hat{\Gamma}_{mn}}$$

$$\tilde{F}_5 = \frac{\lambda_m}{16}$$

$$\tilde{G}_1 = \frac{\left(A_{26}\Lambda_{11} - A_{16}\Lambda_{12}\right)\mu_n^2}{16\left(\Lambda_{11}\Lambda_{66} - A_{16}^2\right)\lambda_m}$$

$$\tilde{G}_2 = \frac{\left(\Lambda_{12}\Lambda_{66} - A_{16}A_{26}\right)\lambda_m^2 + \left(A_{26}^2 - \Lambda_{22}\Lambda_{66}\right)\mu_n^2}{16\mu_n\left(\Lambda_{22}\Lambda_{66} - A_{26}^2\right)}$$

$$\tilde{G}_3 = \frac{\hat{\gamma}_{3mn}}{\hat{\Gamma}_{mn}}, \qquad \tilde{G}_4 = \frac{\hat{\gamma}_{4mn}}{\hat{\Gamma}_{mn}}$$

$$\tilde{G}_6 = \frac{\mu_n}{16}$$

$$\tilde{H}_1 = \frac{\hat{\hat{\eta}}_{1mn}}{\hat{\hat{\Gamma}}_{mn}}, \qquad \tilde{H}_2 = \frac{\hat{\hat{\eta}}_{2mn}}{\hat{\hat{\Gamma}}_{mn}}$$

$$\tilde{I}_1 = \frac{\hat{\hat{i}}_{1mn}}{\hat{\hat{\Gamma}}_{mn}}, \qquad \tilde{I}_2 = \frac{\hat{\hat{i}}_{2mn}}{\hat{\hat{\Gamma}}_{mn}}$$

$$\tilde{\tilde{H}}_1^T = \frac{\hat{\hat{\eta}}_{1mn}^T}{\hat{\hat{\Gamma}}_{mn}}, \qquad \tilde{\tilde{H}}_2^T = \frac{\hat{\hat{\eta}}_{2mn}^T}{\hat{\hat{\Gamma}}_{mn}}$$

$$\tilde{\tilde{I}}_1^T = \frac{\hat{\hat{i}}_{1mn}^T}{\hat{\hat{\Gamma}}_{mn}}, \qquad \tilde{\tilde{I}}_2^T = \frac{\hat{\hat{i}}_{2mn}^T}{\hat{\hat{\Gamma}}_{mn}}$$

Where the constants within these expressions are defined as

$$\hat{\Gamma}_{mn} = \Gamma_{11}\lambda_m^8 + \Gamma_{12}\lambda_m^6\mu_n^2 + \Gamma_{13}\lambda_m^4\mu_n^4 + \Gamma_{14}\lambda_m^2\mu_n^6 + \Gamma_{15}\mu_n^8$$

$$\hat{\hat{\Gamma}}_{mn} = \Gamma_{21}\lambda_m^8 + \Gamma_{22}\lambda_m^6 + \Gamma_{23}\lambda_m^6\mu_n^2 + \Gamma_{24}\lambda_m^4 + \Gamma_{25}\lambda_m^4\mu_n^2 + \Gamma_{26}\lambda_m^4\mu_n^4 + \Gamma_{27}\lambda_m^2 + \Gamma_{28}\lambda_m^2\mu_n^2 + \Gamma_{29}\mu_n^2 + \Gamma_{30}\lambda_m^2\mu_n^4 + \Gamma_{31}\mu_n^4 + \Gamma_{32}\lambda_m^2\mu_n^6 + \Gamma_{33}\mu_n^6 + \Gamma_{34}\mu_n^8 + \Gamma_{35}$$

$$\hat{\phi}_{3mn} = (1/R_1)\left[\phi_{31}\mu_n^7 + \phi_{32}\lambda_m^2\mu_n^5 + \phi_{33}\lambda_m^4\mu_n^3\right] + (1/R_2)\left[\phi_{34}\lambda_m^2\mu_n^5 + \phi_{35}\lambda_m^4\mu_n^3 + \phi_{36}\lambda_m^6\mu_n\right]$$

$$\hat{\phi}_{4mn} = (1/R_1)\left[\phi_{41}\lambda_m^7 + \phi_{42}\lambda_m^5\mu_n^2 + \phi_{43}\lambda_m^3\mu_n^4 + \phi_{44}\lambda_m\mu_n^6\right] + (1/R_2)\left[\phi_{45}\lambda_m^7 + \phi_{46}\lambda_m^5\mu_n^2 + \phi_{47}\lambda_m^3\mu_n^4 + \phi_{48}\lambda_m\mu_n^6\right]$$

$$\hat{\gamma}_{3mn} = (1/R_1)\left[\gamma_{31}\mu_n^7 + \gamma_{32}\lambda_m^2\mu_n^5 + \gamma_{33}\lambda_m^4\mu_n^3 + \gamma_{34}\lambda_m^6\mu_n\right] + (1/R_2)\left[\gamma_{35}\mu_n^7 + \gamma_{36}\lambda_m^2\mu_n^5 + \gamma_{37}\lambda_m^4\mu_n^3 + \gamma_{38}\lambda_m^6\mu_n\right]$$

$$\hat{\gamma}_{4mn} = (1/R_1)\left[\gamma_{41}\lambda_m^5\mu_n^2 + \gamma_{42}\lambda_m^3\mu_n^4 + \gamma_{43}\lambda_m\mu_n^6\right] + (1/R_2)\left[\gamma_{44}\lambda_m^7 + \gamma_{45}\lambda_m^5\mu_n^2 + \gamma_{46}\lambda_m^3\mu_n^4\right]$$

$$\hat{\hat{\eta}}_{1mn} = \eta_{11}\lambda_m^7 + \eta_{12}\lambda_m^5 + \eta_{13}\lambda_m^5\mu_n^2 + \eta_{14}\lambda_m^3 + \eta_{15}\lambda_m^3\mu_n^2 + \eta_{16}\lambda_m^3\mu_n^4 + \eta_{17}\lambda_m + \eta_{18}\lambda_m\mu_n^2 + \eta_{19}\lambda_m\mu_n^4 + \eta_{20}\lambda_m\mu_n^6$$

$$\hat{\hat{\eta}}_{2mn} = \eta_{21}\mu_n^7 + \eta_{22}\mu_n^5 + \eta_{23}\lambda_m^2\mu_n^5 + \eta_{24}\mu_n^3 + \eta_{25}\lambda_m^2\mu_n^3 + \eta_{26}\lambda_m^4\mu_n^3 + \eta_{27}\lambda_m^2\mu_n + \eta_{28}\lambda_m^4\mu_n + \eta_{29}\lambda_m^6\mu_n$$

$$\hat{\hat{\imath}}_{1mn} = \imath_{11}\lambda_m^7 + \imath_{12}\lambda_m^5 + \imath_{13}\lambda_m^5\mu_n^2 + \imath_{14}\lambda_m^3 + \imath_{15}\lambda_m^3\mu_n^2 + \imath_{16}\lambda_m^3\mu_n^4 + \imath_{17}\lambda_m\mu_n^2 + \imath_{18}\lambda_m\mu_n^4 + \imath_{19}\lambda_m\mu_n^6$$

$$\hat{\hat{\imath}}_{2mn} = \imath_{21}\mu_n^7 + \imath_{22}\mu_n^5 + \imath_{23}\lambda_m^2\mu_n^5 + \imath_{24}\mu_n^3 + \imath_{25}\lambda_m^2\mu_n^3 + \imath_{26}\lambda_m^4\mu_n^3 + \imath_{27}\mu_n + \imath_{28}\lambda_m^2\mu_n + \imath_{29}\lambda_m^4\mu_n + \imath_{30}\lambda_m^6\mu_n$$

$$\hat{\hat{\eta}}_{1mn}^T = \eta_{11}^T\lambda_m^7 + \eta_{12}^T\lambda_m^5 + \eta_{13}^T\lambda_m^5\mu_n^2 + \eta_{14}^T\lambda_m^3 + \eta_{15}^T\lambda_m^3\mu_n^2 + \eta_{16}^T\lambda_m^3\mu_n^4 + \eta_{17}^T\lambda_m + \eta_{18}^T\lambda_m\mu_n^2 + \eta_{19}^T\lambda_m\mu_n^4 + \eta_{20}^T\lambda_m\mu_n^6$$

$$\hat{\hat{\eta}}_{2mn}^T = \eta_{21}^T\mu_n^7 + \eta_{22}^T\mu_n^5 + \eta_{23}^T\lambda_m^2\mu_n^5 + \eta_{24}^T\mu_n^3 + \eta_{25}^T\lambda_m^2\mu_n^3 + \eta_{26}^T\lambda_m^4\mu_n^3 + \eta_{27}^T\mu_n + \eta_{28}^T\lambda_m^2\mu_n + \eta_{29}^T\lambda_m^4\mu_n + \eta_{30}^T\lambda_m^6\mu_n$$

$$\hat{\hat{\imath}}_{1mn}^T = \imath_{11}^T\lambda_m^7 + \imath_{12}^T\lambda_m^5 + \imath_{13}^T\lambda_m^5\mu_n^2 + \imath_{14}^T\lambda_m^3 + \imath_{15}^T\lambda_m^3\mu_n^2 + \imath_{16}^T\lambda_m^3\mu_n^4 + \imath_{17}^T\lambda_m + \imath_{18}^T\lambda_m\mu_n^2 + \imath_{19}^T\lambda_m\mu_n^4 + \imath_{20}^T\lambda_m\mu_n^6$$

$$\hat{\hat{\imath}}_{2mn}^T = \imath_{21}^T\mu_n^7 + \imath_{22}^T\mu_n^5 + \imath_{23}^T\lambda_m^2\mu_n^5 + \imath_{24}^T\mu_n^3 + \imath_{25}^T\lambda_m^2\mu_n^3 + \imath_{26}^T\lambda_m^4\mu_n^3 + \imath_{27}^T\mu_n + \imath_{28}^T\lambda_m^2\mu_n + \imath_{29}^T\lambda_m^4\mu_n + \imath_{30}^T\lambda_m^6\mu_n$$

$$\Gamma_{11} = \Lambda_{11}^2\Lambda_{66}^2 - 2A_{16}^2\Lambda_{11}\Lambda_{66} + A_{16}^4$$

$$\Gamma_{12} = 2\Lambda_{11}^2\Lambda_{22}\Lambda_{66} - 4A_{26}^2\Lambda_{11}^2 - 2\Lambda_{12}^2\Lambda_{11}\Lambda_{66} - 4\Lambda_{12}\Lambda_{11}\Lambda_{66}^2 + 8A_{16}A_{26}\Lambda_{12}\Lambda_{11} + 4A_{16}A_{26}\Lambda_{11}\Lambda_{66} - 2A_{16}^2\Lambda_{11}\Lambda_{22} + 4A_{16}^2\Lambda_{12}\Lambda_{66} - 4A_{16}^3A_{26} - 2A_{16}^2\Lambda_{12}^2$$

$$\Gamma_{13} = \Lambda_{12}^4 + \Lambda_{11}^2\Lambda_{22}^2 + 2\Lambda_{11}\Lambda_{22}\Lambda_{66}^2 - 2\Lambda_{11}\Lambda_{66}A_{26}^2 - 2\Lambda_{11}\Lambda_{22}\Lambda_{12}^2 - 4\Lambda_{12}\Lambda_{11}\Lambda_{22}\Lambda_{66} + 8A_{26}^2\Lambda_{11}\Lambda_{12} - 4A_{16}A_{26}\Lambda_{11}\Lambda_{22} + 4\Lambda_{12}^2\Lambda_{66}^2 - 8A_{16}A_{26}\Lambda_{12}\Lambda_{66} - 2A_{16}^2\Lambda_{22}\Lambda_{66} + 6A_{16}^2A_{26}^2 + 8A_{16}^2\Lambda_{12}\Lambda_{22} - 12A_{16}A_{26}\Lambda_{12}^2 + 4\Lambda_{12}^3\Lambda_{66}$$

$$\Gamma_{14} = 2\Lambda_{11}\Lambda_{22}^2\Lambda_{66} - 2A_{26}^2\Lambda_{11}\Lambda_{22} - 2\Lambda_{12}^2\Lambda_{22}\Lambda_{66} - 4\Lambda_{12}\Lambda_{22}\Lambda_{66}^2 + 4A_{26}^2\Lambda_{12}\Lambda_{66} + 4A_{16}A_{26}\Lambda_{22}\Lambda_{66} - 4A_{16}^2\Lambda_{22}^2 + 8A_{16}A_{26}\Lambda_{12}\Lambda_{22} - 4A_{16}A_{26}^3 - 2A_{26}^2\Lambda_{12}^2$$

$$\Gamma_{15} = \Lambda_{22}^2\Lambda_{66}^2 - 2A_{26}^2\Lambda_{22}\Lambda_{66} + A_{26}^4$$

$$\Gamma_{21} = A_{16}^4 - 2A_{16}^2\hat{\Lambda}_{11}\hat{\Lambda}_{66} + \hat{\Lambda}_{11}^2\hat{\Lambda}_{66}^2$$

$$\Gamma_{22} = 2\left(\hat{\Lambda}_{11}\hat{\Lambda}_{66}^2 - A_{16}^2\hat{\Lambda}_{66}\right)d_1 + 2\left(\hat{\Lambda}_{11}^2\hat{\Lambda}_{66} - A_{16}^2\hat{\Lambda}_{11}\right)d_2$$

$$\Gamma_{23} = -2A_{16}^2\hat{\Lambda}_{12}^2 + 4A_{16}^2\hat{\Lambda}_{12}\hat{\Lambda}_{66} - 4A_{16}^3A_{26} - 2\hat{\Lambda}_{11}\hat{\Lambda}_{12}^2\hat{\Lambda}_{66} - 4\hat{\Lambda}_{11}\hat{\Lambda}_{12}\hat{\Lambda}_{66}^2 + 4A_{16}A_{26}\hat{\Lambda}_{11}\hat{\Lambda}_{66} - 4A_{26}^2\hat{\Lambda}_{11}^2 + 8A_{16}A_{26}\hat{\Lambda}_{11}\hat{\Lambda}_{12} - 2A_{16}^2\hat{\Lambda}_{11}\hat{\Lambda}_{22} + 2\hat{\Lambda}_{11}^2\hat{\Lambda}_{22}\hat{\Lambda}_{66}$$

$$\Gamma_{24} = 2\left(2\hat{\Lambda}_{11}\hat{\Lambda}_{66} - A_{16}^2\right)d_1d_2 + \hat{\Lambda}_{11}^2d_2^2 + \hat{\Lambda}_{66}^2d_1^2$$

$$\Gamma_{25} = \left(-2\hat{\Lambda}_{12}^2\hat{\Lambda}_{66} - 4\hat{\Lambda}_{12}\hat{\Lambda}_{66}^2 + 4A_{16}A_{26}\hat{\Lambda}_{66} - 8A_{26}^2\hat{\Lambda}_{11} + 8A_{16}A_{26}\hat{\Lambda}_{12} - 2A_{16}^2\hat{\Lambda}_{22} + 4\hat{\Lambda}_{11}\hat{\Lambda}_{22}\hat{\Lambda}_{66}\right)d_1 + \left(-2\hat{\Lambda}_{11}\hat{\Lambda}_{12}^2 - 4\hat{\Lambda}_{11}\hat{\Lambda}_{12}\hat{\Lambda}_{66} + 2\hat{\Lambda}_{11}\hat{\Lambda}_{66}^2 - 4A_{16}A_{26}\hat{\Lambda}_{11} + 8A_{16}^2\hat{\Lambda}_{12} - 2A_{16}^2\hat{\Lambda}_{66} + 2\hat{\Lambda}_{11}^2\hat{\Lambda}_{22}\right)d_2$$

$$\Gamma_{26} = \hat{\Lambda}_{12}^4 + 4\hat{\Lambda}_{12}^3\hat{\Lambda}_{66} + 6A_{16}^2A_{26}^2 - 12A_{16}A_{26}\hat{\Lambda}_{12}^2 - 8A_{16}A_{26}\hat{\Lambda}_{12}\hat{\Lambda}_{66} + 4\hat{\Lambda}_{12}^2\hat{\Lambda}_{66}^2 - 2\hat{\Lambda}_{11}\hat{\Lambda}_{12}^2\hat{\Lambda}_{22} - 4\hat{\Lambda}_{11}\hat{\Lambda}_{22}\hat{\Lambda}_{12}\hat{\Lambda}_{66} + 2\hat{\Lambda}_{11}\hat{\Lambda}_{22}\hat{\Lambda}_{66}^2 - 4A_{16}A_{26}\hat{\Lambda}_{11}\hat{\Lambda}_{22} + 8A_{16}^2\hat{\Lambda}_{12}\hat{\Lambda}_{22} + 8A_{26}^2\hat{\Lambda}_{11}\hat{\Lambda}_{12} - 2A_{26}^2\hat{\Lambda}_{11}\hat{\Lambda}_{66} - 2A_{16}^2\hat{\Lambda}_{22}\hat{\Lambda}_{66} + \hat{\Lambda}_{11}^2\hat{\Lambda}_{22}^2$$

$$\Gamma_{27} = 2\hat{\Lambda}_{11}d_1d_2^2 + 2\hat{\Lambda}_{66}d_1^2d_2$$

$$\Gamma_{28} = \left(-2\hat{\Lambda}_{12}^2 - 4\hat{\Lambda}_{12}\hat{\Lambda}_{66} + 2\hat{\Lambda}_{66}^2 - 4A_{16}A_{26} + 4\hat{\Lambda}_{11}\hat{\Lambda}_{22}\right)d_1d_2 + \left(2\hat{\Lambda}_{22}\hat{\Lambda}_{66} - 4A_{26}^2\right)d_1^2 + \left(2\hat{\Lambda}_{11}\hat{\Lambda}_{66} - 4A_{16}^2\right)d_2^2$$

$$\Gamma_{29} = 2\hat{\Lambda}_{66}d_1d_2^2 + 2\hat{\Lambda}_{22}d_1^2d_2$$

$$\Gamma_{30} = \left(8A_{26}^2\hat{\Lambda}_{12} - 2A_{26}^2\hat{\Lambda}_{66} + 2\hat{\Lambda}_{11}\hat{\Lambda}_{22}^2 + 2\hat{\Lambda}_{22}\hat{\Lambda}_{66}^2 - 2\hat{\Lambda}_{12}^2\hat{\Lambda}_{22} - 4\hat{\Lambda}_{12}\hat{\Lambda}_{22}\hat{\Lambda}_{66} - 4A_{16}A_{26}\hat{\Lambda}_{22}\right)d_1 + \left(8A_{16}A_{26}\hat{\Lambda}_{12} + 4A_{16}A_{26}\hat{\Lambda}_{66} - 2A_{26}^2\hat{\Lambda}_{11} + 4\hat{\Lambda}_{11}\hat{\Lambda}_{22}\hat{\Lambda}_{66} - 2\hat{\Lambda}_{12}^2\hat{\Lambda}_{66} - 4\hat{\Lambda}_{12}\hat{\Lambda}_{66}^2 - 8A_{16}^2\hat{\Lambda}_{22}\right)d_2$$

$$\Gamma_{31} = \left(4\hat{\Lambda}_{22}\hat{\Lambda}_{66} - 2A_{26}^2\right)d_1d_2 + \hat{\Lambda}_{22}^2d_1^2 + \hat{\Lambda}_{66}^2d_2^2$$

$$\Gamma_{32} = -4A_{16}A_{26}^3 - 2A_{26}^2\hat{\Lambda}_{12}2 + 4A_{26}^2\hat{\Lambda}_{12}\hat{\Lambda}_{66} - 2\hat{\Lambda}_{12}^2\hat{\Lambda}_{22}\hat{\Lambda}_{66} - 4\hat{\Lambda}_{12}\hat{\Lambda}_{22}\hat{\Lambda}_{66}^2 + 4A_{16}A_{26}\hat{\Lambda}_{22}\hat{\Lambda}_{66} - 4A_{16}^2A_{26}^2 + 8A_{16}A_{26}\hat{\Lambda}_{12}\hat{\Lambda}_{22} - 2A_{26}^2\hat{\Lambda}_{11}\hat{\Lambda}_{22} + 2\hat{\Lambda}_{11}\hat{\Lambda}_{22}^2\hat{\Lambda}_{66}$$

$$\Gamma_{33} = \left(-2A_{26}^2\hat{\Lambda}_{22} + 2\hat{\Lambda}_{22}^2\hat{\Lambda}_{66}\right)d_1 + \left(-2A_{26}^2\hat{\Lambda}_{66} + 2\hat{\Lambda}_{22}\hat{\Lambda}_{66}^2\right)d_2$$

$$\Gamma_{34} = -2A_{26}^2\hat{\Lambda}_{22}\hat{\Lambda}_{66} + \hat{\Lambda}_{22}^2\hat{\Lambda}_{66}^2 + A_{26}^4$$

$$\Gamma_{35} = d_1^2d_2^2$$

$$\phi_{31} = A_{16}A_{26}^2\Lambda_{22} - A_{16}\Lambda_{22}^2\Lambda_{66} + A_{26}\Lambda_{12}\Lambda_{22}\Lambda_{66} - A_{26}^3\Lambda_{12}$$

$$\phi_{32} = A_{16}\Lambda_{11}\Lambda_{22}^2 - A_{16}\Lambda_{12}^2\Lambda_{22} + 2A_{16}\Lambda_{12}\Lambda_{22}\Lambda_{66} - 2A_{16}A_{26}^2\Lambda_{12} - 2A_{26}\Lambda_{11}\Lambda_{22}\Lambda_{66} - A_{26}\Lambda_{11}\Lambda_{12}\Lambda_{22} + 2A_{26}^3\Lambda_{11} + A_{26}\Lambda_{12}^3$$

$$\phi_{33} = -A_{16}^3\Lambda_{22} + 3A_{16}^2A_{26}\Lambda_{12} - 2A_{16}\Lambda_{12}^2\Lambda_{66} - 2A_{16}A_{26}^2\Lambda_{11} + A_{16}\Lambda_{11}\Lambda_{22}\Lambda_{66} + A_{26}\Lambda_{11}\Lambda_{12}\Lambda_{66}$$

$$\phi_{34} = A_{16}A_{26}^2\Lambda_{22} - A_{26}^3\Lambda_{12} + A_{26}\Lambda_{12}\Lambda_{22}\Lambda_{66} - A_{16}\Lambda_{22}^2\Lambda_{66}$$

$$\phi_{35} = -2A_{26}\Lambda_{11}\Lambda_{22}\Lambda_{66} + 2A_{26}^3\Lambda_{11} - 2A_{16}A_{26}^2\Lambda_{12} - A_{16}\Lambda_{12}^2\Lambda_{22} + 2A_{16}\Lambda_{12}\Lambda_{22}\Lambda_{66} + A_{26}\Lambda_{12}^3 + A_{16}\Lambda_{11}\Lambda_{22}^2 - A_{26}\Lambda_{12}\Lambda_{11}\Lambda_{22}$$

$$\phi_{36} = -2A_{16}\Lambda_{12}^2\Lambda_{66} + 3A_{16}^2A_{26}\Lambda_{12} + A_{16}\Lambda_{11}\Lambda_{22}\Lambda_{66} - A_{16}^3\Lambda_{22} - 2A_{16}A_{26}^2\Lambda_{11} + A_{26}\Lambda_{12}\Lambda_{11}\Lambda_{66}$$

$$\phi_{41} = 2A_{16}^2\Lambda_{11}\Lambda_{66} - \Lambda_{11}^2\Lambda_{66}^2 - A_{16}^4$$

$$\phi_{42} = -3A_{16}^2\Lambda_{12}\Lambda_{66} + 3A_{16}^3A_{26} + 3\Lambda_{12}\Lambda_{11}\Lambda_{66}^2 + 2A_{16}^2\Lambda_{11}\Lambda_{22} - 8A_{16}A_{26}\Lambda_{12}\Lambda_{11} + 4A_{26}^2\Lambda_{11}^2 - 2\Lambda_{11}^2\Lambda_{22}\Lambda_{66} - 3A_{16}A_{26}\Lambda_{11}\Lambda_{66} + 2\Lambda_{11}\Lambda_{12}^2\Lambda_{66} + 2A_{16}^2\Lambda_{12}^2$$

$$\phi_{43} = A_{16}^2\Lambda_{22}\Lambda_{66} - 3A_{16}^2A_{26}^2 + 4A_{16}A_{26}\Lambda_{12}\Lambda_{66} + 9A_{16}A_{26}\Lambda_{12}^2 - 6A_{26}^2\Lambda_{12}\Lambda_{11} + 3A_{16}A_{26}\Lambda_{11}\Lambda_{22} - 2\Lambda_{12}^2\Lambda_{66}^2 - 6A_{16}^2\Lambda_{12}\Lambda_{22} + 2\Lambda_{12}^2\Lambda_{11}\Lambda_{22} + 3\Lambda_{12}\Lambda_{11}\Lambda_{22}\Lambda_{66} - \Lambda_{11}^2\Lambda_{22}^2 - \Lambda_{11}\Lambda_{22}\Lambda_{66}^2 - \Lambda_{12}^4 + A_{26}^2\Lambda_{11}\Lambda_{66} - 3\Lambda_{12}^3\Lambda_{66}$$

$$\phi_{44} = 2A_{16}^2\Lambda_{22}^2 - 4A_{16}A_{26}\Lambda_{12}\Lambda_{22} - A_{16}A_{26}\Lambda_{22}\Lambda_{66} + A_{16}A_{26}^3 + A_{26}^2\Lambda_{11}\Lambda_{22} - \Lambda_{11}\Lambda_{22}^2\Lambda_{66} + A_{26}^2\Lambda_{12}^2 + \Lambda_{12}^2\Lambda_{22}\Lambda_{66} + \Lambda_{12}\Lambda_{22}\Lambda_{66}^2 - A_{26}^2\Lambda_{12}\Lambda_{66}$$

$$\phi_{45} = A_{16}^2\Lambda_{12}\Lambda_{66} - \Lambda_{12}\Lambda_{11}\Lambda_{66}^2 + A_{16}A_{26}\Lambda_{11}\Lambda_{66} - A_{16}^3A_{26}$$

$$\phi_{46} = -4A_{16}A_{26}\Lambda_{12}\Lambda_{66} + 3A_{16}^2A_{26}^2 + 2\Lambda_{12}^2\Lambda_{66}^2 + 2A_{16}^2\Lambda_{12}\Lambda_{22} - 3A_{16}A_{26}\Lambda_{12}^2 + 2A_{26}^2\Lambda_{11}\Lambda_{12} - \Lambda_{11}\Lambda_{22}\Lambda_{12}\Lambda_{66} + \Lambda_{12}^3\Lambda_{66} - A_{16}A_{26}\Lambda_{11}\Lambda_{22} + \Lambda_{11}\Lambda_{22}\Lambda_{66}^2 - A_{16}^2\Lambda_{22}\Lambda_{66} - A_{26}^2\Lambda_{11}\Lambda_{66}$$

$$\phi_{47} = 3A_{16}A_{26}\Lambda_{22}\Lambda_{66} - 3A_{16}A_{26}^3 + 4A_{16}A_{26}\Lambda_{12}\Lambda_{22} + 3A_{26}^2\Lambda_{12}\Lambda_{66} - A_{26}^2\Lambda_{12}^2 - 3\Lambda_{12}\Lambda_{22}\Lambda_{66}^2 - \Lambda_{12}^2\Lambda_{22}\Lambda_{66} - A_{26}^2\Lambda_{11}\Lambda_{22} - 2A_{16}^2\Lambda_{22}^2 + \Lambda_{11}\Lambda_{22}^2\Lambda_{66}$$

$$\phi_{48} = \Lambda_{22}^2\Lambda_{66}^2 - 2A_{26}^2\Lambda_{22}\Lambda_{66} + A_{26}^4$$

$$\gamma_{31} = A_{16}A_{26}\Lambda_{22}\Lambda_{66} + A_{26}^2\Lambda_{12}\Lambda_{66} - \Lambda_{12}\Lambda_{22}\Lambda_{66}^2 - A_{16}A_{26}^3$$

$$\gamma_{32} = 3A_{16}^2A_{26}^2 + 2A_{16}^2\Lambda_{12}\Lambda_{22} - A_{16}A_{26}\Lambda_{11}\Lambda_{22} - A_{16}^2\Lambda_{22}\Lambda_{66} - 3A_{16}A_{26}\Lambda_{12}^2 + 2A_{26}^2\Lambda_{12}\Lambda_{11} - \\ - \Lambda_{12}\Lambda_{11}\Lambda_{22}\Lambda_{66} - A_{26}^2\Lambda_{11}\Lambda_{66} - 4A_{16}A_{26}\Lambda_{12}\Lambda_{66} + 2\Lambda_{12}^2\Lambda_{66}^2 + \Lambda_{12}^3\Lambda_{66} + \Lambda_{11}\Lambda_{22}\Lambda_{66}^2$$

$$\gamma_{33} = -3A_{16}^3A_{26} - A_{16}^2\Lambda_{12}^2 + 4A_{16}A_{26}\Lambda_{12}\Lambda_{11} + 3A_{16}A_{26}\Lambda_{11}\Lambda_{66} - A_{16}^2\Lambda_{11}\Lambda_{22} - \Lambda_{11}\Lambda_{12}^2\Lambda_{66} + \\ + \Lambda_{11}^2\Lambda_{22}\Lambda_{66} - 2A_{26}^2\Lambda_{11}^2 - 3\Lambda_{11}\Lambda_{12}\Lambda_{66}^2 + 3A_{16}^2\Lambda_{12}\Lambda_{66}$$

$$\gamma_{34} = A_{16}^4 + \Lambda_{11}^2\Lambda_{66}^2 - 2A_{16}^2\Lambda_{11}\Lambda_{66}$$

$$\gamma_{35} = 2A_{26}^2\Lambda_{22}\Lambda_{66} - \Lambda_{22}^2\Lambda_{66}^2 - A_{26}^4$$

$$\gamma_{36} = 3A_{16}A_{26}^3 - 8A_{16}A_{26}\Lambda_{12}\Lambda_{22} + 2A_{26}^2\Lambda_{11}\Lambda_{22} - 3A_{16}A_{26}\Lambda_{22}\Lambda_{66} + 2A_{26}^2\Lambda_{12}^2 + 2\Lambda_{12}^2\Lambda_{22}\Lambda_{66} + \\ + 3\Lambda_{12}\Lambda_{22}\Lambda_{66}^2 - 3A_{26}^2\Lambda_{12}\Lambda_{66} - 2\Lambda_{11}\Lambda_{22}^2\Lambda_{66} + 4A_{16}^2\Lambda_{22}^2$$

$$\gamma_{37} = -3A_{16}^2A_{26}^2 + 9A_{16}A_{26}\Lambda_{12}^2 - 6A_{26}^2\Lambda_{11}\Lambda_{12} + A_{26}^2\Lambda_{11}\Lambda_{66} + 3A_{16}A_{26}\Lambda_{11}\Lambda_{22} - \Lambda_{12}^4 - 3\Lambda_{12}^3\Lambda_{66} + \\ + 3\Lambda_{11}\Lambda_{22}\Lambda_{12}\Lambda_{66} - 2\Lambda_{12}^2\Lambda_{66}^2 + 2\Lambda_{12}^2\Lambda_{11}\Lambda_{22} + 4A_{16}A_{26}\Lambda_{12}\Lambda_{66} - 6A_{16}^2\Lambda_{12}\Lambda_{22} - \Lambda_{12}^2\Lambda_{22}^2 - \\ - \Lambda_{11}\Lambda_{22}\Lambda_{66}^2 + A_{16}^2\Lambda_{22}\Lambda_{66}$$

$$\gamma_{38} = -A_{16}A_{26}\Lambda_{11}\Lambda_{66} + A_{16}^3A_{26} + A_{16}^2\Lambda_{12}^2 + \Lambda_{12}\Lambda_{11}\Lambda_{66}^2 - 4A_{16}A_{26}\Lambda_{12}\Lambda_{11} + \Lambda_{12}^2\Lambda_{11}\Lambda_{66} - \\ A_{16}^2\Lambda_{12}\Lambda_{66} + A_{16}^2\Lambda_{11}\Lambda_{22} = 2A_{26}^2\Lambda_{11}^2 - \Lambda_{11}^2\Lambda_{22}\Lambda_{66}$$

$$\gamma_{41} = A_{16}^2A_{26}\Lambda_{11} - A_{16}^3\Lambda_{12} + A_{16}\Lambda_{12}\Lambda_{11}\Lambda_{66} - A_{26}\Lambda_{11}^2\Lambda_{66}$$

$$\gamma_{42} = -2A_{16}^2A_{26}\Lambda_{12} + 2A_{16}^3\Lambda_{22} - A_{16}\Lambda_{12}\Lambda_{11}\Lambda_{22} + \Lambda_{12}^3A_{16} - A_{26}\Lambda_{12}^2\Lambda_{11} + A_{26}\Lambda_{11}^2\Lambda_{22} + \\ 2A_{26}\Lambda_{12}\Lambda_{11}\Lambda_{66} - 2A_{16}\Lambda_{11}\Lambda_{22}\Lambda_{66}$$

$$\gamma_{43} = 3A_{16}A_{26}^2\Lambda_{12} + A_{16}\Lambda_{12}\Lambda_{22}\Lambda_{66} + A_{26}\Lambda_{11}\Lambda_{22}\Lambda_{66} - A_{26}^3\Lambda_{11} - 2A_{16}^2A_{26}\Lambda_{22} - 2A_{26}\Lambda_{12}^2\Lambda_{66}$$

$$\gamma_{44} = A_{16}\Lambda_{12}\Lambda_{11}\Lambda_{66} - A_{16}^3\Lambda_{12} + A_{16}^2A_{26}\Lambda_{11} - A_{26}\Lambda_{11}^2\Lambda_{66}$$

$$\gamma_{45} = -2A_{16}^2A_{26}\Lambda_{12} - A_{16}\Lambda_{12}\Lambda_{11}\Lambda_{22} - A_{26}\Lambda_{12}^2\Lambda_{11} + A_{16}\Lambda_{12}^3 + A_{26}\Lambda_{11}^2\Lambda_{22} - 2A_{16}\Lambda_{11}\Lambda_{22}\Lambda_{66} + \\ 2A_{26}\Lambda_{12}\Lambda_{11}\Lambda_{66} + 2A_{16}^3\Lambda_{22}$$

$$\gamma_{46} = 3A_{16}A_{26}^2\Lambda_{12} - 2A_{16}^2A_{26}\Lambda_{22} - A_{26}^3\Lambda_{11} - 2A_{26}\Lambda_{12}^2\Lambda_{66} + A_{26}\Lambda_{11}\Lambda_{22}\Lambda_{66} + A_{16}\Lambda_{12}\Lambda_{22}\Lambda_{66}$$

$$\eta_{11} = \left(A_{16}^2 \hat{\Lambda}_{66} - \hat{\Lambda}_{11}\hat{\Lambda}_{66}^2\right)\overline{\Lambda}_1$$

$$\eta_{12} = \left\{-\hat{\Lambda}_{66}^2 d_1 + \left(A_{16}^2 - 2\hat{\Lambda}_{11}\hat{\Lambda}_{66}\right)d_1\right\}$$

$$\eta_{13} = \left(-4A_{16}A_{26}\hat{\Lambda}_{12} - 2A_{16}A_{26}\hat{\Lambda}_{66} + A_{16}^2\hat{\Lambda}_{22} + \hat{\Lambda}_{12}^2\hat{\Lambda}_{66} + 2\hat{\Lambda}_{12}\hat{\Lambda}_{66}^2 - 2\hat{\Lambda}_{11}\hat{\Lambda}_{22}\hat{\Lambda}_{66} + 4A_{26}^2\hat{\Lambda}_{11}\right)\overline{\Lambda}_1 + \left(A_{16}^2\hat{\Lambda}_{12} + \hat{\Lambda}_{11}\hat{\Lambda}_{66}^2 - 2A_{16}A_{26}\hat{\Lambda}_{11} + \hat{\Lambda}_{12}\hat{\Lambda}_{11}\hat{\Lambda}_{66} - A_{16}^2\hat{\Lambda}_{66}\right)\overline{\Lambda}_2$$

$$\eta_{14} = -\left(2\hat{\Lambda}_{66}d_1d_2 + \hat{\Lambda}_{11}d_2^2\right)\overline{\Lambda}_1$$

$$\eta_{15} = \left\{\left(4A_{26}^2 - 2\hat{\Lambda}_{22}\hat{\Lambda}_{66}\right)d_1 + \left(2A_{16}A_{26} + 2\hat{\Lambda}_{12}\hat{\Lambda}_{66} - 2\hat{\Lambda}_{11}\hat{\Lambda}_{22} + \hat{\Lambda}_{12}^2 - \hat{\Lambda}_{66}^2\right)d_2\right\}\overline{\Lambda}_1 + \left\{\left(\hat{\Lambda}_{12}\hat{\Lambda}_{66} - 2A_{16}A_{26} + \hat{\Lambda}_{66}^2\right)d_1 + \left(\hat{\Lambda}_{11}\hat{\Lambda}_{66} + \hat{\Lambda}_{11}\hat{\Lambda}_{12} - 2A_{16}^2\right)d_2\right\}\overline{\Lambda}_2$$

$$\eta_{16} = \left(2\hat{\Lambda}_{12}\hat{\Lambda}_{22}\hat{\Lambda}_{66} - 4A_{26}^2\hat{\Lambda}_{12} + \hat{\Lambda}_{12}^2\hat{\Lambda}_{22} + 2A_{16}A_{26}\hat{\Lambda}_{22} - \hat{\Lambda}_{11}\hat{\Lambda}_{22}^2 - \hat{\Lambda}_{22}\hat{\Lambda}_{66}^2 + A_{26}^2\hat{\Lambda}_{66}\right)\overline{\Lambda}_1 + \left(-3\hat{\Lambda}_{12}^2\hat{\Lambda}_{66} - 2\hat{\Lambda}_{12}\hat{\Lambda}_{66}^2 + \hat{\Lambda}_{11}\hat{\Lambda}_{22}\hat{\Lambda}_{66} + \hat{\Lambda}_{12}\hat{\Lambda}_{11}\hat{\Lambda}_{22} + 6A_{16}A_{26}\hat{\Lambda}_{12} + 2A_{16}A_{26}\hat{\Lambda}_{66} - \hat{\Lambda}_{12}^3 - 2A_{16}^2\hat{\Lambda}_{22} - 2A_{26}^2\hat{\Lambda}_{11}\right)\overline{\Lambda}_2$$

$$\eta_{17} = -d_1d_2^2\overline{\Lambda}_1$$

$$\eta_{18} = \left(\hat{\Lambda}_{12} + \hat{\Lambda}_{66}\right)d_1d_2\overline{\Lambda}_2 - \left(2\hat{\Lambda}_{22}d_1d_2 + \hat{\Lambda}_{66}d_2^2\right)\overline{\Lambda}_1$$

$$\eta_{19} = \left\{-\hat{\Lambda}_{22}^2 d_1 + \left(A_{26}^2 - 2\hat{\Lambda}_{22}\hat{\Lambda}_{66}\right)d_2\right\}\overline{\Lambda}_1 + \left\{\left(\hat{\Lambda}_{12}\hat{\Lambda}_{22} + \hat{\Lambda}_{22}\hat{\Lambda}_{66} - 2A_{26}^2\right)d_1 + \left(\hat{\Lambda}_{66}^2 + \hat{\Lambda}_{12}\hat{\Lambda}_{66} - - 2A_{16}A_{26}\right)d_2\right\}\overline{\Lambda}_2$$

$$\eta_{20} = \left(A_{26}^2\hat{\Lambda}_{22} - \hat{\Lambda}_{22}^2\hat{\Lambda}_{66}\right)\overline{\Lambda}_1 + \left(\hat{\Lambda}_{12}\hat{\Lambda}_{22}\hat{\Lambda}_{66} + \hat{\Lambda}_{22}\hat{\Lambda}_{66}^2 - A_{26}^2\hat{\Lambda}_{66} + A_{26}^2\hat{\Lambda}_{12} - 2A_{16}A_{26}\hat{\Lambda}_{22}\right)\overline{\Lambda}_2$$

$$\eta_{21} = \left(A_{26}\hat{\Lambda}_{22}\hat{\Lambda}_{66} - A_{26}^3\right)\overline{\Lambda}_2$$

$$\eta_{22} = \left(A_{26}\hat{\Lambda}_{22}d_1 + A_{26}\hat{\Lambda}_{66}d_2\right)\hat{\Lambda}_2$$

$$\eta_{23} = \left(2A_{16}\hat{\Lambda}_{22}^2 + 2A_{26}^3 - 2A_{26}\hat{\Lambda}_{12}\hat{\Lambda}_{22} - 2A_{26}\hat{\Lambda}_{22}\hat{\Lambda}_{66}\right)\overline{\Lambda}_1 + \left(A_{26}\hat{\Lambda}_{12}^2 + A_{16}A_{26}^2 - 2A_{16}\hat{\Lambda}_{12}\hat{\Lambda}_{22} - A_{16}\hat{\Lambda}_{22}\hat{\Lambda}_{66} + A_{26}\hat{\Lambda}_{11}\hat{\Lambda}_{22}\right)\overline{\Lambda}_2$$

$$\eta_{24} = A_{26} d_1 d_2 \overline{\Lambda}_2$$

$$\eta_{25} = \left(4 A_{16} \hat{\Lambda}_{22} - 2 A_{26} \hat{\Lambda}_{12} - 2 A_{26} \hat{\Lambda}_{66}\right) d_2 \overline{\Lambda}_1 + \left\{\left(A_{16} \hat{\Lambda}_{22} - A_{26} \hat{\Lambda}_{66} - 2 A_{26} \hat{\Lambda}_{12}\right) d_1 + \left(-2 A_{16} \hat{\Lambda}_{12} + A_{26} \hat{\Lambda}_{11} - A_{16} \hat{\Lambda}_{66}\right) d_2\right\} \overline{\Lambda}_2$$

$$\eta_{26} = \left(2 A_{16} \hat{\Lambda}_{22} \hat{\Lambda}_{66} - 4 A_{16} A_{26}^2 - 2 A_{16} \hat{\Lambda}_{12} \hat{\Lambda}_{22} + 2 A_{26} \hat{\Lambda}_{12}^2 + 2 A_{26} \hat{\Lambda}_{12} \hat{\Lambda}_{66}\right) \overline{\Lambda}_1 + \left(A_{16} \hat{\Lambda}_{12}^2 + A_{16}^2 A_{26} - A_{26} \hat{\Lambda}_{11} \hat{\Lambda}_{66} + A_{16} \hat{\Lambda}_{11} \hat{\Lambda}_{22} - 2 A_{26} \hat{\Lambda}_{11} \hat{\Lambda}_{12}\right) \overline{\Lambda}_2$$

$$\eta_{27} = 2 A_{16} d_2^2 \overline{\Lambda}_1 + A_{16} d_1 d_2 \overline{\Lambda}_2$$

$$\eta_{28} = \left(2 A_{16} \hat{\Lambda}_{66} - 2 A_{16} \hat{\Lambda}_{12}\right) d_2 \overline{\Lambda}_1 + \left(A_{16} \hat{\Lambda}_{66} d_1 + A_{16} \hat{\Lambda}_{11} d_2\right) \overline{\Lambda}_2$$

$$\eta_{29} = \left(-2 A_{16} \hat{\Lambda}_{12} \hat{\Lambda}_{66} + 2 A_{16}^2 A_{26}\right) \overline{\Lambda}_1 + \left(-A_{16}^3 + A_{16} \hat{\Lambda}_{11} \hat{\Lambda}_{66}\right) \overline{\Lambda}_2$$

$$\iota_{11} = \left(A_{16} \hat{\Lambda}_{11} \hat{\Lambda}_{66} - A_{16}^3\right) \overline{\Lambda}_1$$

$$\iota_{12} = \left(A_{16} \hat{\Lambda}_{66} d_1 + A_{16} \hat{\Lambda}_{11} d_2\right) \overline{\Lambda}_1$$

$$\iota_{13} = \left(-2 A_{26} \hat{\Lambda}_{11} \hat{\Lambda}_{12} + A_{16} \hat{\Lambda}_{12}^2 - A_{26} \hat{\Lambda}_{11} \hat{\Lambda}_{66} + A_{16}^2 A_{26} + A_{16} \hat{\Lambda}_{11} \hat{\Lambda}_{22}\right) \overline{\Lambda}_1 + \left(2 A_{16}^3 + 2 A_{26} \hat{\Lambda}_{11}^2 - -2 A_{16} \hat{\Lambda}_{11} \hat{\Lambda}_{12} - 2 A_{16} \hat{\Lambda}_{11} \hat{\Lambda}_{66}\right) \overline{\Lambda}_2$$

$$\iota_{14} = A_{16} d_1 d_2 \overline{\Lambda}_1$$

$$\iota_{15} = \left\{\left(-2 A_{26} \hat{\Lambda}_{12} - A_{26} \hat{\Lambda}_{66} + A_{16} \hat{\Lambda}_{22}\right) d_1 + \left(A_{26} \hat{\Lambda}_{11} - 2 A_{16} \hat{\Lambda}_{12} - A_{16} \hat{\Lambda}_{66}\right) d_2\right\} \overline{\Lambda}_1 + \left(4 A_{26} \hat{\Lambda}_{11} - 2 A_{16} \hat{\Lambda}_{66} - 2 A_{16} \hat{\Lambda}_{12}\right) d_1 \overline{\Lambda}_2$$

$$\iota_{16} = \left(A_{26} \hat{\Lambda}_{12}^2 + A_{26} \hat{\Lambda}_{11} \hat{\Lambda}_{22} + A_{16} A_{26}^2 - 2 A_{16} \hat{\Lambda}_{12} \hat{\Lambda}_{22} - A_{16} \hat{\Lambda}_{22} \hat{\Lambda}_{66}\right) \overline{\Lambda}_1 + \left(2 A_{26} \hat{\Lambda}_{11} \hat{\Lambda}_{66} + 2 A_{16} \hat{\Lambda}_{12} \hat{\Lambda}_{66} - 2 A_{26} \hat{\Lambda}_{11} \hat{\Lambda}_{12} - 4 A_{16}^2 A_{26} + 2 A_{16} \hat{\Lambda}_{12}^2\right) \overline{\Lambda}_2$$

$$\iota_{17} = A_{26} d_1 d_2 \overline{\Lambda}_1 + 2 A_{26} d_1^2 \overline{\Lambda}_2$$

$$\iota_{18} = \left(A_{26} \hat{\Lambda}_{66} d_2 + A_{26} \hat{\Lambda}_{22} d_1\right) \overline{\Lambda}_1 + \left(2 A_{26} \hat{\Lambda}_{66} - 2 A_{26} \hat{\Lambda}_{12}\right) d_1 \overline{\Lambda}_2$$

$$\iota_{19} = \left(A_{26}\hat{\Lambda}_{22}\hat{\Lambda}_{66} - A_{26}^3\right)\overline{\Lambda}_1 + 2\left(A_{16}A_{26}^2 - A_{26}\hat{\Lambda}_{12}\hat{\Lambda}_{66}\right)\overline{\Lambda}_2$$

$$\iota_{21} = \left(A_{26}^2\hat{\Lambda}_{66} - \hat{\Lambda}_{22}\hat{\Lambda}_{66}^2\right)\overline{\Lambda}_2$$

$$\iota_{22} = \left\{\left(A_{26}^2 - 2\hat{\Lambda}_{22}\hat{\Lambda}_{66}\right)d_1 - \hat{\Lambda}_{66}^2 d_2\right\}\overline{\Lambda}_2$$

$$\iota_{23} = \left(\hat{\Lambda}_{12}\hat{\Lambda}_{22}\hat{\Lambda}_{66} + \hat{\Lambda}_{22}\hat{\Lambda}_{66}^2 - A_{26}^2\hat{\Lambda}_{66} + A_{26}^2\hat{\Lambda}_{12} - 2A_{16}A_{26}\hat{\Lambda}_{22}\right)\overline{\Lambda}_1 + \left(-2\hat{\Lambda}_{11}\hat{\Lambda}_{22}\hat{\Lambda}_{66} + A_{26}^2\hat{\Lambda}_{11} - 2A_{16}A_{26}\hat{\Lambda}_{66} + 4A_{16}^2\hat{\Lambda}_{22} - 4A_{16}A_{26}\hat{\Lambda}_{12} + \hat{\Lambda}_{12}^2\hat{\Lambda}_{66} + 2\hat{\Lambda}_{12}\hat{\Lambda}_{66}^2\right)\overline{\Lambda}_2$$

$$\iota_{24} = \left(-\hat{\Lambda}_{22}d_1^2 - 2\hat{\Lambda}_{66}d_1d_2\right)\overline{\Lambda}_2$$

$$\iota_{25} = \left\{\left(\hat{\Lambda}_{12}\hat{\Lambda}_{22} + \hat{\Lambda}_{22}\hat{\Lambda}_{66} - 2A_{26}^2\right)d_1 + \left(\hat{\Lambda}_{12}\hat{\Lambda}_{66} + \hat{\Lambda}_{66}^2 - 2A_{16}A_{26}\right)d_2\right\}\overline{\Lambda}_1 + \left\{\left(\hat{\Lambda}_{12}^2 - \hat{\Lambda}_{66}^2 - -2\hat{\Lambda}_{11}\hat{\Lambda}_{22} + 2A_{16}A_{26} + 2\hat{\Lambda}_{12}\hat{\Lambda}_{66}\right)d_1 + \left(-2\hat{\Lambda}_{11}\hat{\Lambda}_{66} + 4A_{16}^2\right)d_2\right\}\overline{\Lambda}_2$$

$$\iota_{26} = \left(-\hat{\Lambda}_{12}^3 + \hat{\Lambda}_{11}\hat{\Lambda}_{22}\hat{\Lambda}_{12} - 3\hat{\Lambda}_{12}^3\hat{\Lambda}_{66} + \hat{\Lambda}_{11}\hat{\Lambda}_{22}\hat{\Lambda}_{66} - 2\hat{\Lambda}_{12}\hat{\Lambda}_{66}^2 - 2A_{26}^2\hat{\Lambda}_{11} + 6A_{16}A_{26}\hat{\Lambda}_{12} + 2A_{16}A_{26}\hat{\Lambda}_{66} - 2A_{16}^2\hat{\Lambda}_{22}\right)\overline{\Lambda}_1 + \left(2\hat{\Lambda}_{11}\hat{\Lambda}_{12}\hat{\Lambda}_{66} - \hat{\Lambda}_{11}\hat{\Lambda}_{66}^2 + \hat{\Lambda}_{11}\hat{\Lambda}_{12}^2 + 2A_{16}A_{26}\hat{\Lambda}_{11} - \hat{\Lambda}_{11}^2\hat{\Lambda}_{22} + A_{16}^2\hat{\Lambda}_{66} - 4A_{16}^2\hat{\Lambda}_{12}\right)\overline{\Lambda}_2$$

$$\iota_{27} - -d_1^2 d_2\overline{\Lambda}_2$$

$$\iota_{28} = \left(\hat{\Lambda}_{12} + \hat{\Lambda}_{66}\right)d_1d_2\overline{\Lambda}_1 - \left(2\hat{\Lambda}_{11}d_1d_2 + \hat{\Lambda}_{66}d_1^2\right)\overline{\Lambda}_2$$

$$\iota_{29} = \left\{\left(\hat{\Lambda}_{12}\hat{\Lambda}_{66} + \hat{\Lambda}_{66}^2 - 2A_{16}A_{26}\right)d_1 + \left(\hat{\Lambda}_{11}\hat{\Lambda}_{12} + \hat{\Lambda}_{11}\hat{\Lambda}_{66} - 2A_{16}^2\right)d_2\right\}\overline{\Lambda}_1 + \left\{\left(A_{16}^2 - 2\hat{\Lambda}_{11}\hat{\Lambda}_{66}\right)d_1 - \hat{\Lambda}_{11}^2 d_2\right\}\overline{\Lambda}_2$$

$$\iota_{30} = \left(\hat{\Lambda}_{11}\hat{\Lambda}_{12}\hat{\Lambda}_{66} + \hat{\Lambda}_{11}\hat{\Lambda}_{66}^2 - 2A_{16}A_{26}\hat{\Lambda}_{11} + A_{16}^2\hat{\Lambda}_{12} - A_{16}^2\hat{\Lambda}_{66}\right)\overline{\Lambda}_1 + \left(A_{16}^2\hat{\Lambda}_{11} - \hat{\Lambda}_{11}^2\hat{\Lambda}_{66}\right)\overline{\Lambda}_2$$

$$\eta_{11}^T = \left(A_{16}^2\hat{\Lambda}_{66} - \hat{\Lambda}_{11}\hat{\Lambda}_{66}^2\right)\hat{\Omega}_{11}^T + \left(A_{16}\hat{\Lambda}_{11}\hat{\Lambda}_{66} - A_{16}^3\right)\hat{\Omega}_{12}^T$$

$$\eta_{12}^T = \left\{-\hat{\Lambda}_{66}^2 d_1 + \left(-2\hat{\Lambda}_{11}\hat{\Lambda}_{66} + A_{16}^2\right)d_2\right\}\hat{\Omega}_{11}^T + \left(A_{16}\hat{\Lambda}_{66}d_1 + A_{16}\hat{\Lambda}_{11}d_2\right)\hat{\Omega}_{12}^T$$

$$\eta_{13}^T = \left(-4A_{16}A_{26}\hat{\Lambda}_{12} - 2A_{16}A_{26}\hat{\Lambda}_{66} + A_{16}^2\hat{\Lambda}_{22} + \hat{\Lambda}_{12}^2\hat{\Lambda}_{66} + 2\hat{\Lambda}_{12}\hat{\Lambda}_{66}^2 - 2\hat{\Lambda}_{11}\hat{\Lambda}_{22}\hat{\Lambda}_{66} + 4A_{26}^2\hat{\Lambda}_{11}\right)\hat{\Omega}_{11}^T + \left(-2A_{16}\hat{\Lambda}_{12}\hat{\Lambda}_{66} + 3A_{16}^2A_{26} + A_{16}\hat{\Lambda}_{12}^2 + A_{16}\hat{\Lambda}_{11}\hat{\Lambda}_{22} - A_{26}\hat{\Lambda}_{11}\hat{\Lambda}_{66} - 2A_{26}\hat{\Lambda}_{11}\hat{\Lambda}_{12}\right)\hat{\Omega}_{12}^T + \left(A_{16}^2\hat{\Lambda}_{12} + \hat{\Lambda}_{11}\hat{\Lambda}_{66}^2 - 2A_{16}A_{26}\hat{\Lambda}_{11} + \hat{\Lambda}_{12}\hat{\Lambda}_{11}\hat{\Lambda}_{66} - A_{16}^2\hat{\Lambda}_{66}\right)\hat{\Omega}_{22}^T$$

$$\eta_{14}^T = \left(-2\hat{\Lambda}_{66}d_1d_2 - \hat{\Lambda}_{11}d_2^2\right)\hat{\Omega}_{11}^T + A_{16}d_1d_2\hat{\Omega}_{12}^T$$

$$\eta_{15}^T = \left\{\left(-2\hat{\Lambda}_{22}\hat{\Lambda}_{66} + 4A_{26}^2\right)d_1 + \left(2A_{16}A_{26} + 2\hat{\Lambda}_{12}\hat{\Lambda}_{66} + \hat{\Lambda}_{12}^2 - 2\hat{\Lambda}_{11}\hat{\Lambda}_{22} - \hat{\Lambda}_{66}^2\right)d_2\right\}\hat{\Omega}_{11}^T + \left\{\left(-A_{26}\hat{\Lambda}_{66} - 2A_{26}\hat{\Lambda}_{12} + A_{16}\hat{\Lambda}_{22}\right)d_1 + \left(-4A_{16}\hat{\Lambda}_{12} + A_{16}\hat{\Lambda}_{66} + A_{26}\hat{\Lambda}_{11}\right)d_2\right\}\hat{\Omega}_{12}^T + \left\{\left(\hat{\Lambda}_{66}^2 + \hat{\Lambda}_{12}\hat{\Lambda}_{66} - 2A_{16}A_{26}\right)d_1 + \left(\hat{\Lambda}_{11}\hat{\Lambda}_{66} + \hat{\Lambda}_{11}\hat{\Lambda}_{12} - 2A_{16}^2\right)d_2\right\}\hat{\Omega}_{22}^T$$

$$\eta_{16}^T = \left(2\hat{\Lambda}_{12}\hat{\Lambda}_{22}\hat{\Lambda}_{66} - 4A_{26}^2\hat{\Lambda}_{12} + \hat{\Lambda}_{12}^2\hat{\Lambda}_{22} + 2A_{16}A_{26}\hat{\Lambda}_{22} - \hat{\Lambda}_{11}\hat{\Lambda}_{22}^2 - \hat{\Lambda}_{22}\hat{\Lambda}_{66}^2 + A_{26}^2\hat{\Lambda}_{66}\right)\hat{\Omega}_{11}^T + \left(-4A_{16}\hat{\Lambda}_{12}\hat{\Lambda}_{22} + A_{16}\hat{\Lambda}_{22}\hat{\Lambda}_{66} - 3A_{16}A_{26}^2 + 3A_{26}\hat{\Lambda}_{12}^2 + 2A_{26}\hat{\Lambda}_{12}\hat{\Lambda}_{66} + A_{26}\hat{\Lambda}_{11}\hat{\Lambda}_{22}\right)\hat{\Omega}_{12}^T + \left(-3\hat{\Lambda}_{12}^2\hat{\Lambda}_{66} - 2\hat{\Lambda}_{12}\hat{\Lambda}_{66}^2 + \hat{\Lambda}_{11}\hat{\Lambda}_{22}\hat{\Lambda}_{66} + \hat{\Lambda}_{12}\hat{\Lambda}_{11}\hat{\Lambda}_{22} + 6A_{16}A_{26}\hat{\Lambda}_{12} + 2A_{16}A_{26}\hat{\Lambda}_{66} - \hat{\Lambda}_{12}^3 - 2A_{16}^2\hat{\Lambda}_{22} - 2A_{26}^2\hat{\Lambda}_{11}\right)\hat{\Omega}_{22}^T$$

$$\eta_{17}^T = -d_1d_2^2\hat{\Omega}_{11}^T$$

$$\eta_{18}^T = \left(-2\hat{\Lambda}_{22}d_1d_2 - \hat{\Lambda}_{66}d_2^2\right)\hat{\Omega}_{11}^T + \left(2A_{16}d_2^2 + A_{26}d_1d_2\right)\hat{\Omega}_{12}^T + \left(\hat{\Lambda}_{12} + \hat{\Lambda}_{66}\right)d_1d_2\hat{\Omega}_{22}^T$$

$$\eta_{19}^T = \left\{-\hat{\Lambda}_{22}^2d_1 + \left(A_{26}^2 - 2\hat{\Lambda}_{22}\hat{\Lambda}_{66}\right)d_2\right\}\hat{\Omega}_{11}^T + \left\{A_{26}\hat{\Lambda}_{22}d_1 + \left(-2A_{26}\hat{\Lambda}_{12} + 4A_{16}\hat{\Lambda}_{22} - A_{26}\hat{\Lambda}_{66}\right)d_2\right\}\hat{\Omega}_{12}^T + \left\{\left(\hat{\Lambda}_{22}\hat{\Lambda}_{66} - 2A_{26}^2 + \hat{\Lambda}_{12}\hat{\Lambda}_{22}\right)d_1 + \left(\hat{\Lambda}_{66}^2 + \hat{\Lambda}_{12}\hat{\Lambda}_{66} - 2A_{16}A_{26}\right)d_2\right\}\hat{\Omega}_{22}^T$$

$$\eta_{20}^T = \left(A_{26}^2\hat{\Lambda}_{22} - \hat{\Lambda}_{22}^2\hat{\Lambda}_{66}\right)\hat{\Omega}_{11}^T + \left(-2A_{26}\hat{\Lambda}_{12}\hat{\Lambda}_{22} + 2A_{16}\hat{\Lambda}_{22}^2 - A_{26}\hat{\Lambda}_{22}\hat{\Lambda}_{66} + A_{26}^3\right)\hat{\Omega}_{12}^T + \left(\hat{\Lambda}_{12}\hat{\Lambda}_{22}\hat{\Lambda}_{66} + \hat{\Lambda}_{22}\hat{\Lambda}_{66}^2 - A_{26}^2\hat{\Lambda}_{66} + A_{26}^2\hat{\Lambda}_{12} - 2A_{16}A_{26}\hat{\Lambda}_{22}\right)\hat{\Omega}_{22}^T$$

$$\eta_{21}^T = \left(-\hat{\Lambda}_{22}^2\hat{\Lambda}_{66} + A_{26}^2\hat{\Lambda}_{22}\right)\hat{\Omega}_{12}^T + \left(A_{26}\hat{\Lambda}_{22}\hat{\Lambda}_{66} - A_{26}^3\right)\hat{\Omega}_{22}^T$$

$$\eta_{22}^T = \left\{\left(A_{26}^2 - 2\hat{\Lambda}_{22}\hat{\Lambda}_{66}\right)d_2 - \hat{\Lambda}_{22}^2d_1\right\}\hat{\Omega}_{12}^T + \left(A_{26}\hat{\Lambda}_{22}d_1 + A_{26}\hat{\Lambda}_{66}d_2\right)\hat{\Omega}_{22}^T$$

$$\eta_{23}^{T} = \left(2A_{16}\hat{\Lambda}_{22}^{2} + 2A_{26}^{3} - 2A_{26}\hat{\Lambda}_{12}\hat{\Lambda}_{22} - 2A_{26}\hat{\Lambda}_{22}\hat{\Lambda}_{66}\right)\hat{\Omega}_{11}^{T} + \left(-\hat{\Lambda}_{11}\hat{\Lambda}_{22}^{2} + \hat{\Lambda}_{12}^{2}\hat{\Lambda}_{22} + 3\hat{\Lambda}_{12}\hat{\Lambda}_{22}\hat{\Lambda}_{66} - 3A_{26}^{2}\hat{\Lambda}_{12}\right)\hat{\Omega}_{12}^{T} + \left(A_{26}\hat{\Lambda}_{12}^{2} + A_{16}A_{26}^{2} - 2A_{16}\hat{\Lambda}_{12}\hat{\Lambda}_{22} - A_{16}\hat{\Lambda}_{22}\hat{\Lambda}_{66} + A_{26}\hat{\Lambda}_{11}\hat{\Lambda}_{22}\right)\hat{\Omega}_{22}^{T}$$

$$\eta_{24}^{T} = \left(-\hat{\Lambda}_{66}d_{2}^{2} - 2\hat{\Lambda}_{22}d_{1}d_{2}\right)\hat{\Omega}_{12}^{T} + A_{26}d_{1}d_{2}\hat{\Omega}_{22}^{T}$$

$$\eta_{25}^{T} = \left(4A_{16}\hat{\Lambda}_{22} - 2A_{26}\hat{\Lambda}_{12} - 2A_{26}\hat{\Lambda}_{66}\right)d_{2}\hat{\Omega}_{11}^{T} + \left\{\left(2A_{26}^{2} - \hat{\Lambda}_{22}\hat{\Lambda}_{66} + \hat{\Lambda}_{12}\hat{\Lambda}_{22}\right)d_{1} + \left(\hat{\Lambda}_{12}^{2} - 2\hat{\Lambda}_{11}\hat{\Lambda}_{22} + 3\hat{\Lambda}_{12}\hat{\Lambda}_{66}d_{2}\right)\right\}\hat{\Omega}_{12}^{T} + \left\{\left(A_{16}\hat{\Lambda}_{22} - A_{26}\hat{\Lambda}_{66} - 2A_{26}\hat{\Lambda}_{12}\right)d_{1} + \left(-2A_{16}\hat{\Lambda}_{12} + + A_{26}\hat{\Lambda}_{11} - A_{16}\hat{\Lambda}_{66}\right)d_{2}\right\}\hat{\Omega}_{22}^{T}$$

$$\eta_{26}^{T} = \left(2A_{16}\hat{\Lambda}_{22}\hat{\Lambda}_{66} - 4A_{16}A_{26}^{2} - 2A_{16}\hat{\Lambda}_{12}\hat{\Lambda}_{22} + 2A_{26}\hat{\Lambda}_{12}^{2} + 2A_{26}\hat{\Lambda}_{12}\hat{\Lambda}_{66}\right)\hat{\Omega}_{11}^{T} + \left(-\hat{\Lambda}_{11}\hat{\Lambda}_{22}\hat{\Lambda}_{66} - -2\hat{\Lambda}_{12}^{2}\hat{\Lambda}_{66} + 2A_{26}^{2}\hat{\Lambda}_{11} + 2A_{16}A_{26}\hat{\Lambda}_{12} - 4A_{16}A_{26}\hat{\Lambda}_{66} - A_{16}^{2}\hat{\Lambda}_{22} + \hat{\Lambda}_{11}\hat{\Lambda}_{12}\hat{\Lambda}_{22} - \hat{\Lambda}_{12}^{3}\right)\hat{\Omega}_{12}^{T} + \left(A_{16}\hat{\Lambda}_{12}^{2} + A_{16}^{2}A_{26} - A_{26}\hat{\Lambda}_{11}\hat{\Lambda}_{66} + A_{16}\hat{\Lambda}_{11}\hat{\Lambda}_{22} - 2A_{26}\hat{\Lambda}_{11}\hat{\Lambda}_{12}\right)\hat{\Omega}_{22}^{T}$$

$$\eta_{27}^{T} = -d_{1}d_{2}^{2}\hat{\Omega}_{12}^{T}$$

$$\eta_{28}^{T} = 2A_{16}d_{2}^{2}\hat{\Omega}_{11}^{T} + \left\{-\hat{\Lambda}_{11}d_{2}^{2} + \left(\hat{\Lambda}_{12} - \hat{\Lambda}_{66}\right)d_{1}d_{2}\right\}\hat{\Omega}_{12}^{T} + A_{16}d_{1}d_{2}\hat{\Omega}_{22}^{T}$$

$$\eta_{29}^{T} = \left(2A_{16}\hat{\Lambda}_{66} - 2A_{16}\hat{\Lambda}_{12}\right)d_{2}\hat{\Omega}_{11}^{T} + \left\{\left(\hat{\Lambda}_{12}\hat{\Lambda}_{66} - 2A_{16}A_{26}\right)d_{1} + \left(-\hat{\Lambda}_{11}\hat{\Lambda}_{66} - A_{16}^{2} + \hat{\Lambda}_{11}\hat{\Lambda}_{12}\right)d_{2}\right\}\hat{\Omega}_{12}^{T} + \left(A_{16}\hat{\Lambda}_{66}d_{1} + A_{16}\hat{\Lambda}_{11}d_{2}\right)\hat{\Omega}_{22}^{T}$$

$$\eta_{30}^{T} = \left(-2A_{16}\hat{\Lambda}_{12}\hat{\Lambda}_{66} + 2A_{16}^{2}A_{26}\right)\hat{\Omega}_{11}^{T} + \left(A_{16}^{2}\hat{\Lambda}_{12} + \hat{\Lambda}_{11}\hat{\Lambda}_{12}\hat{\Lambda}_{66} - 2A_{16}A_{26}\hat{\Lambda}_{11}\right)\hat{\Omega}_{12}^{T} + \left(A_{16}\hat{\Lambda}_{11}\hat{\Lambda}_{66} - A_{16}^{3}\right)\hat{\Omega}_{22}^{T}$$

$$\iota_{11}^{T} = \left(A_{16}\hat{\Lambda}_{11}\hat{\Lambda}_{66} - A_{16}^{3}\right)\hat{\Omega}_{11}^{T} + \left(A_{16}^{2}\hat{\Lambda}_{11} - \hat{\Lambda}_{11}^{2}\hat{\Lambda}_{66}\right)\hat{\Omega}_{12}^{T}$$

$$\iota_{12}^{T} = \left\{\left(A_{16}^{2} - 2\hat{\Lambda}_{11}\hat{\Lambda}_{66}\right)d_{1} - \hat{\Lambda}_{11}^{2}d_{2}\right\}\hat{\Omega}_{12}^{T} + \left(A_{16}\hat{\Lambda}_{66}d_{1} + A_{16}\hat{\Lambda}_{11}d_{2}\right)\hat{\Omega}_{11}^{T}$$

$$\iota_{13}^{T} = \left(-2A_{26}\hat{\Lambda}_{11}\hat{\Lambda}_{12} + A_{16}\hat{\Lambda}_{12}^{2} - A_{26}\hat{\Lambda}_{11}\hat{\Lambda}_{66} + A_{16}^{2}A_{26} + A_{16}\hat{\Lambda}_{11}\hat{\Lambda}_{22}\right)\hat{\Omega}_{11}^{T} + \left(-3A_{16}^{2}\hat{\Lambda}_{12} + 3\hat{\Lambda}_{11}\hat{\Lambda}_{12}\hat{\Lambda}_{66} - \hat{\Lambda}_{11}^{2}\hat{\Lambda}_{22} + \hat{\Lambda}_{11}\hat{\Lambda}_{12}^{2}\right)\hat{\Omega}_{12}^{T} + \left(2A_{16}^{3} + 2A_{26}\hat{\Lambda}_{11}^{2} - 2A_{16}\hat{\Lambda}_{11}\hat{\Lambda}_{12} - 2A_{16}\hat{\Lambda}_{11}\hat{\Lambda}_{66}\right)\hat{\Omega}_{22}^{T}$$

$$\iota_{14}^{T} = A_{16}d_1d_2\hat{\Omega}_{11}^{T} + \left(-2\hat{\Lambda}_{11}d_1d_2 - \hat{\Lambda}_{66}d_1^{2}\right)\hat{\Omega}_{12}^{T}$$

$$\iota_{15}^{T} = \left\{\left(-2A_{26}\hat{\Lambda}_{12} - A_{26}\hat{\Lambda}_{66} + A_{16}\hat{\Lambda}_{22}\right)d_1 + \left(A_{26}\hat{\Lambda}_{11} - 2A_{16}\hat{\Lambda}_{12} - A_{16}\hat{\Lambda}_{66}\right)d_2\right\}\hat{\Omega}_{11}^{T} + \left\{\left(3\hat{\Lambda}_{12}\hat{\Lambda}_{66} - 2\hat{\Lambda}_{11}\hat{\Lambda}_{22} + \hat{\Lambda}_{12}^{2}\right)d_1 + \left(2A_{16}^{2} + \hat{\Lambda}_{11}\hat{\Lambda}_{12} - \hat{\Lambda}_{11}\hat{\Lambda}_{66}\right)d_2\right\}\hat{\Omega}_{12}^{T} + \left(4A_{26}\hat{\Lambda}_{11} - -2A_{16}\hat{\Lambda}_{66} - 2A_{16}\hat{\Lambda}_{12}\right)d_1\hat{\Omega}_{22}^{T}$$

$$\iota_{16}^{T} = \left(A_{26}\hat{\Lambda}_{12}^{2} + A_{26}\hat{\Lambda}_{11}\hat{\Lambda}_{22} + A_{16}A_{26}^{2} - 2A_{16}\hat{\Lambda}_{12}\hat{\Lambda}_{22} - A_{16}\hat{\Lambda}_{22}\hat{\Lambda}_{66}\right)\hat{\Omega}_{11}^{T} + \left(-\hat{\Lambda}_{12}^{3} - 2\hat{\Lambda}_{12}^{2}\hat{\Lambda}_{66} + 2A_{16}^{2}\hat{\Lambda}_{22} + 2A_{16}A_{26}\hat{\Lambda}_{12} - A_{26}^{2}\hat{\Lambda}_{11} + \hat{\Lambda}_{11}\hat{\Lambda}_{12}\hat{\Lambda}_{22} - \hat{\Lambda}_{11}\hat{\Lambda}_{22}\hat{\Lambda}_{66}\right)\hat{\Omega}_{12}^{T} + \left(2A_{26}\hat{\Lambda}_{11}\hat{\Lambda}_{66} + 2A_{16}\hat{\Lambda}_{12}\hat{\Lambda}_{66} - 2A_{26}\hat{\Lambda}_{11}\hat{\Lambda}_{12} - 4A_{16}^{2}A_{26} + 2A_{16}\hat{\Lambda}_{12}^{2}\right)\hat{\Omega}_{22}^{T}$$

$$\iota_{17}^{T} = -d_1^{2}d_2\hat{\Omega}_{12}^{T}$$

$$\iota_{18}^{T} = A_{26}d_1d_2\hat{\Omega}_{11}^{T} + \left\{\left(\hat{\Lambda}_{12} - \hat{\Lambda}_{66}\right)d_1d_2 - \hat{\Lambda}_{22}d_1^{2}\right\}\hat{\Omega}_{12}^{T} + 2A_{26}d_1^{2}\hat{\Omega}_{22}^{T}$$

$$\iota_{19}^{T} = \left(A_{26}\hat{\Lambda}_{66}d_2 + A_{26}\hat{\Lambda}_{22}d_1\right)\hat{\Omega}_{11}^{T} + \left\{\left(-\hat{\Lambda}_{22}\hat{\Lambda}_{66} - A_{26}^{2} + \hat{\Lambda}_{12}\hat{\Lambda}_{22}\right)d_1 + \left(\hat{\Lambda}_{12}\hat{\Lambda}_{66} - 2A_{16}A_{26}\right)d_2\right\}\hat{\Omega}_{12}^{T} + \left(2A_{26}\hat{\Lambda}_{66} - 2A_{26}\hat{\Lambda}_{12}\right)d_1\hat{\Omega}_{22}^{T}$$

$$\iota_{20}^{T} = \left(A_{26}\hat{\Lambda}_{22}\hat{\Lambda}_{66} - A_{26}^{3}\right)\hat{\Omega}_{11}^{T} + \left(A_{26}^{2}\hat{\Lambda}_{12} + \hat{\Lambda}_{12}\hat{\Lambda}_{22}\hat{\Lambda}_{66} - 2A_{16}A_{26}\hat{\Lambda}_{22}\right)\hat{\Omega}_{12}^{T} + \left(2A_{16}A_{26}^{2} - 2A_{26}\hat{\Lambda}_{12}\hat{\Lambda}_{66}\right)\hat{\Omega}_{22}^{T}$$

$$\iota_{21}^{T} = \hat{\Omega}_{12}^{T}\left(A_{26}\hat{\Lambda}_{22}\hat{\Lambda}_{66} - A_{26}^{3}\right) + \hat{\Omega}_{22}^{T}\left(A_{26}^{2}\hat{\Lambda}_{66} - \hat{\Lambda}_{22}\hat{\Lambda}_{66}^{2}\right)$$

$$\iota_{22}^{T} = \hat{\Omega}_{12}^{T}\left(A_{26}\hat{\Lambda}_{22}d_1 + A_{26}\hat{\Lambda}_{66}d_2\right) + \hat{\Omega}_{22}^{T}\left\{\left(A_{26}^{2} - 2\hat{\Lambda}_{22}\hat{\Lambda}_{66}\right)d_1 - \hat{\Lambda}_{66}^{2}d_2\right\}$$

$$\iota_{23}^{T} = \hat{\Omega}_{11}^{T}\left(\hat{\Lambda}_{12}\hat{\Lambda}_{22}\hat{\Lambda}_{66} + \hat{\Lambda}_{22}\hat{\Lambda}_{66}^{2} - A_{26}^{2}\hat{\Lambda}_{66} + A_{26}^{2}\hat{\Lambda}_{12} - 2A_{16}A_{26}\hat{\Lambda}_{22}\right) + \hat{\Omega}_{12}^{T}\left(A_{26}\hat{\Lambda}_{11}\hat{\Lambda}_{22} + A_{26}\hat{\Lambda}_{12}^{2} - 2A_{16}\hat{\Lambda}_{12}\hat{\Lambda}_{22} - A_{16}\hat{\Lambda}_{22}\hat{\Lambda}_{66} - 2A_{26}\hat{\Lambda}_{12}\hat{\Lambda}_{66} + 3A_{16}A_{26}^{2}\right) + \hat{\Omega}_{22}^{T}\left(-2\hat{\Lambda}_{11}\hat{\Lambda}_{22}\hat{\Lambda}_{66} + A_{26}^{2}\hat{\Lambda}_{11} - 2A_{16}A_{26}\hat{\Lambda}_{66} + 4A_{16}^{2}\hat{\Lambda}_{22} - 4A_{16}A_{26}\hat{\Lambda}_{12} + \hat{\Lambda}_{12}^{2}\hat{\Lambda}_{66} + 2\hat{\Lambda}_{12}\hat{\Lambda}_{66}^{2}\right)$$

$$\iota_{24}^{T} = \hat{\Omega}_{12}^{T} A_{26} d_1 d_2 - \hat{\Omega}_{22}^{T}\left(\hat{\Lambda}_{22} d_1^2 + 2\hat{\Lambda}_{66} d_1 d_2\right)$$

$$\iota_{25}^{T} = \hat{\Omega}_{11}^{T}\left\{\left(\hat{\Lambda}_{12}\hat{\Lambda}_{22} + \hat{\Lambda}_{22}\hat{\Lambda}_{66} - 2A_{26}^2\right)d_1 + \left(\hat{\Lambda}_{12}\hat{\Lambda}_{66} + \hat{\Lambda}_{66}^2 - 2A_{16}A_{26}\right)d_2\right\} + \hat{\Omega}_{12}^{T}\left\{\left(-4A_{26}\hat{\Lambda}_{12} + A_{26}\hat{\Lambda}_{66} + A_{16}\hat{\Lambda}_{22}\right)d_1 + \left(-2A_{16}\hat{\Lambda}_{12} - A_{16}\hat{\Lambda}_{66} + A_{26}\hat{\Lambda}_{11}\right)d_2\right\} + \hat{\Omega}_{22}^{T}\left\{\left(\hat{\Lambda}_{12}^2 - \hat{\Lambda}_{66}^2 - 2\hat{\Lambda}_{11}\hat{\Lambda}_{22} + 2A_{16}A_{26} + 2\hat{\Lambda}_{12}\hat{\Lambda}_{66}\right)d_1 + \left(-2\hat{\Lambda}_{11}\hat{\Lambda}_{66} + 4A_{16}^2\right)d_2\right\}$$

$$\iota_{26}^{T} = \hat{\Omega}_{11}^{T}\left(-\hat{\Lambda}_{12}^3 + \hat{\Lambda}_{11}\hat{\Lambda}_{22}\hat{\Lambda}_{12} - 3\hat{\Lambda}_{12}^2\hat{\Lambda}_{66} + \hat{\Lambda}_{11}\hat{\Lambda}_{22}\hat{\Lambda}_{66} - 2\hat{\Lambda}_{12}\hat{\Lambda}_{66}^2 - 2A_{26}^2\hat{\Lambda}_{11} + 6A_{16}A_{26}\hat{\Lambda}_{12} + 2A_{16}A_{26}\hat{\Lambda}_{66} - 2A_{16}^2\hat{\Lambda}_{22}\right) + \hat{\Omega}_{12}^{T}\left(A_{16}\hat{\Lambda}_{11}\hat{\Lambda}_{22} - 4A_{26}\hat{\Lambda}_{11}\hat{\Lambda}_{12} + A_{26}\hat{\Lambda}_{11}\hat{\Lambda}_{66} + 3A_{16}\hat{\Lambda}_{12}^2 + 2A_{16}\hat{\Lambda}_{12}\hat{\Lambda}_{66} - 3A_{16}^2A_{26}\right) + \hat{\Omega}_{22}^{T}\left(2\hat{\Lambda}_{11}\hat{\Lambda}_{12}\hat{\Lambda}_{66} - \hat{\Lambda}_{11}\hat{\Lambda}_{66}^2 + \hat{\Lambda}_{11}\hat{\Lambda}_{12}^2 + 2A_{16}A_{26}\hat{\Lambda}_{11} - \hat{\Lambda}_{11}^2\hat{\Lambda}_{22} + A_{16}^2\hat{\Lambda}_{66} - 4A_{16}^2\hat{\Lambda}_{12}\right)$$

$$\iota_{27}^{T} = -\hat{\Omega}_{22}^{T} d_1^2 d_2$$

$$\iota_{28}^{T} = \hat{\Omega}_{11}^{T}\left\{\left(\hat{\Lambda}_{12} + \hat{\Lambda}_{66}\right)d_1 d_2\right\} + \hat{\Omega}_{12}^{T}\left(A_{16}d_1 d_2 + 2A_{26}d_1^2\right) + \hat{\Omega}_{22}^{T}\left(-2\hat{\Lambda}_{11}d_1 d_2 - \hat{\Lambda}_{66}d_1^2\right)$$

$$\iota_{29}^{T} = \hat{\Omega}_{11}^{T}\left\{\left(\hat{\Lambda}_{12}\hat{\Lambda}_{66} + \hat{\Lambda}_{66}^2 - 2A_{16}A_{26}\right)d_1 + \left(\hat{\Lambda}_{11}\hat{\Lambda}_{12} + \hat{\Lambda}_{11}\hat{\Lambda}_{66} - 2A_{16}^2\right)d_2\right\} + \hat{\Omega}_{12}^{T}\left\{\left(4A_{26}\hat{\Lambda}_{11} - 2A_{16}\hat{\Lambda}_{12} - A_{16}\hat{\Lambda}_{66}\right)d_1 + A_{16}\hat{\Lambda}_{11}d_2\right\} + \hat{\Omega}_{22}^{T}\left\{\left(-2\hat{\Lambda}_{11}\hat{\Lambda}_{66} + A_{16}^2\right)d_1 - \hat{\Lambda}_{11}^2 d_2\right\}$$

$$\iota_{30}^{T} = \hat{\Omega}_{11}^{T}\left(\hat{\Lambda}_{11}\hat{\Lambda}_{12}\hat{\Lambda}_{66} + \hat{\Lambda}_{11}\hat{\Lambda}_{66}^2 - 2A_{16}A_{26}\hat{\Lambda}_{11} + A_{16}^2\hat{\Lambda}_{12} - A_{16}^2\hat{\Lambda}_{66}\right) + \hat{\Omega}_{12}^{T}\left(A_{16}^3 + 2A_{26}\hat{\Lambda}_{11}^2 - 2A_{16}\hat{\Lambda}_{11}\hat{\Lambda}_{12} - A_{16}\hat{\Lambda}_{11}\hat{\Lambda}_{66}\right) + \hat{\Omega}_{22}^{T}\left(A_{16}^2\hat{\Lambda}_{11} - \hat{\Lambda}_{11}^2\hat{\Lambda}_{66}\right)$$

and

$$\overline{\Lambda}_i = d_i a \qquad (i = 1,2)$$

$$\hat{\Omega}_{\alpha\beta}^{T} = \hat{B}_{\alpha\beta}^{T} + \frac{2\overline{h}^2}{3}\overline{\lambda}_{\alpha\beta} \qquad (\alpha,\beta = 1,2)$$

$$\hat{B}_{\alpha\beta}^{T} = {}^{/}B_{\alpha\beta}^{T} - {}^{//}B_{\alpha\beta}^{T}$$

$$ {}^{/}B_{\alpha\beta}^{T} = \sum_{k=1}^{{}^{/}n} \int_{(x_3)_{k-1}}^{(x_3)_k} \left({}^{/}\hat{\lambda}_{\alpha\beta} \right)_{(k)} x_3 dx_3 $$

{Note: ${}^{//}B_{\alpha\beta}^{T}$ is obtained by replacing the single prime (/) with a double prime (//).}